<u>**Final Report**</u>

Contract No. BDV29-977-13

Develop Epoxy Grout Pourback Guidance and Test Methods to Eliminate Thermal/Shrinkage Cracking at Post-Tensioning Anchorages

Phase II

Prepared for:

Research Center
Florida Department of Transportation
605 Suwannee Street, M.S. 30
Tallahassee, FL 32399-0450

Prepared by:

Irtishad Ahmad, Ph.D., P.E., Professor
Florida International University

Nakin Suksawang, Ph.D., P.E., Assistant Professor
Florida Institute of Technology

Khaled Sobhan, Ph.D., Professor
Florida Atlantic University

John A. Corven, P.E., President and Chief Engineer
Corven Engineering, Inc.

Ehssan Amir Sayyafi, E.I., Graduate Research Assistant
Florida International University

Sharmila Pant and Fernando Martinez, E.I., Graduate Research Assistants
Florida Atlantic University

January 2016

DISCLAIMER

The opinions, findings, and conclusions expressed in this publication are those of the authors and not necessarily those of the State of Florida Department of Transportation.

METRIC CONVERSION CHART

SYMBOL	WHEN YOU KNOW	MULTIPLY BY	TO FIND	SYMBOL
LENGTH				
in	Inches	25.4	millimeters	mm
ft	Feet	0.305	meters	m
yd	Yards	0.914	meters	m
mi	Miles	1.61	kilometers	km
mm	Millimeters	0.039	inches	in
m	Meters	3.28	feet	ft
m	Meters	1.09	yards	yd
km	Kilometers	0.621	miles	mi
SYMBOL	**WHEN YOU KNOW**	**MULTIPLY BY**	**TO FIND**	**SYMBOL**
AREA				
in²	square inches	645.2	square millimeters	mm²
ft²	square feet	0.093	square meters	m²
yd²	square yard	0.836	square meters	m²
ac	Acres	0.405	hectares	ha
mi²	square miles	2.59	square kilometers	km²
mm²	square millimeters	0.0016	square inches	in²
m²	square meters	10.764	square feet	ft²
m²	square meters	1.195	square yards	yd²
ha	Hectares	2.47	acres	ac
km²	square kilometers	0.386	square miles	mi²
SYMBOL	**WHEN YOU KNOW**	**MULTIPLY BY**	**TO FIND**	**SYMBOL**
VOLUME				
fl oz	fluid ounces	29.57	milliliters	mL
gal	Gallons	3.785	liters	L
ft³	cubic feet	0.028	cubic meters	m³
yd³	cubic yards	0.765	cubic meters	m³
mL	Milliliters	0.034	fluid ounces	fl oz
L	Liters	0.264	gallons	gal
m³	cubic meters	35.314	cubic feet	ft³
m³	cubic meters	1.307	cubic yards	yd³
NOTE: volumes greater than 1000 L shall be shown in m³				

1. Report No.	2. Government Accession No.	3. Recipient's Catalog No.

4. Title and Subtitle	5. Report Date
Develop Epoxy Grout Pourback Guidance and Test Methods to Eliminate Thermal/Shrinkage Cracking at Post-Tensioning Anchorages: Phase II	December 2015
	6. Performing Organization Code

7. Author(s) Irtishad Ahmad, Nakin Suksawang, Khaled Sobhan and John Corven	8. Performing Organization Report No.

9. Performing Organization Name and Address	10. Work Unit No. (TRAIS)
Department of Civil and Environmental Engineering and OHL School of Construction.	
	11. Contract or Grant No.
Florida International University 10555 West Flagler Street, EC 3680, Miami, FL 33174	BDV29-977-13

12. Sponsoring Agency Name and Address	13. Type of Report and Period Covered
Research Center State of Florida Department of Transportation 605 Suwannee Street, M.S. 30, Tallahassee, Florida 32399-0450	Final Report February 2012 – January 2016
	14. Sponsoring Agency Code
	99700-3596-119

15. Supplementary Notes
Mr. Rick Vallier of the Structures Design Office at the Florida Department of Transportation served as the Project Manager for this project.

16. Abstract

This research report contains guidance for eliminating thermal and shrinkage cracking in epoxy grout pourbacks used in post-tensioned anchorages. In this study, an experimental investigation of a selected epoxy grout pourback material and finite element analysis on the full-scale pourback specimens using the same pourback material were conducted. The study was undertaken to better understand the pourbacks' failure mechanisms and provide guidelines and methods for eliminating them. Additionally, field investigation of epoxy grout pourbacks cracking was made at two bridge sites in Tampa and Miami. Based on a comprehensive literature review, manufacturer and contractor feedbacks, field investigation, and full-scale testing potential factors affecting epoxy grout pourback were determined to be the pourback size, shapes (particularly shapes with obtuse corner), ambient condition and concrete substrate's temperature. The results of the full-scale testing and finite element analysis indicated that the primary cause of pourback failure was due to thermal cracking. The manufacturer-provided peak exothermic temperature did not reflect what was measured in the full-scale specimens as well as in the researchers' own laboratory test, which were significantly higher. It was found that both the peak exothermic temperature and the maximum thermal stress increased as the volume-to-surface (V/S) ratio increased. It should be noted that the V/S ratios calculated in this report were based on the volume divided by the area of the exposed surfaces (the face of the epoxy grout not in contact with the concrete) in ft. The shapes also played a significant role particularly shapes with obtuse corners. The thermal cracks found in the field and full-scale specimens were full-depth cracks that penetrated through the epoxy grout. Therefore, it is recommended that these cracks should be immediately sealed. To avoid the thermal cracks, it is highly recommended, based on the findings of this study, that the V/S ratio of the epoxy grout be limited to 0.30 ft and 0.35 ft for irregular (S-type) and rectangular (R-type) shaped pourbacks, respectively.

17. Key Word	18. Distribution Statement
Post-tensioning, epoxy grout, pourback, cracking, thermal, shrinkage	

19. Security Classif. (of this report)	20. Security Classif. (of this page)	21. No. of Pages	22. Price
Unclassified	Unclassified	112	

Form DOT F 1700.7 (8-72)   Reproduction of completed page authorized

ACKNOWLEDGEMENTS

EXECUTIVE SUMMARY

Epoxy grout pourbacks at end anchorages of post-tensioning tendons provide an essential level of corrosion protection. This is especially true when the anchorages are adjacent to expansion joints or other bridge deck discontinuities where water can flow freely to the tendon anchorage. Water may easily pass through the mastic coating and onto the post-tensioning anchorage. However, the current practice includes permanent anchorage caps providing another barrier. Within a few years of installation, the tendon may fail as a result of strand corrosion in the anchorage. In order to mitigate this problem, this study was undertaken to develop guidance for eliminating thermal/shrinkage cracking in epoxy grout pourbacks at post-tensioned anchorages. Post-tensioning end anchorages are protected by a four-level system composed of grout, heavy-duty permanent grout caps with sealing o-ring, an applied coating, and enclosure with epoxy grout pourback as adopted by the Florida Department of Transportation (FDOT) in its *FDOT Structures Manual* (2010, now replaced with January 2016 edition). FDOT experienced occurrences of cracking on larger epoxy grout pourbacks, which are suspected to be caused by the pourback shrinkage strains relative to the substrate and/or thermal strains that occur as a result of the exothermic nature of the epoxy grout curing. Therefore, there is a need to develop best practice guidance for the construction of epoxy grout pourbacks to avoid the current cracking problems on larger pourbacks. This study describes the investigation of a selected epoxy grout pourback material, 420 Epoxy Grout System, from E-Bond Epoxies, Inc. (Ft. Lauderdale, FL.).

The following tasks were conducted as part of this investigation: (a) Literature search on the current use of epoxy grout pourbacks for anchorage corrosion protection in Florida bridges; (b) Inspection of Florida bridges with epoxy grout cracking; (c) Determination of selected physical properties of an FDOT-approved (commonly used) epoxy grout from laboratory tests and manufacturer data; (d) Full-scale testing on complex and regular geometric shapes; (e) Finite element thermal and stress analysis on the selected epoxy grout pourback material and validation with experimental results; and (f) Development of guidelines to minimize the probability of cracking.

Field investigation of epoxy grout pourbacks cracking was made at two bridge sites in Tampa and Miami. Based on a comprehensive literature review, manufacturer and contractor feedbacks, field investigation, and full-scale testing, potential factors affecting epoxy grout pourback were determined to be the pourback size, shapes (particularly shapes with obtuse corner), and ambient condition and concrete substrates temperature.

Two physical properties tests were conducted in the Florida International University (FIU) laboratory: (1) the compressive strength test and (2) the peak exothermic test. The results of the compressive strength test compared very well with the corresponding data obtained from the manufacturer's product data sheet. This test was conducted for three temperatures (55°F, 75°F, and 110°F) at several elapsed times from 8 hours to 28 days using 2-inch cube specimens in accordance with ASTM C-579. Based on the compressive strength results, there was no significant variation between specimens tested at low temperature, i.e., 55°F, and controlled specimens tested at room temperature of 75°F. However, significant early-age compressive strength reduction existed when testing the specimens at high temperature of 110°F with approximately 25% reduction as compared to specimens tested at room temperature. It was

decided by the investigators and the FDOT project manager not to conduct other physical properties tests, such as the modulus of elasticity and the tensile strength test, and instead use the manufacturer's data for FEM analysis. The peak exothermic temperature test was conducted for the standard size (12 in. × 12 in. × 3in.) and three other volume/surface ratios. A comparison of the results showed that the laboratory finding of 103°C for the standard-sized specimen was considerably higher than the manufacturer-provided data, which was 60°C. In general, higher peak exothermic temperature is associated with higher thermal stresses and cracking potential. Therefore, epoxy materials with lower peak exothermic temperature should be preferred when there is a choice. The peak exothermic temperature test was performed on small-scale specimens with a volume-to-surface area (V/S) ratio ranging from 0.19 to 1.0 in accordance with ASTM D 2471. As expected, as the V/S ratio increased, so did the peak exothermic temperature.

The full-scale test consisted of testing rectangular (R-type) and irregular (S-type) pourbacks with V/S ratios of 0.26 ft., 0.32 ft., and 0.37 ft. The S-type pourback was modeled from the cracked pourback found at the LeRoy Selmon Crosstown Expressway. The full-scale specimens were instrumented with multiple thermocouples and a vibrating wire strain gauge to capture the temperature profile and localized strain, respectively. Based on the full-scale data and observation, specimens with V/S ratio of 0.37 ft. experienced full-depth cracks. Additionally, full-depth cracks were also observed on the S-type specimen with V/S ratio of 0.32 ft. The cracks appeared within the first 24 hours and concentrated in regions with high exothermic temperature. Therefore, it was concluded that these cracks were caused by exothermic temperature rather than shrinkage. It is also very important that these cracks are immediately sealed, considering that they occurred in the heavy-duty permanent grout caps regions. A finite element analysis was developed to perform a parametric study for better understanding of the cracking mechanism of epoxy grout pourback system and the influence of V/S ratio. The model was calibrated and validated using the data obtained from the full-scale test.

The following recommendations were made from this study:
- Cracks observed on the specimens were not surface cracks but penetrated all the way through the epoxy pourbacks. Hence, it is highly recommended that any cracks found in the pourbacks should be injected and sealed as soon as possible to avoid chloride-laden water to leak through.
- Finite element analysis is a valid tool for predicting field behavior of epoxy grout pourback systems. It is recommended that parametric studies (V/S ratios under considerations and materials data) using FEM analysis be undertaken for developing design charts.
- Manufacturer-provided peak exothermic temperature data should be verified.
- It is recommended that the maximum value of V/S ratio of the epoxy grout pourbacks be limited to 0.3 ft. for irregular (S-type) shape and to 0.35 ft. for regular (R-type) shapes. FEM analysis can be undertaken when V/S ratio exceeds these limits.

TABLE OF CONTENTS

LIST OF TABLES

LIST OF ACRONYMS

ASTM   American Society for Testing and Materials

ANSYS   Analysis System

FE   Finite Element

FEM   Finite Element Method

FDOT   Florida Department of Transportation

CHAPTER 1 – INTRODUCTION

1.1 Background and Problem Statement

Pourbacks at end anchorages of post-tensioning tendons provide an essential level of corrosion protection. This is especially true when the anchorages are adjacent to expansion joints or other bridge deck discontinuities where water can flow freely to the tendon anchorage. Figure 1-1 shows an anchorage of a tendon in an expansion joint span of the Mid-Bay Bridge, where no pourback was provided. Water easily passed through the mastic coating and into the post-tensioning anchorage. Within seven years of installation, the tendon failed as a result of strand corrosion in the anchorage.

Figure 1-1: Tendon failure on the Mid-Bay Bridge

Early segmental bridges incorporated cementitious pourbacks to protect end anchorages. Figure 1-2 shows a single pourback that encases three anchorages of the span-by-span approaches on the Sunshine Skyway Bridge. Unfortunately, the details of the pourbacks, and the methods of placing the materials, led to significant cracking of the pourbacks.

Figure 1-2: Pourback cracking on the Sunshine Skyway Bridge

Larger epoxy grout pourbacks at the post-tensioning anchorages may crack due to the pourback shrinkage strains relative to the substrate and/or thermal strains that occur as a result of the exothermic nature of the epoxy grout curing. Therefore, this research project addressed the need to develop epoxy grout pourback guidance and test methods to eliminate thermal/shrinkage cracking at post-tensioning anchorages.

1.2 Objectives and Scope

The goal of this research was to develop best practices for pourback construction. The primary objectives were to develop epoxy grout pourback guidance and test methods to eliminate thermal/shrinkage cracking at post-tensioning anchorages. To accomplish these objectives, the following tasks were completed:

- Literature search on the current use of epoxy grout pourbacks for anchorage corrosion protection in Florida bridges
- Inspection of Florida bridges with epoxy grout cracking
- Determination of selected physical properties of an FDOT-approved (commonly used) epoxy grout from laboratory tests and manufacturer data
- Full-scale testing on complex and regular geometric shapes
- Finite element thermal and stress analysis on the selected epoxy grout pourback material and validation with experimental results
- Development of guidelines to minimize the probability of cracking

1.3 Report Organization

The report is organized as follows: Chapter 1 describes the research background, statement of the problem, and study objectives. Chapter 2 discusses the literature review performed on the current state of knowledge on epoxy pourback cracking. Chapter 3 discusses field inspections of epoxy grout pourbacks at two Florida post-tensioned segmental bridges. Chapter 4 explains the experimental methodology for the evaluation of the physical properties of the epoxy grouts and finite element modeling for result validation. Chapter 5 presents the results of the experimental and finite element modeling phases. Finally, Chapter 6 provides relevant conclusions, best practices guidelines, and recommendations for further work.

CHAPTER 2 – LITERATURE REVIEW

2.1 Introduction and Background

Partly as a result of the problems with post-tensioned bridges, the Florida Departments of Transportation (FDOT) has undertaken major activities, resulting in the development of the state of the art technologies for the prevention of corrosion in pre-tensioned and post-tensioned concrete bridge elements. The protection of strands under tensile force is essential for extending the bridge service life. The FDOT standards for grouting are nationally recognized as the best practice for strands protection. Very rigorous testing and grouting procedures required are aimed at preventing the existence of voids, which could contain water and oxygen, the two elements needed to initiate corrosion activities. (Please note that the FDOT's latest policy includes flexible filler along with grout. See FDOT Bulletin 15-03, 2015. The flexible filler policy will be included in the 2016 FDOT Structures Manual.)

The FDOT implemented new policies and procedures (Florida Department of Transportation, 2010) to enhance the long-term durability of their post-tensioned bridges. These policies and procedures are developed through extensive researches that are highlighted in a ten volume publication titled *New Directions for Florida Post-Tensioned Bridges* by Corven Engineering, Inc. (2002) who served as a co-principal investigator of this research project. Five strategies for providing corrosion protection have been adopted for post-tensioned bridges: (1) enhanced post-tensioned systems; (2) fully grouted tendons; (3) multi-level anchor protection; (4) watertight bridges; and (5) multiple tendon paths. These strategies are developed by examining six levels of protection for typical post-tensioning systems consisting of: (1) exterior surface; (2) concrete or epoxy cover; (3) duct; (4) grout; (5) strands' sheathing or coating; and (6) strand or bar (Figure 2-1).

Out of these six levels, three and four levels of protection were adopted by FDOT Structures Manual for strands and anchorages, respectively. The anchorages are protected by a four-level system comprised of grout, heavy-duty permanent grout caps with sealing o-ring, an applied coating, and enclosure with epoxy grout pourback.
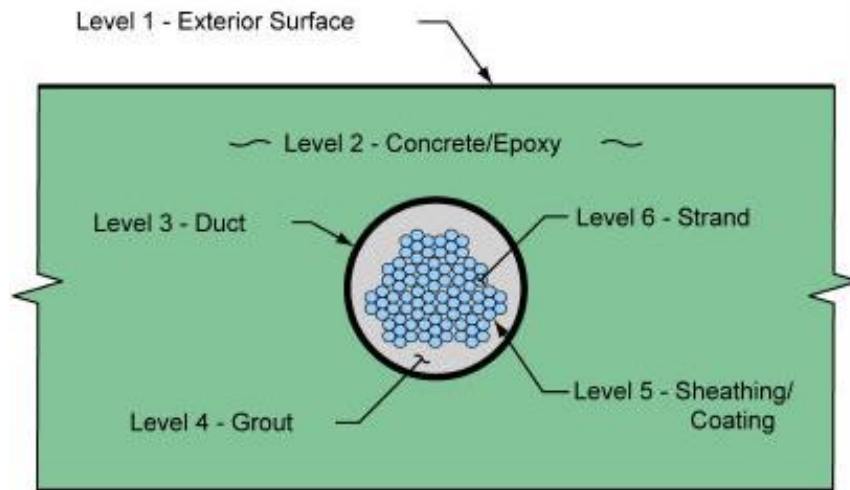
Figure 2-1: Level of protection for corrosion protection (Source: Corven Engineering, Inc., 2002, Volume 1)

Another research project, titled *Post-Tensioning Grout Bleed, Duct, and Anchorage Protection Test* that was conducted by Hamilton and Alvarez (2002) at the University of Florida (UF) evaluate the performance of epoxy grout pourbacks. In this project, Dr. Hamilton and his research team constructed full-scale mockup anchorage ends (Figure 2-2) to determine if thermal expansion and drying shrinkage cause cracking of the pourback. Based on their results, no discernible cracking was observed or detected on the exterior of the pourback specimens. Furthermore, they did not detect any sign of change in the bond at the interface between the epoxy and concrete. However, they did recommend that further study of epoxy grout pourback should be conducted.

While the rehabilitation of the Florida Keys project was a success, not all epoxy grout pourbacks yielded positive results. Larger epoxy grout pourbacks tend to suffer from thermal/shrinkage cracking due to excessive exothermic heat generated during the curing period. Considering that the full-scale mockup anchorage ends tested at UF were quite large and that no cracking was observed, lead us to hypothesize that the leading causes of the cracking in epoxy grout pourback found in the field are related to several variables: mixture proportions, environment, design

details, and construction practices. This research effort will investigate these variables to help develop best practices for pourback construction.
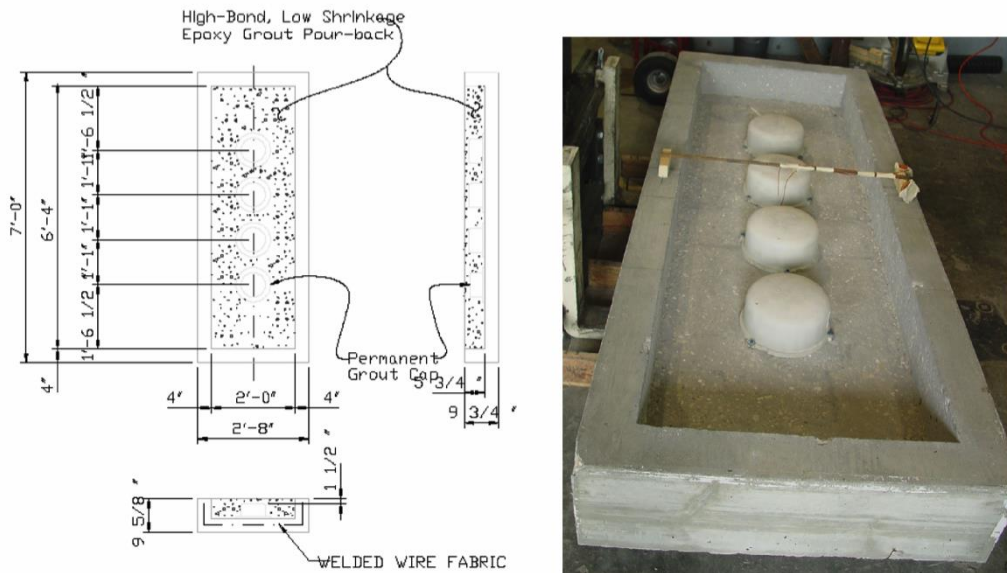
Figure 2-2: Epoxy pourback specimen design details (Hamilton and Alvarez, 2002)

Figure 2-3: Epoxy grout pourbacks in the Florida Keys Bridges

2.2 Factors Affecting the Cracking

As stated above, there are three main factors affecting the cracking of the finished pourback: (1) the mixture proportions, (2) environments, and (3) design details and construction practices. However, it should be noted that the mixture proportions cannot be controlled or specified by the

FDOT since the epoxy grouts are proprietary products that come pre-proportioned by the manufacturer with strict mixing guidelines. These factors will be described in more details in the following sections:

2.2.1 Effect of mixture proportions on epoxy grout cracking

The mixture proportions play one of the biggest roles in the determination of factors contributing to cracking of the finished pourback. At the time this research was conducted, there were five epoxy grouts listed on the Qualified Products List, namely the E3HP Epoxy Grout, Sikadur 42 Grout Pak PT, Masterflow 648 CP Plus, Magmaflow Grout-Pak, and E-Bond 420 Grout System. All these products do not have the same physical properties, but they do meet or exceed FDOT 926-14 specifications (Standard Specifications for Road and Bridge Construction, 2010). The product data sheets for two of these epoxy grouts, namely the E3HP and the 420 epoxy grout system (E-Bond, Ft. Lauderdale), are shown in Figures 2-4(a) and 2-4(b). It is possible that one product will perform best in a certain environments while the other performs best in a different environment. This research evaluated the selected physical properties of one of these products, namely 420 epoxy grout system, and its thermal and shrinkage behavior in full-scale models.

(Please note that, The QPL list is now the *Approved Product List* since the end of 2014. There are now six products on the APL for Epoxy Compounds Type Q. E3-DP by Euclid Chemical is now also on the list. See FDOT (2015), Approved Product List.)

2.2.2 Effect of environment on epoxy grout cracking

The environments in which the epoxy grout is mixed, placed, and cured and to which it is exposed during its life have a significant effect on the physical properties of the epoxy grout. Low temperatures reduce the compressive strength as shown below in the product data sheet (see Figure 2-4a). The reduction in compressive strength could also lead to reduced tensile strength and elastic modulus. These factors may increase the cracking potential should the epoxy grout exhibit high early-age thermal/shrinkage strains. Furthermore, if the ambient temperature is low, the temperature gradient between the epoxy grout and concrete would be quite large; when these are combined with the difference in coefficient of thermal expansion, the epoxy grout may crack. The opposite is also true. High temperatures may increase the compressive strength but have a negative impact on the gel time and peak exothermic temperature, which can lead to thermal/shrinkage cracking. We considered some of these factors when designing the full-scale experimental setup.

E³-HP

HIGH PERFORMANCE EPOXY GROUT SYSTEM

DESCRIPTION

E³-HP high performance epoxy grout is a performance standard for epoxy grouts. E³-HP is formulated from a new resin technology. Further, a proprietary aggregate blend has created a grout which exceeds all current performance standards. This product is characterized by high bearing surface, low creep and excellent flowability. E³-HP is clearly the choice for the toughest and most demanding epoxy installations where bond to existing foundation and machinery is critical.

PRIMARY APPLICATIONS

- Turbines, compressors or stamping machines with dynamic loading
- Quick re-grouts and start-ups
- Industrial areas requiring maximum bond to foundation with maximum bearing
- Pour-backs for post tension projects

FEATURES/BENEFITS

- Fast return to service
- High chemical resistance
- Excellent bond, machinery to foundation
- Low shrinkage, low creep
- Excellent bearing
- Superior stability under elevated service temperatures of up to 220°F (105°C)

TECHNICAL INFORMATION

Typical Engineering Data
Test results developed under laboratory conditions.
Compressive Strength,
ASTM C 579 2" (50 mm) cubes @ 70°F (21°C)

Age	Strength
4 hours	700 psi (5 MPa)
6 hours	5,000 psi (34 MPa)
8 hours	8,000 psi (55 MPa)
1 day	11,900 psi (82 MPa)
3 days	13,100 psi (90 MPa)
7 days	13,600 psi (94 MPa)
28 days	14,800 psi (102 MPa)

Creep Data, ASTM C 181
3 days.......... 1.9×10^{-4} in./in. (1.9×10^{-4} mm/mm)
7 days.......... 2.4×10^{-4} in./in. (2.4×10^{-4} mm/mm)
28 days....... 3.6×10^{-4} in./in. (3.6×10^{-4} mm/mm)
120 days...... 7.1×10^{-4} in./in. (7.1×10^{-4} mm/mm)
Coefficient of Thermal Expansion, ASTM C 531
2.0×10^{-5} in./in./°F (3.6×10^{-5} mm/mm/°C)
Bond to Concrete: Exceeds tensile and shear strength of concrete.

Chemical Resistance: ASTM D 543 excellent resistance to most chemicals. Specific recommendations available upon request.
Abrasion Resistance: Greater than concrete.
Flexural Strength, ASTM C 580
1 day......................................3,600 psi (25 MPa)
28 days..................................4,100 psi (28 MPa)
Modulus of Elasticity, ASTM C 580
1 day............................ 1.2×10^6 psi (8.5×10^3 MPa)
28 days.................... 1.5×10^6 psi (10.5×10^3 MPa)
Tensile Strength, ASTM C 307
1 day......................................1,900 psi (13 MPa)
28 days..................................2,200 psi (15 MPa)
Gel Time, ASTM D 2471
@73°F (23°C) .... 109 minutes
Peak Exotherm, ASTM D 2471
@73°F (23°C) ....116°F (47°C) @ 126 minutes
Heat Deflection Temperature..........192°F (89°C)
Appearance: E³-HP is a three part epoxy grout system which consists of a Part A (resin), Part B (hardener) and Part C (aggregate). After mixing and placing, the color is similar to that of concrete though the grout may always appear somewhat darker than the surrounding concrete

Figure 2-4(a): E3HP Epoxy Grout PT Data Sheet (from manufacturer Euclid)

420 EPOXY GROUT SYSTEM

FORMULATED AND LABELED FOR PROFESSIONAL USE ONLY
NOT FOR SALE TO OR USE BY THE GENERAL PUBLIC

420

PRODUCT DATA   PRODUCT DATA   PRODUCT DATA   PRODUCT DATA

Formulated to comply with 926-14 Specific Requirements for Type Q Compounds

DESCRIPTION

E-Bond 420 Epoxy Grout system is a pre-proportioned, 3-component, 100% solids, moisture-tolerant, non-shrink epoxy. This product is characterized by high bearing surface, low creep and excellent flowability that produces a low exothermic reaction.

WHERE TO USE

• To protect the anchorages of post-tensioning tendons or bars on segmental bridge projects
• Seating of base plates • Grouting under equipment where easy access is available
• Industrial areas requiring maximum bond to foundation with maximum bearing • Quick re-grouts and start ups

FEATURES

- Ready to mix, pre-proportioned kit
- Excellent flowability
- Long working time
- 100% solids, no solvents
- Fast strength gain
- High compressive strength
- Moisture Tolerant

BENEFITS

- Fast return to service
- Minimal shrinkage/expansion
- Impermeable and resistant to chemicals, corrosion, impact and stress
- High vibration resistance
- Excellent bond, machinery to foundation
- High effective bearing area
- Low heat development for large pours

PHYSICAL PROPERTIES

Property	Test Method	Results
Gel Time	(ASTM D-2471)	150 minutes
Tensile Properties 7 day	(ASTM C-307)	3,500-4,000 psi (24-28 MPa)
Flexural Properties 7 day @ 77F (25C)	(ASTM-C580)	> 5,000 psi (35 MPa)
Thermal Compatibility 5 cycles	(ASTM C-884) (with aggregate)	passed
Peak Exotherm 12 in. x12 in. x 3 in. Specimen	(ASTM D-2471)	140°F (60°C)
Linear Shrinkage 7 day	(ASTM C-531)	<.01%
Flowability and Bearing Area	(ASTM C-1339)	>97%
Coefficient of Thermal Expansion 74F to 210F (23C to 99C)	(ASTM C-531)	< 30 x 10-7 in/in/F
Modulus of Elasticity 7 day @ 77F (25C)	(ASTM C-580)	1,700,000 – 1,800,000 psi (11724-12414 MPa)
Compressive Properties 7 day @ 73F (23C)	(ASTM-C-579B) Test Method B	14,250 psi (99 MPa)
Water Absorption 7 days	(ASTM-C-413)	.4%
Heat Deflection Temp	(ASTM D-648)	152° F (67°C)
Slant Shear 7 days	(ASTM C-882)	>5,000 psi

For Best Performance

- Precondition the components to 70°F (23°C) to 80°F (27°C) for 24 hrs before use.

- Minimum ambient, surface, aggregate and epoxy temperatures should be 50°F (10°C) and rising at the time of application.

- Store at 55°F to 90°F (15°C to 32°C).

- Protect from moisture.

- Protect from freezing.

- Do not add solvents or water to epoxy material.

- Do not alter or change the recommended proportions when blending the components.

Figure 2-4(b): Product data sheet for 420 epoxy grout system (E-Bond, Ft. Lauderdale)

2.2.3 Effect of design and construction on epoxy grout cracking

There are many factors at the construction site that can affect the epoxy grout cracking such as the quality control, quality assurance, material handling and storage, and workmanship. These factors are of importance when it is necessary to minimize cracking but would be difficult to replicate all scenarios in laboratory environment. This research reviewed current and past construction practices through inspection reports and informal communications with contractors and producers. Additionally, field inspections of bridges with known epoxy grout pourbacks cracking were conducted to understand the severity of the cracking problems. This information was used to develop testing protocols of full-scale pourback specimens.

The design details can also affect the epoxy grout cracking due to the large contact area or more specifically the ratio of the volume of the specimen to its exposed surface area (V/S ratio). It is a known fact that there is some form of relationship between the thermal/shrinkage rate and V/S ratio. However, this relationship is not well established and was investigated as part of this research. Another important design detail that may eliminate or minimize thermal/shrinkage cracking is the inclusion of reinforcing steel found in FDOT Type 12 (post-tensioning anchorage protection, FDOT 2016 *Design Standards* Index No. 21802.)

2.3 Cracks Evaluation Methods

Available technologies related to the detection of cracks in epoxy grout could be divided into four main categories: (1) visual, (2) sounding, (3) reflection methods, and (4) imaging.

1. Visual - The visual method is the simplest non-destructive methods. A simple example is a crack microscope, which can help magnified hairline cracks. The problem with this method is that microcracks and delamination are not visually identifiable.

2. Sounding – The sounding method is similar to the reflection method but using low-tech human ear to discern the change in pitch. A simple example is the chain drag delamination survey that involves dragging lengths of chain across a concrete surface. A distinctly hollow, drum-like sound is heard when delamination is encountered. Another similar test is the hammer sounding test that involves tapping a concrete surface with a hammer. This method could be very cost-effective when use in the combination with the visual method.

3. Reflection Methods – The nondestructive techniques which rely on sending various forms of sonic waves and investigating the return responses are referred to as reflection methods. Most reflection methods are best suited for investigating local and small areas and are time consuming if they are conducted on a point-by-point basis. Such methods include impact echo and ultrasonic pulse velocity with shear waves for concrete bridges and can potentially be used for detecting cracks in epoxy grout.

4. Imaging – Nondestructive techniques in the imaging category are those which provide images, allow visual inspection, such as radiographic imaging or tomographic systems. In general these techniques are difficult to implement in the field condition, expensive and only allow inspection of very small areas. Ground penetrating radar can provide 2-D and 3-D images of epoxy grout but are very expensive.

CHAPTER 3 – FIELD INSPECTION OF EPOXY GROUT POURBACKS

3.1 Field Inspection

As a first step to developing a comprehensive experimental program to evaluate the performance and to better understand the epoxy grout pourbacks failure mechanism, field inspection of epoxy grout pourbacks was conducted on two bridges. These two bridges were the SR 826/836 Interchange Bridge #11 in Miami, FL, and the LeRoy Selmon Crosstown Expressway in Tampa, FL. Both bridges were newly constructed post-tensioned concrete segmental bridges. The former bridge had no epoxy grout pourback problems while some pourback cracking was found on the latter bridge. Part of the reason for this is two-fold, first, the diurnal temperature variation is lower in Miami than in Tampa, and second, the size of the pourbacks on the SR 826/836 Interchange Bridge #11 was much smaller. Unlike the SR 826/836 Interchange Bridge #11, the dead-ends on the LeRoy Selmon Crosstown Expressway comprise multiple anchorage points that are spread throughout the entire depth of the bridge segment (Figure 3-1). To simplify the pourback construction, one large formwork encapsulating multiple anchorages was used. As a consequence, a few epoxy grout pourbacks experienced some cracking. Thus, only the finding of the LeRoy Selmon Crosstown Expressway is reported here.

Figure 3-1: Typical concrete dead-end segment. Notice the multiple anchorage points spread throughout the entire segment cross-section.

3.2 Pourbacks Description

Three different large pourbacks' geometry were used on the LeRoy Selmon Crosstown Expressway as shown in Figure 3-2. These pourbacks were 4 to 6 in thick and were irregular shapes depending on the pattern of the anchorages on the dead-end segment. One common feature between the shapes was the volume-to-surface ratio with an average value of 0.31 as illustrated in Figure 3-3.
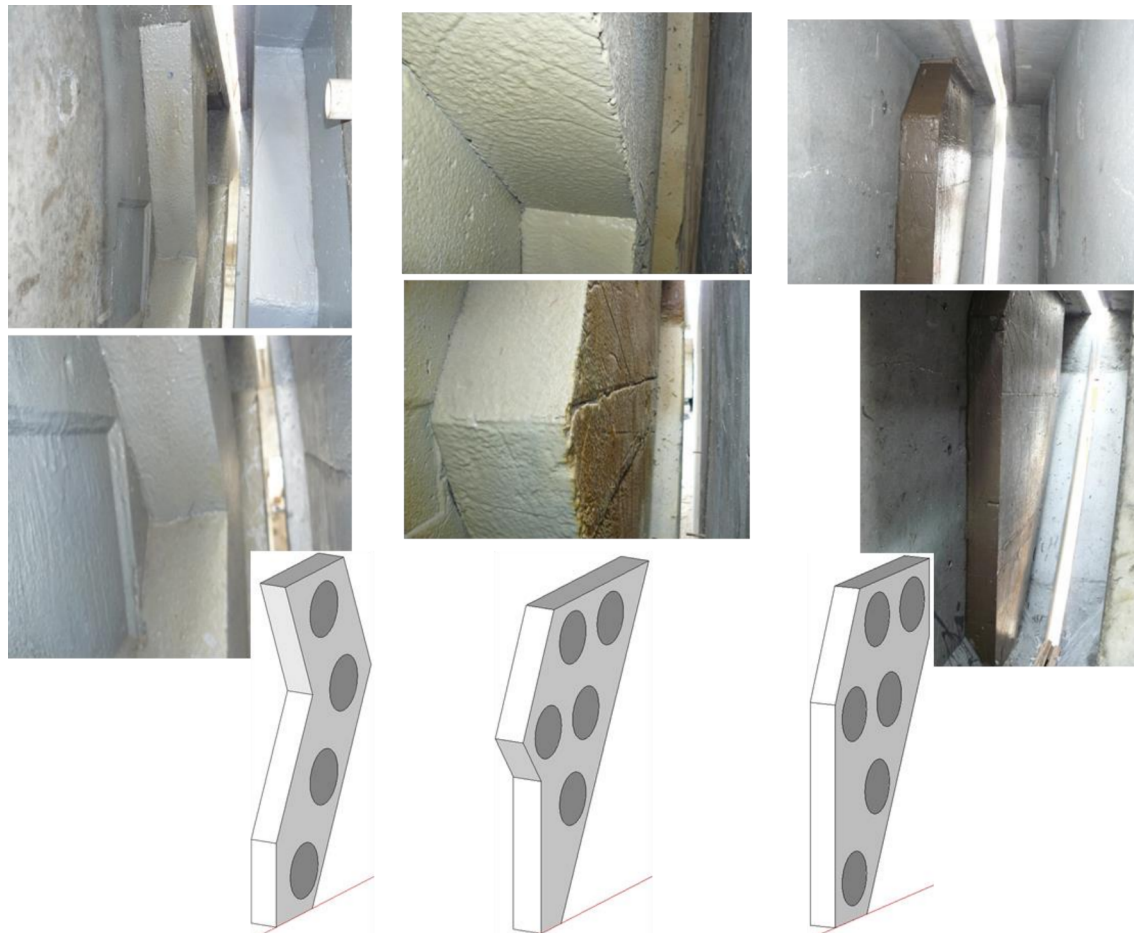
Figure 3-2: Pourbacks geometry on the LeRoy Selmon Crosstown Expressway

3.3 Findings

Overall, only pattern 3 (P3 in Figure 3-3) experienced cracking and spalling. The cracking seemed to be initiated from the sharp corner but some cracks were also found at other locations as shown in Figure 3-4. Figure 3-5 illustrates a summary of the field observation and proposed solutions for preventing epoxy pourbacks cracking.
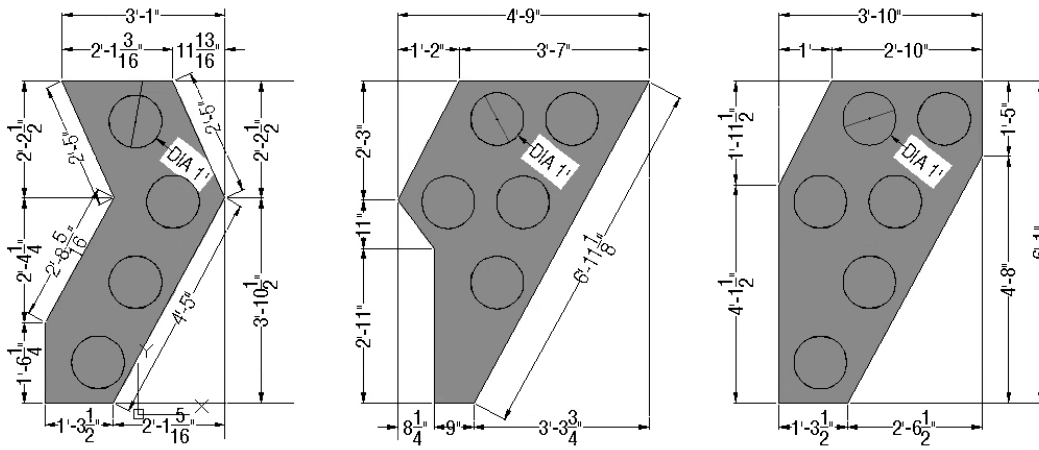
Figure 3-3: Volume-to-surface ratio and dimension of pourbacks

(a)

(b)

Figure 3-4: Typical location of cracks

Field Observation
- Cracks across the entire width
- Extended across the widest and/or narrowest regions of the pourback
- Range in size and location
- Appear to originate near the corners of the mass

Manufacturer Concerns
- Sharp corners
- Large size

Manufacturer Proposed Solution
- Soften corner of the form
- Reduce large size of the mass

- Reduce the exotherm experienced while curing by individual anchor protection
- Less amount of material
- Increase formwork
- More Labor

Figure 3-5: Summary of field inspection of epoxy grout pourbacks.

CHAPTER 4 – RESEARCH METHODOLOGY

4.1 Introduction

Several researchers studied the cement exothermal hydration reaction of early age concrete, but not the epoxy grout which is the subject of this research. Normally, temperature measurement by embedded temperature sensors is used, followed by validation with finite element model. Similar methodology was used in this investigation. For temperature measurement, two techniques were used in this research: embedded temperature sensors and infrared thermography as a non-destructive technique.

At the time this research project was conducted, there were five epoxy grouts listed on the FDOT Qualified Products List, namely:

(1) E3HP Epoxy Grout,
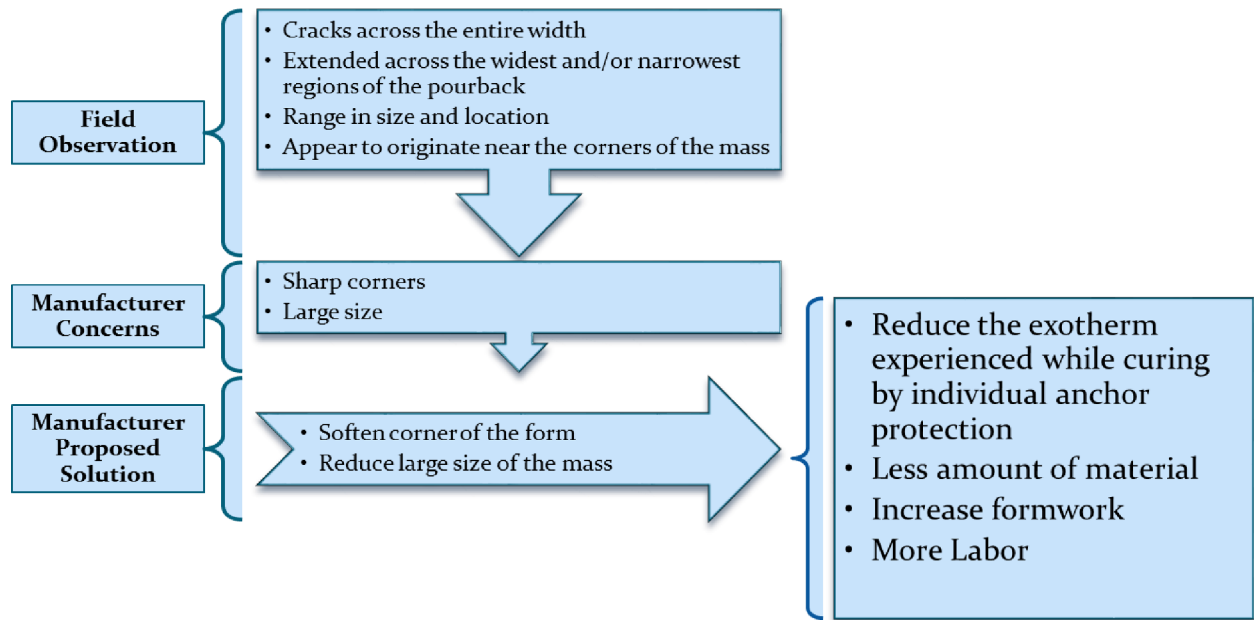
(2) Sikadur 42 Grout Pak PT,

(3) Masterflow 648 CP Plus,

(4) Magmaflow Grout-Pak,

(5) E-Bond 420 Grout System,

(Please note that, The QPL list is now the *Approved Product List*" (FDOT 2015) since the end of 2014. There are now six products on the APL for Epoxy Compounds Type Q. E3-DP by Euclid Chemical is now also on the list.)

All these products do not have the same physical properties but they do meet or exceed FDOT (2014) *926-14 specifications*. It is possible that one product will perform best in a certain environment while the other performs best in a different environment.

(Please note, spec. 926-14 is not listed in the current FDOT Specifications (January 2016). It was listed in the 2014 Specifications as Type Q epoxies. It is now listed in the January 2016 Specifications under 926-9 (Specific Requirements for Type Q Compounds)).

A preliminary laboratory and numerical investigation was conducted on three of these products, E3HP Epoxy Grout, Masterflow 648 CP Plus, and E-Bond 420 Grout System. Cube specimens made from E3HP Epoxy Grout and E-Bond Grout System were tested in FIU Structural Laboratory to evaluate the time-temperature behavior. The third product, Masterflow 648 CP Plus, was studied numerically using finite element model. The objective of the preliminary experiments was to investigate the thermal behavior of selected epoxy grouts and to determine of the accuracy and robustness of the instrumentations and the data acquisition system to be used

later in the full-scale experiments and subsequent FEM analysis. The results of this preliminary investigation are provided in Appendix A.

Although there are several methods to model the early age behavior of concrete, no research has been done for these epoxy grouts. Therefore, due to the lack of data on the thermal and mechanical properties of these epoxy grouts such as thermal conductivity, specific heat, Poisson's ratio, density, modulus of elasticity, and tensile stress at early age, the laboratory or in situ verification of numerical predictions is quite difficult. Although necessary physical and mechanical properties are provided in the manufacturer's product data sheet, two properties, namely the compressive strength and the peak exothermic temperature, were determined in the laboratory for verification purposes.

4.2 Compressive Strength Testing

This task involves the evaluation of compressive strength of the epoxy grouts on the 420 epoxy grout (E-Bond) in accordance with ASTM C-579 using method B at 55˚F, 75˚F, and 110˚F. At each temperature, three 2 in. cube specimens were tested at 8 hours, 16 hours, 24 hours, 3 days, 7 days, 14 days, and 28 days. Figure 4-1 illustrates the casting and testing of epoxy specimens.
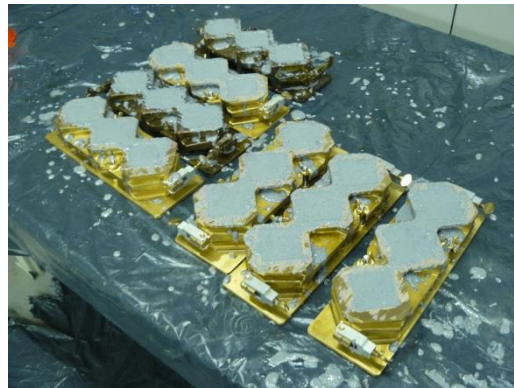
(a)
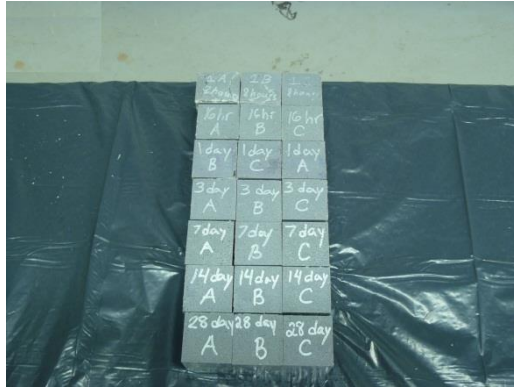
(b)

(c)

Figure 4-1: Sample preparation and testing

4.3 Laboratory Peak Exothermic Temperature

The Peak Exothermic Temperature of the epoxy grout was measured in the laboratory following ASTM D 2471 specifications. Epoxy specimens were prepared at four different volume to surface (V/S) ratios of 1, 0.45, 0.3, and 0.1875 (in inch) with corresponding dimensions of 12 × 12 × 3 inches (standard), 4.5 × 4.5 × 1.5 inches, 3 × 3 × 1 inches, and 3 × 3 × 0.5 inches, respectively. Specimen setup and data acquisition procedure are shown in Figure 4-2**.**
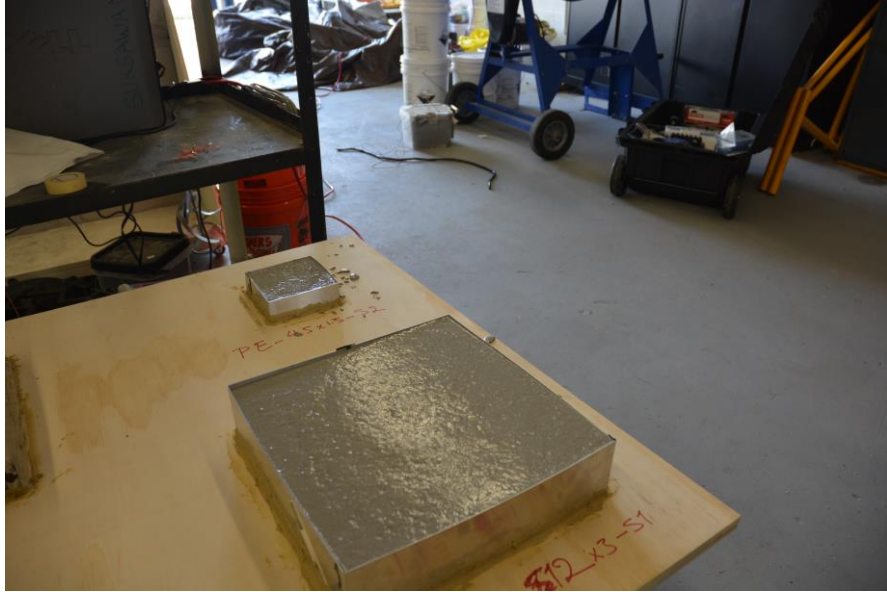
(a)
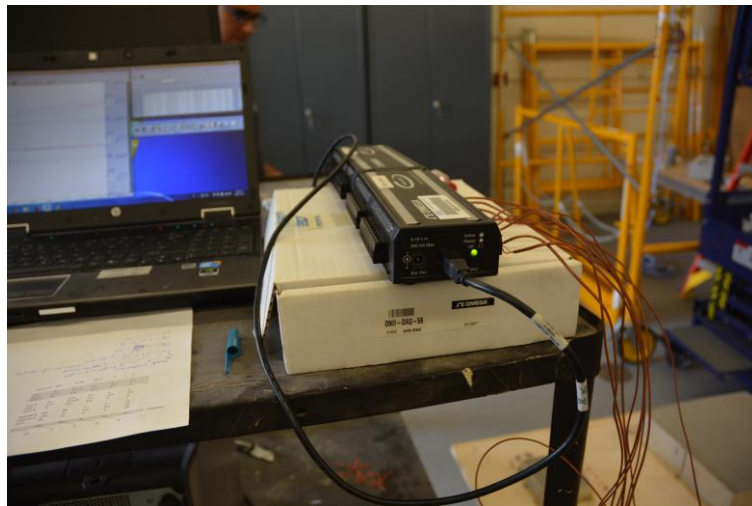
(b)

Figure 4-2: Peak exothermic test setup in the laboratory

4.4 Testing of Full-Scale Epoxy Pourback Specimens

4.4.1 Pourback Specimens

The full-scale epoxy grout testing consisted of two sets of epoxy pourbacks: 1) irregular shaped pourbacks (S-type) as illustrated in Figure 4-3; and 2) rectangular shaped pourbacks (R-type) as illustrated in Figures 4-4. For each set, three different volume-to-surface (V/S) ratios were

investigated: 0.26, 0.32. and 0.37 (expressed in ft.). These V/S ratios were based on actual pourback size commonly found in the field. The pourback specimens were cast against reinforced concrete wall.   E-Bond epoxy grout system specifies, "Grout depth of 1 in. (25 mm) minimum required and maximum of 6 in (152 mm). If multiple pours are needed apply additional layer while the proceeding lift is still tacky." Researchers followed the specifications as stated. Actual grout caps were also used to simulate field condition. The grout caps were filled with grout prior to mounting them to the reinforced concrete wall.
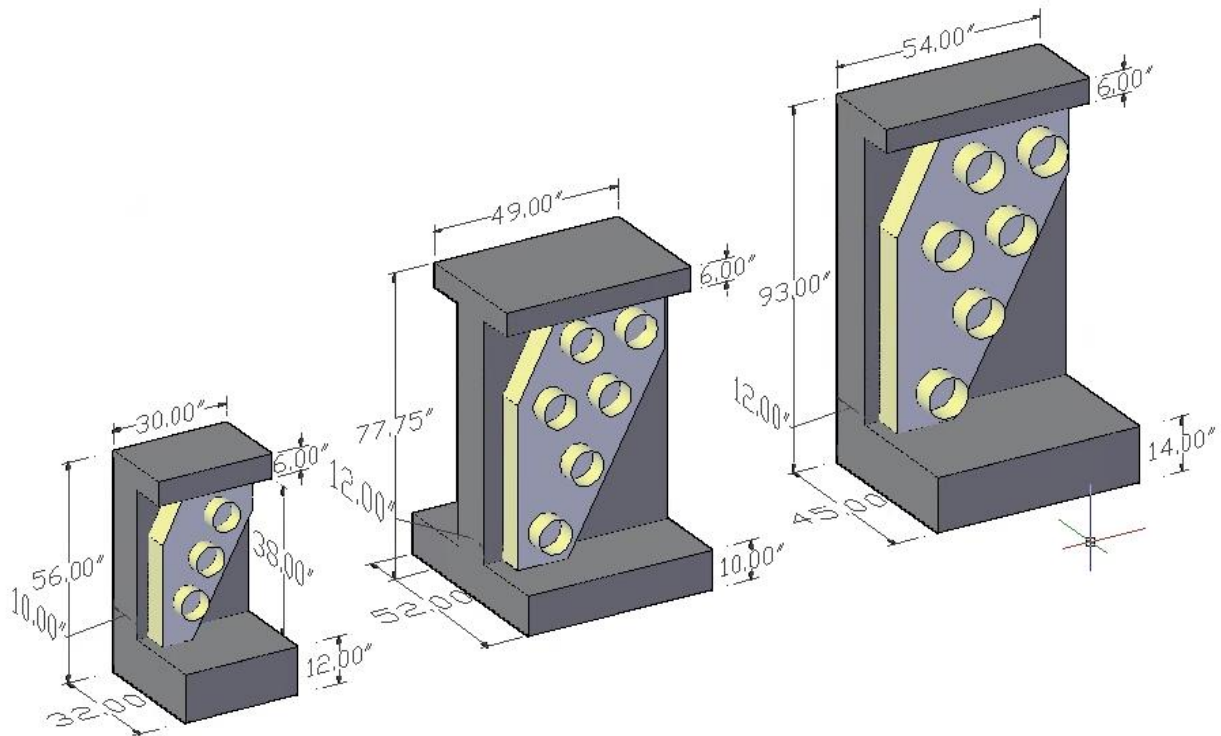
(a)

	S2	S2.5	S3
Number of grout caps	3	6	6
Ambient temperature (F)	68	68	68
Volume/surface ratio	0.26	0.32	0.37
Construction method	Full Depth		
Reinforcement	Non		
Concrete temperature	Ambient: 68° F		
Initial temperature of epoxy	Ambient: 68° F (Store epoxy in laboratory for 48 hours at 68° F before casting)		
Concrete surface	Hydro blast		

(b)

(c)

Figure 4-3: Complex geometric shapes and properties (S-type)
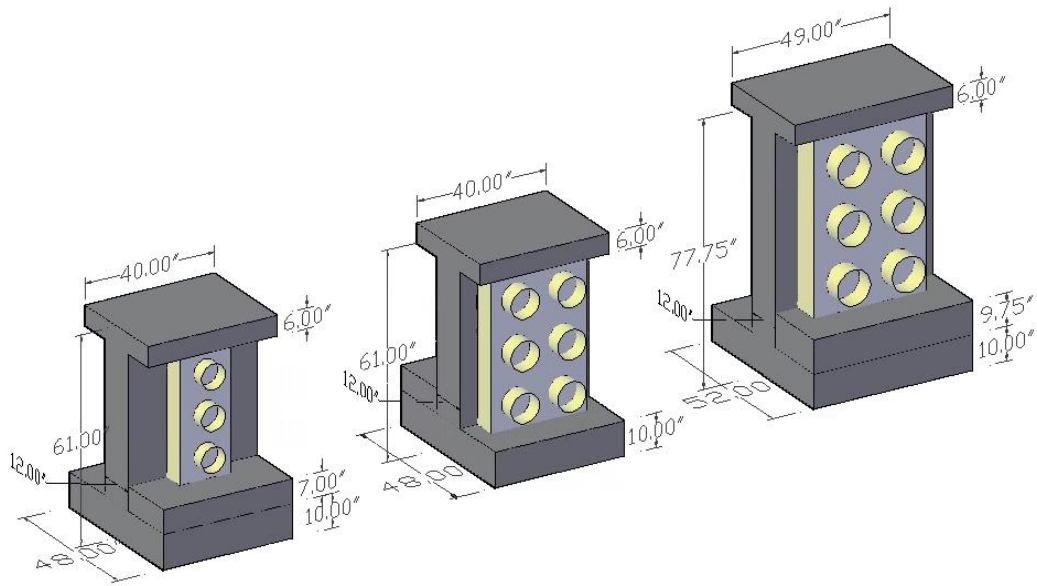
(a)

	R2	R2.5	R3
Number of grout caps	3	6	6
Ambient temperature (F)	68	68	68
Volume/surface ratio	0.26	0.32	0.37
Construction method	Full Depth		
Reinforcement	Non		
Concrete temperature	Ambient: 68° F		
Initial temperature of epoxy	Ambient: 68° F (Store epoxy in laboratory for 48 hours at 68° F before casting)		
Concrete surface	Hydro blast		

(b)

(c)

Figure 4-4: Regular geometric shapes and properties (R-type)

4.4.2 *Instrumentation*

The pourback specimens were instrumented using 12 thermocouples and a vibrating wire strain gauge for each specimen as shown in Figure 4-5. These gauges were designed to monitor the temperature gradients in the pourback specimens and the strain at the center of the pourback specimens.

Two separate data collection systems were used to accommodate all 78 sensors. The data were collected every 10 minutes intervals for a period of 48 hours after casting.
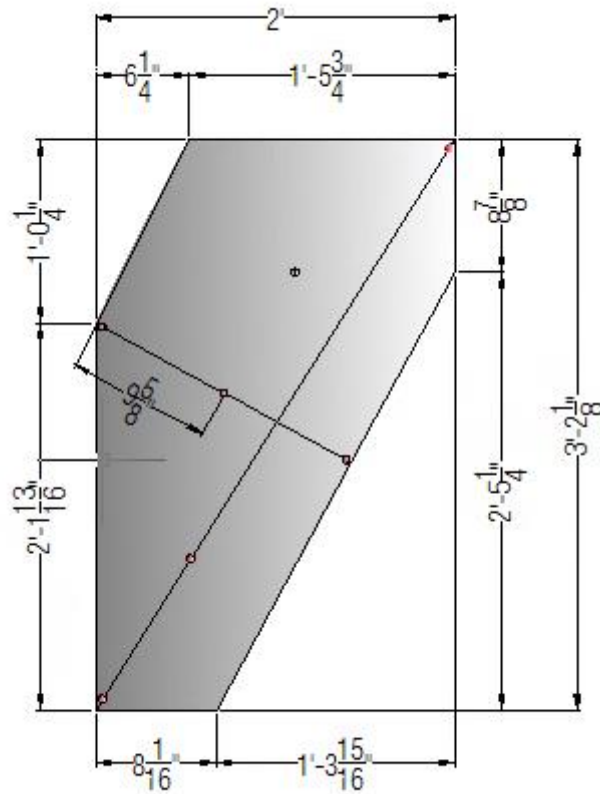
(a)
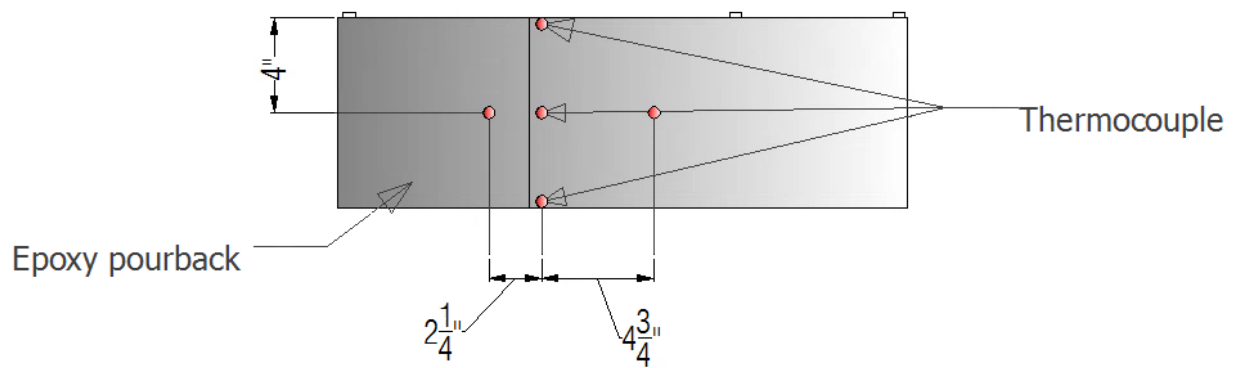
(b)

Figure 4-5: Instrumentation plan

4.4.3 *Casting Epoxy Grout*

Wooded forms with plastic lining were used to mold the pourback. The forms were made such that a 12 in gap was left open to allow pouring of the epoxy grout. The grout was mixed in a 5 gallons bucket in accordance with the manufacturer specification using a hand mixer. After the epoxy grout was mixed, it was hand poured into the form. Once the epoxy grout reached the opening, the gap was sealed and the remaining portion was pour from a small opening from the top. Figure 4-6 illustrates the mixing and casting of the epoxy grout.

Figure 4-6: Mixing and casting of epoxy pourback

4.5 Finite Element Modeling with ANSYS

Finite element modeling is a crucial part of this research needed to perform a parametric study for better understanding the cracking mechanism of epoxy grout pourback system. Figure 4-7 shows the analysis procedure available in the ANSYS (Stolarski and Yoshimoto, 2011) finite element modeling for transient thermal and stress analysis. The three-dimensional element type SOLID70 3D was used for the transient thermal analysis. The SOLID70 element has a three-dimensional thermal conduction capability. The element has eight nodes with a single degree of freedom, temperature, at each node. The element is applicable to a three-dimensional, steady-state, or transient thermal analysis. The element can also compensate for mass transport heat flow from a constant velocity field. Similarly, the three dimensional element type SOLID185 3D was used for the stress analysis. The SOLID185 element has eight nodes with three degrees of freedom at each node: translations in the nodal x, y, and z directions. The element has plasticity, hyperelasticity, stress stiffening, creep, large deflection, and large strain capabilities. It also has mixed formulation capability for simulating deformations of nearly incompressible elastoplastic materials and fully incompressible hyperelastic materials.
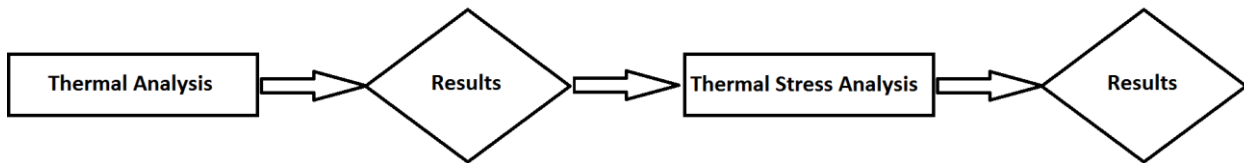

Figure 4-7: Analysis procedure

The process of stress analysis is similar to that for analyzing thermal distribution as a function of time. The mechanical properties of the epoxy grout, the analysis type, and the boundary conditions were changed. Thermal distributions were applied as time functions to constitute a body load on the concrete. Figure 4-8 presents a typical finite element modeling algorithm for transient thermal distribution and thermally induced stresses on the structural behavior.
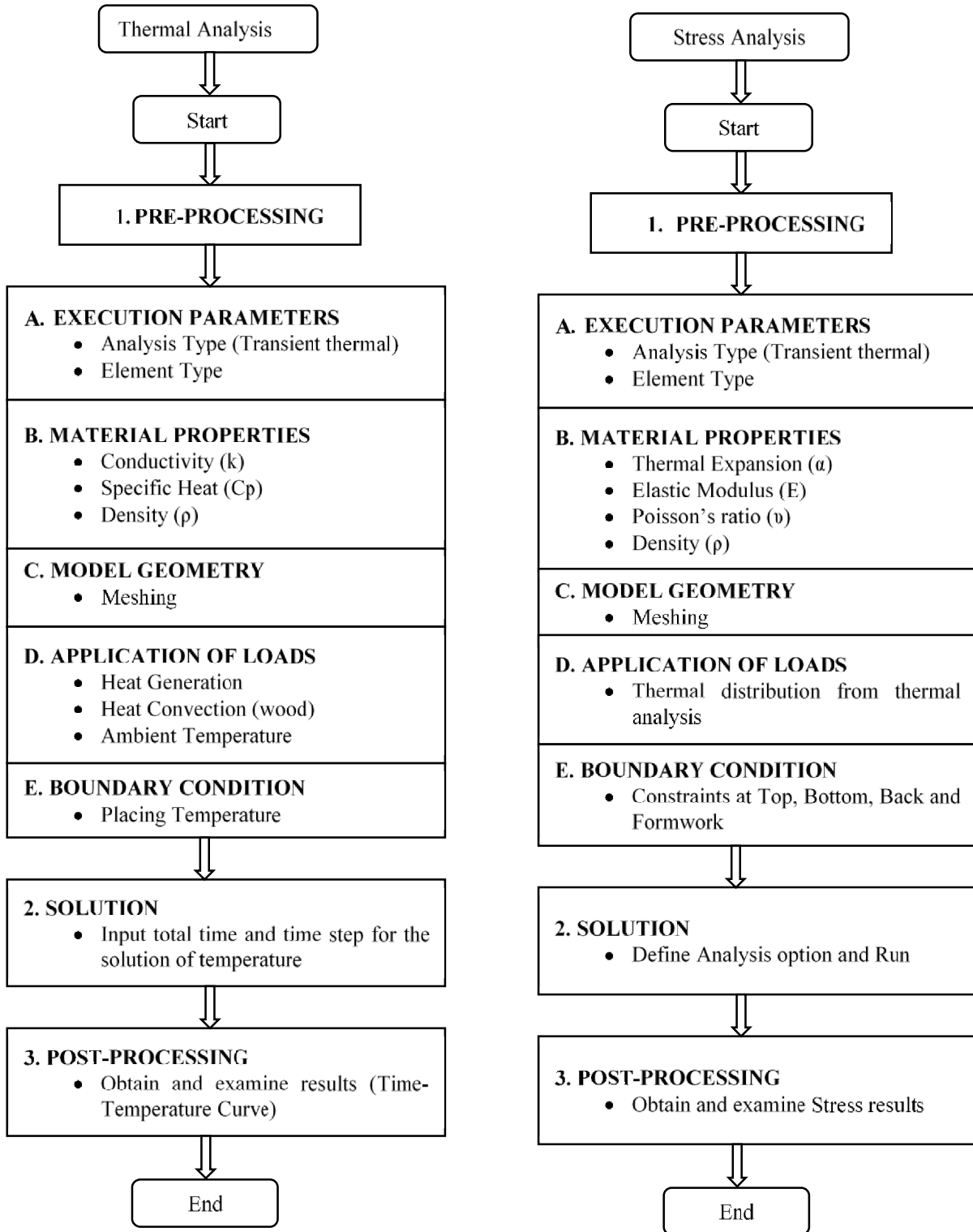
Thermal Analysis

Thermal Analysis

↓

Start

↓

1. PRE-PROCESSING

↓

A. EXECUTION PARAMETERS
- Analysis Type (Transient thermal)
- Element Type

B. MATERIAL PROPERTIES
- Conductivity (k)
- Specific Heat (Cp)
- Density (ρ)

C. MODEL GEOMETRY
- Meshing

D. APPLICATION OF LOADS
- Heat Generation
- Heat Convection (wood)
- Ambient Temperature

E. BOUNDARY CONDITION
- Placing Temperature

↓

2. SOLUTION
- Input total time and time step for the solution of temperature

↓

3. POST-PROCESSING
- Obtain and examine results (Time-Temperature Curve)

↓

End

Stress Analysis

Stress Analysis

↓

Start

↓

1. PRE-PROCESSING

↓

A. EXECUTION PARAMETERS
- Analysis Type (Transient thermal)
- Element Type

B. MATERIAL PROPERTIES
- Thermal Expansion (α)
- Elastic Modulus (E)
- Poisson's ratio (υ)
- Density (ρ)

C. MODEL GEOMETRY
- Meshing

D. APPLICATION OF LOADS
- Thermal distribution from thermal analysis

E. BOUNDARY CONDITION
- Constraints at Top, Bottom, Back and Formwork

↓

2. SOLUTION
- Define Analysis option and Run

↓

3. POST-PROCESSING
- Obtain and examine Stress results

↓

End

Figure 4-8: Process of thermal and stress analysis (after Kim, 2010)

Several material properties are needed for the thermal and stress analysis. For the thermal and stress analyses, the thermal conductivity, specific heat, coefficient of thermal expansion, modulus of elasticity, Poisson's Ratio, and the density of the material are needed. The thermal conductivity is defined as a uniform flow of heat through a unit thickness of material between two faces subjected to a unit temperature difference during a unit time. Specific heat is the amount of heat needed to change the temperature of 1g of material by 1°C. The coefficient of thermal expansion is defined as the change in volume per degree of temperature.

CHAPTER 5 – RESULTS

5.1 Compressive Strength

Figure 5-1 illustrates the compressive strengths of epoxy grout cubes that were tested at three different temperatures, 75°F, 110°F, and 55°F. Overall, there is very little temperature effect on the compressive strength at later age (28 days compressive strength). However, at early-age, particularly during the first 3 days, the specimens exposed to 110°F had a 24% strength reduction when compared to specimens at the temperature of 55°F and 75°F. There are very little differences between the specimens exposed to 55°F and 75°F. The 7-day compressive strength at room temperature (16.17 ksi) compares very well with the data (14.25 ksi) provided in the manufacturer's data sheet for this product (Figure 2-4b).
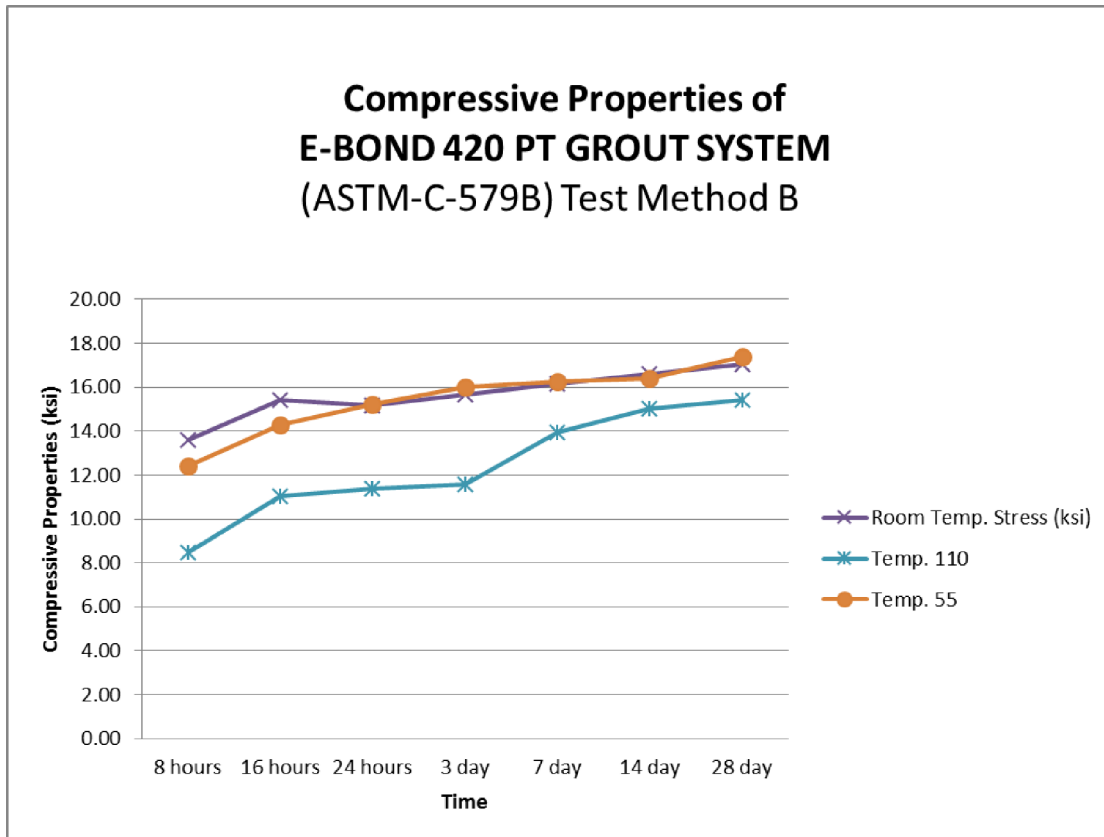
Figure 5-1: Compressive strength of epoxy grout specimens

5.2 Peak Exothermic Temperature Test

Peak Exothermic Temperatures of the E-Bond specimens determined in the laboratory according to ASTM D 2741 are shown in Table 5-1. It should be noted that the Peak Exothermic Temperature of the standard specimen (12 x 12 x 3 inch.) was found to be 103.67^0C, while the manufacturer's product data sheet (Figure 2-4b) reported the corresponding value as 60^0C. This difference may have implications in the thermal/shrinkage cracking behavior. In general, higher peak exothermic temperature is associated with higher thermal stresses and cracking potential. We recommend manufacturer-provided peak exothermic temperature data be verified.

Table 5-1: Variations of Peak Exothermic Temperature with V/S Ratios

						Peak exo temp Celsius		
length	width	height	volume	surface	v/s	Sample 1	Sample 2	Average
12	12	3	432	432	1	101.13	106.2	103.665
4.5	4.5	1.5	30.375	67.5	0.45	56.78	58.77	57.775
3	3	1	9	30	0.3	34.32	33.53	33.925
3	3	0.5	4.5	24	0.1875	32.75	32.82	32.785

Figure 5-2 shows the variations of the Peak Exothermic Temperature with the volume-to-surface (V/S) ratios. It is observed that the PET increases with increasing V/S ratios, which is consistent with the field behavior of full-scale specimens, described later.
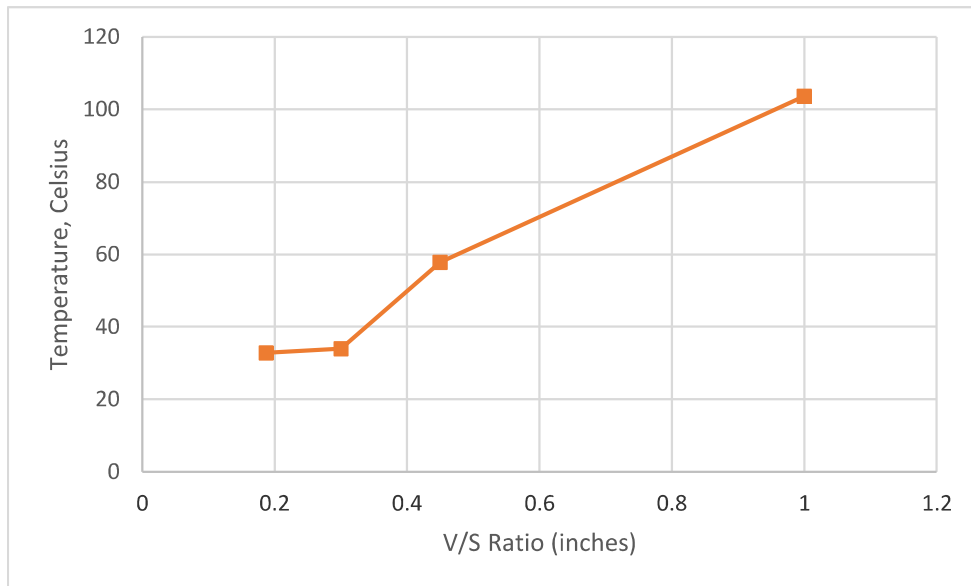

Figure 5-2: Variations in peak exothermic temperature with V/S

5.3 Behavior of Full-Scale Specimens

5.3.1 *Strain Data*

The strain data was obtained from the vibrating wire (VW) strain gauges. Figure 5-3 illustrates the strain in the middle of the specimens for all six full-scale specimens. Based on the product data sheet (Figure 2-4b) for E-Bond specimens, the cracking strain is approximately 2000×10^{-6}, as indicated by the dotted horizontal line in Figure 5-3. It is observed that the cracking in epoxy pourbacks begins at early-age approximately 20 hours (1200 minutes) after casting, particularly for specimens S2.5 and S3 (irregular shaped pourback with V/S ratios of 0.33 and 0.37, respectively). From the strain data, specifically for S3, the cracks observed on the specimens were not surface cracks but penetrated all the way through the epoxy pourbacks. Hence, it is highly recommended that any cracks found in the pourbacks should be injected and sealed as soon as possible to avoid chloride-laden water to leak through.
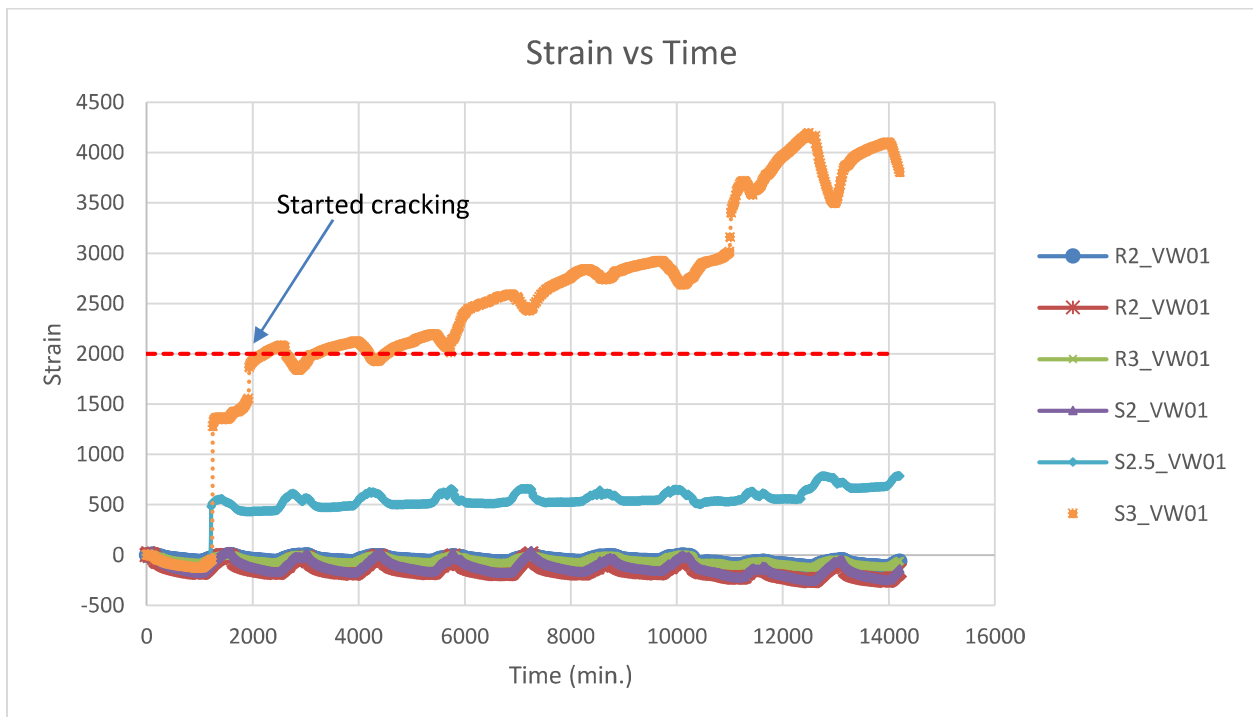
Figure 5-3: Vibrating wire strain versus time for full-scale specimens.

5.3.2 *Visual Inspection*

The specimens were visually inspected daily to confirm the strain data as well as to check other locations where the vibrating wire strain gauges were not installed. Three specimens, S2.5, S3, and R3, had cracks. The irregular shaped pourbacks had diagonal cracks in the center of the

31

specimen (see Figure 5-4) while the rectangular shaped pourback had a horizontal crack forming towards the top.

Figure 5-4: Cracks in pourback specimens

5.4 Finite Element Analysis of Full-Scale Specimens

5.3.1 Material Properties

Table 5-1 shows the essential material properties for the concrete slab and the E-Bond epoxy grout system that were used for the thermal and stress analysis. These included density, thermal conductivity, specific heat, co-efficient of thermal expansion, elastic modulus, and Poisson's ratio.

5.3.2 Analysis Procedure

The process flowchart used in the finite element analysis shown in Figure 5-5. For the calculation of thermal stresses in FEM, it was necessary to get the temperature of each node with respect to time as body forces. The time-temperature curves were developed and compared with the observed behavior of the full-scale specimens. The heat generation values were obtained through a trial and error procedure. Figure 5-6 shows typical temperature contour plots obtained from FEM thermal analysis.

5.3.3 Comparison of Time-Temperature Behavior

The time-temperature behavior measured in the full-scale specimens and calculated by FEM thermal analysis was compared for all thermocouple locations. In the full-scale experiments, a total of ten thermocouples were inserted at various locations of each specimen. The location of the sensors are provided in Figure 4-5. Time-temperature curves obtained after the final iteration in ANSYS at the sensor location TCO2 for R3 (V/S=0.37), and the corresponding experimental values are shown in Figure 5-7. It can be seen from the graphs that there is a good agreement between the ANSYS results and the experimental observation. The time-temperature graphs for all locations are provided in Appendix B.

Table 5-2: Material Properties Used in FEM Analysis of Full-Scale Specimens

Concrete Slab	Standard Test	Units	Value
Thermal conductivity		kJ/(m·h·°C)	2.3
Specific heat	ASTM E1269 -11	kJ/(kg·°C)	0.23
Heat-transfer film coefficient (air exposure)		kcal/(m^2·h·°C	4.3
Density		kg/m^3	2,400
Young Modulus	ASTM C580	MPa	30,000
Poisson's ratio		--	0.18
Thermal Expansion Coefficient	ASTM C531	m/m/°C	1.0×10^{-6}
420 Epoxy Grout System	**Standard Test**	**Units**	**Value**
Thermal conductivity		kJ/(m·h·°C)	2.3
Specific heat	ASTM E1269 -11	kJ/(kg·°C)	0.23
Heat-transfer film coefficient (wood forms)		kcal/(m^2·h·°C	8.5
Heat-transfer film coefficient (air exposure)		kcal/(m^2·h·°C	4.3
Density		kg/m^3	1,986
Young Modulus	ASTM C580	MPa	12,000
Poisson's ratio		--	0.4
Thermal Expansion Coefficient	ASTM C531	m/m/°C	5.4×10^{-6}
Plastic End Caps	**Standard Test**	**Units**	**Value**
Thermal conductivity		kJ/(m·h·°C)	0.68351
Specific heat	ASTM E1269 -11	kJ/(kg·°C)	1.05
Density		kg/m^3	1,400
Young Modulus	ASTM C580	MPa	3,000
Poisson's ratio		--	0.4
Thermal Expansion Coefficient	ASTM C531	m/m/°C	3.6×10^{-5}

```
        ┌─────────────────────┐                            ┌─────────────────────┐
        │  Thermal Analysis   │                            │   Stress Analysis   │
        └─────────────────────┘                            └─────────────────────┘
                  ║                                                   ║
                  ▼                                                   ▼
        ┌─────────────────────┐                            ┌─────────────────────┐
        │       Start         │                            │       Start         │
        └─────────────────────┘                            └─────────────────────┘
                  ║                                                   ║
                  ▼                                                   ▼
        ┌─────────────────────┐                            ┌─────────────────────┐
        │  1. PRE-PROCESSING  │                            │  1.  PRE-PROCESSING │
        └─────────────────────┘                            └─────────────────────┘
                  ║                                                   ║
                  ▼                                                   ▼
```

┌───────────────────────────────────┐   ┌───────────────────────────────────┐
│ **A. EXECUTION PARAMETERS**   │   │ **A. EXECUTION PARAMETERS**   │
│   • Analysis Type (Transient   │   │   • Analysis Type (Transient   │
│   thermal)   │   │   thermal)   │
│   • Element Type   │   │   • Element Type   │
├───────────────────────────────────┤   ├───────────────────────────────────┤
│ **B. MATERIAL PROPERTIES**   │   │ **B. MATERIAL PROPERTIES**   │
│   • Conductivity (k)   │   │   • Thermal Expansion (α)   │
│   • Specific Heat (Cp)   │   │   • Elastic Modulus (E)   │
│   • Density (ρ)   │   │   • Poisson's ratio (υ)   │
│   │   │   • Density (ρ)   │
├───────────────────────────────────┤   ├───────────────────────────────────┤
│ **C. MODEL GEOMETRY**   │   │ **C. MODEL GEOMETRY**   │
│   • Meshing   │   │   • Meshing   │
├───────────────────────────────────┤   ├───────────────────────────────────┤
│ **D. APPLICATION OF LOADS**   │   │ **D. APPLICATION OF LOADS**   │
│   • Heat Generation   │   │   • Thermal distribution from   │
│   • Heat Convection (wood)   │   │   thermal analysis   │
│   • Ambient Temperature   │   ├───────────────────────────────────┤
├───────────────────────────────────┤   │ **E. BOUNDARY CONDITION**   │
│ **E. BOUNDARY CONDITION**   │   │   • Constraints at Top, Bottom,   │
│   • Placing Temperature   │   │   Back and Formwork   │
└───────────────────────────────────┘   └───────────────────────────────────┘

┌───────────────────────────────────┐   ┌───────────────────────────────────┐
│ **2. SOLUTION**   │   │ **2. SOLUTION**   │
│   • Input total time and time   │   │   • Define Analysis option and Run│
│   step for the solution of   │   │   │
│   temperature   │   │   │
└───────────────────────────────────┘   └───────────────────────────────────┘

┌───────────────────────────────────┐   ┌───────────────────────────────────┐
│ **3. POST-PROCESSING**   │   │ **3. POST-PROCESSING**   │
│   • Obtain and examine results   │   │   • Obtain and examine Stress   │
│   (Time-Temperature Curve)   │   │   results   │
└───────────────────────────────────┘   └───────────────────────────────────┘

```
        ┌─────────────────────┐                            ┌─────────────────────┐
        │        End          │                            │        End          │
        └─────────────────────┘                            └─────────────────────┘
```

Figure 5-5: Process flowchart used in the FEM analysis (after Kim, 2010)
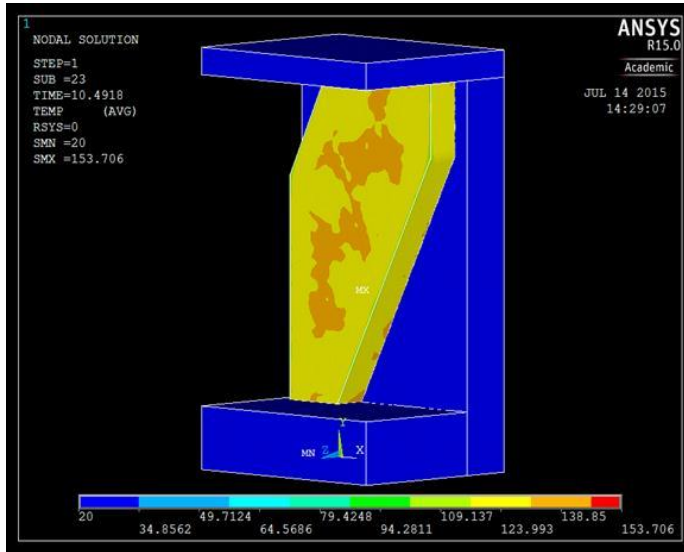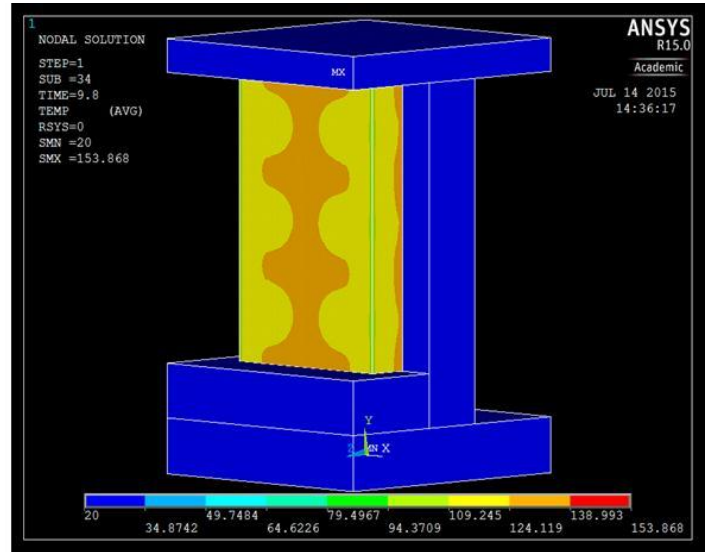
Pourback S3 (V/S=0.37)   Pourback R3 (V/S=0.37)

Figure 5-6: Temperature contour plots obtained by FEM thermal analysis.
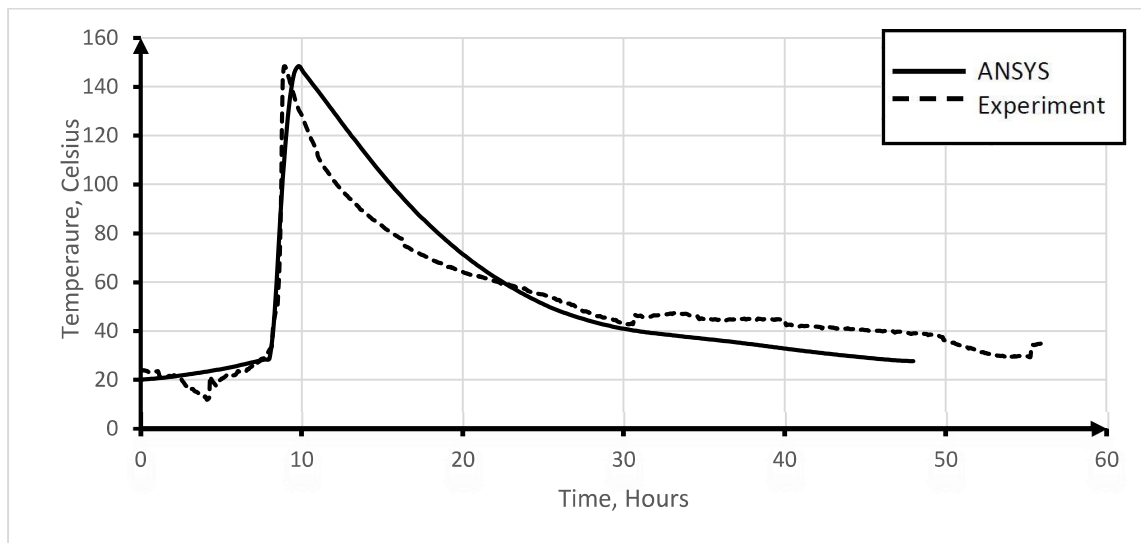
Figure 5-7: Comparison of time-temperature plots at sensor location TCO2 for the R3 Model.

5.3.4 Comparison of Maximum Temperature between FEM and Experimental Observation

Maximum temperatures reached for different V/S ratios are shown in Figure 5-8. The trends observed from the plot indicate that the rate of increase in maximum temperature stabilizes with increasing V/S ratios for the S-type specimens, illustrated by both FEM analysis and the experiments. The same cannot be concluded for the R-type specimens, in which the rate of increase in maximum temperature with V/S ratios is rather steep. As a whole, it can be said that maximum temperature increases as the V/S ratio increases. This trend is also in agreement with the results obtained in the laboratory test for peak exothermic temperature (Figure 5-2).
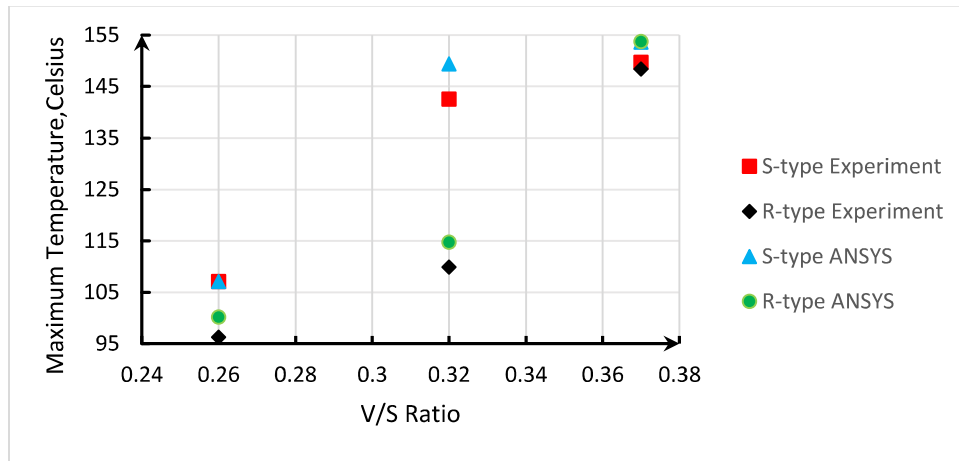
Figure 5-8: Variation in maximum temperature with V/S ratio (FEM and experiments)

5.3.5 Comparison of Crack Locations between FEM Analysis and Experimental Observations

Figure 5-9 shows the experimentally observed crack locations for the S3 specimen and the location of the tensile cracks determined by the maximum tensile stresses computed by FEM analysis utilizing the strength criteria provided in manufacturer's product data sheet (Figure 2-4). The maximum tensile strength of the E-Bond epoxy ranges between 24 to 28 MPa as reported in the product data sheet. Figure 5-9 indicates a remarkable agreement between the actual and predicted crack locations. This agreement is consistent with the crack locations observed in two other specimens, R3 and S2.5, shown in Figures 5-10 and 5-11, respectively.

36
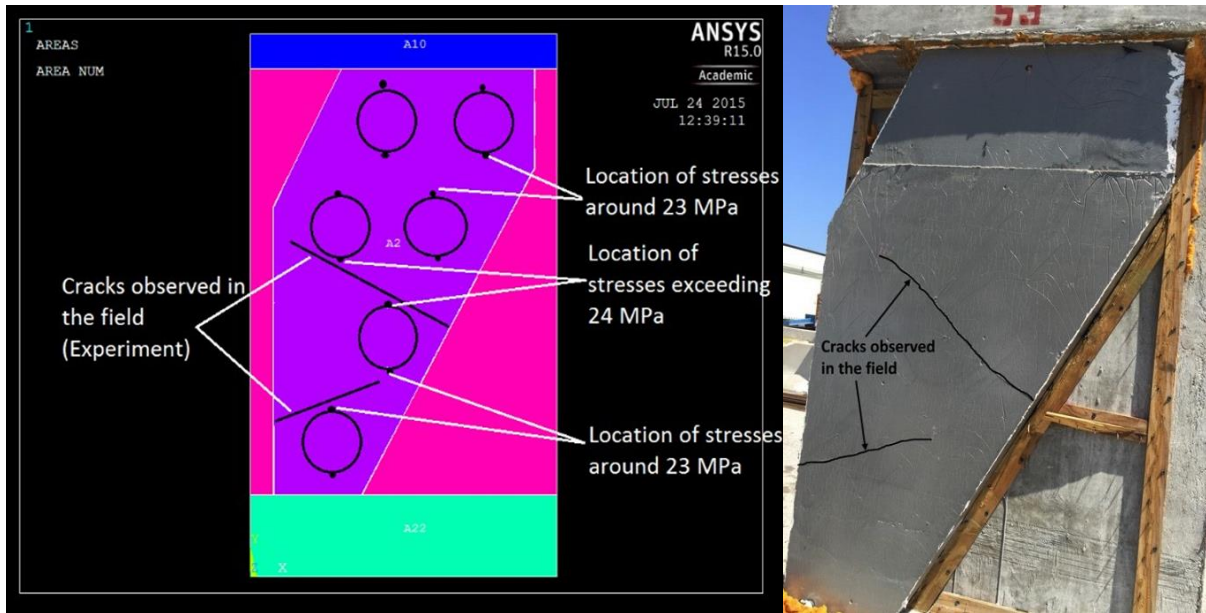
Figure 5-9: Comparison of crack locations between FEM and experimental observations for S3 specimen
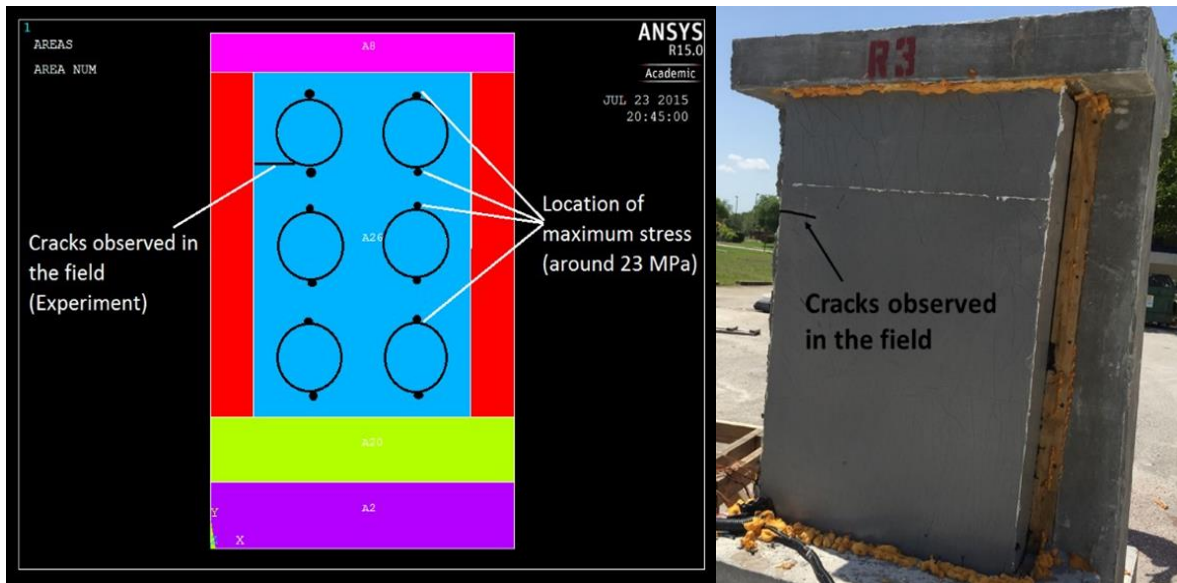
Figure 5-10: Comparison of crack locations between FEM and experimental observations for R3 specimen
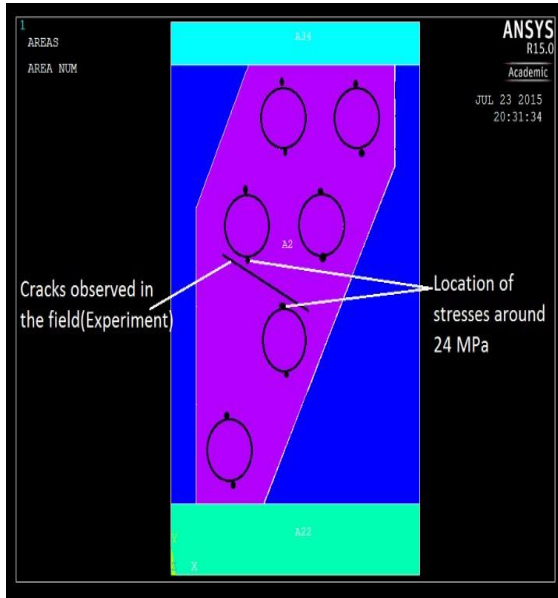
Figure 5-11: Comparison of crack locations between FEM and experimental observations for S2.5 specimen

5.3.6 Variation of Maximum Tensile Stress with V/S Ratios

Figure 5-12 shows the maximum tensile stresses computed by FEM analysis for all specimens and V/S ratios. The observed trends indicate that the rate of increase in maximum tensile stress stabilizes with increasing V/S ratios for the S-type specimens. The same cannot be concluded for the R-type specimens in which the rate of increase in maximum tensile stress with V/S ratios is rather steep. This pattern is similar to the variations in maximum temperature shown in Figure 5-8.

The dotted line in Figure 5-12 indicates the tensile strength (24 MPa) of the E-Bond epoxy reported in the manufacturer's product data sheet. A significant finding from this plot is that the S-type specimens reach cracking stress when V/S ratio exceeds 0.32 ft. For the R-type specimens, the cracking stress is reached at a higher V/S ratio of 0.37 ft.

38
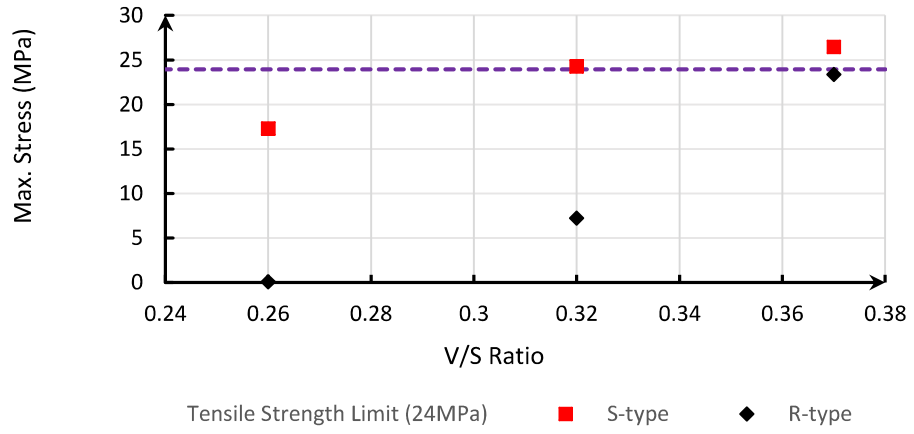
Figure 5-12: Variation in maximum tensile stress with V/S Ratio (FEM analysis)

CHAPTER 6 – CONCLUSIONS AND RECOMMENDATIONS

6.1 Findings

Epoxy grout pourbacks at end anchorages of post-tensioning tendons provide an essential level of corrosion protection. This is especially true when the anchorages are adjacent to expansion joints or other bridge deck discontinuities where water can flow freely to the tendon anchorage. Water may easily pass through the mastic coating and onto the post-tensioning anchorage. However, the current practice includes permanent anchorage caps providing another barrier. Within few years of installation, the tendon may fail as a result of strand corrosion in the anchorage. In order to mitigate this problem, this study was undertaken to develop guidance for eliminating thermal/shrinkage cracking in epoxy grout pourbacks at post-tensioned anchorages.

The following tasks were conducted as part of this investigation: (a) Literature search on the current use of epoxy grout pourbacks for anchorage corrosion protection in Florida bridges; (b) Inspection of Florida bridges with epoxy grout cracking; (c) Determination of selected physical properties of an FDOT approved (commonly used) epoxy grout from laboratory tests and Finite element thermal and stress analysis on the selected epoxy grout pourback material and validate with experimental results.manufacturer data; (d) Full scale testing on complex and regular geometric shapes; (e) Finite element thermal and stress analysis on the selected epoxy grout pourback material and validation with experimental results; and (f) Development of guidelines to minimize the probability of cracking.

Field investigation of epoxy grout pourbacks cracking was made at two bridge sites in Tampa and Miami. Based on a comprehensive literature review, manufacturer and contractor feedbacks, field investigation, and full-scale testing, potential factors affecting epoxy grout pourback were determined to be the pourback size, shapes (particularly shapes with obtuse corner), and ambient condition, and concrete substrates temperature.

The significant findings from the experimental and finite element analysis performed under this study are as follows:

- The time-temperature curves predicted by the ANSYS finite element model closely matched the data obtained from field experiments.
- Thermal stresses predicted by FEM around the vicinity of the actual physical crack observed in the field showed close agreement with the limiting tensile strength.
- The peak exothermic temperature as measured in the laboratory and in the full-scale specimens were found to be significantly higher than the data provided by the manufacturer's product data sheet.
- Both the peak exothermic temperature and the maximum thermal stress increased as V/S ratio increased.

- For the S-type, the maximum thermal stress reached or exceeded the tensile strength of 24 MPa at V/S ratio between 0.32 and 0.37. For the R-type, this limit was reached at V/S ratio of about 0.37.
- Cracking in the selected epoxy pourback begins at early-age approximately 20 hours (1200 minutes) after casting.

6.2 Recommendations

- Cracks observed on the specimens were not surface cracks but penetrated all the way through the epoxy pourbacks. Hence, it is highly recommended that any cracks found in the pourbacks should be injected and sealed with an FDOT approved epoxy sealant, as soon as possible to avoid chloride-laden water to leak through.
- Finite element analysis is a valid tool for predicting field behavior of epoxy grout pourback systems. It is recommended that parametric studies (V/S ratios under considerations and materials data) using FEM analysis be undertaken for developing design charts.
- Since higher peak exothermic temperature is associated with higher thermal stresses and cracking potential, it is recommended that the manufacture-provided peak exothermic temperature data should be verified.
- It is recommended that the maximum value of V/S ratio of the epoxy grout pourbacks be limited to 0.30 ft. for irregular (S-type) shape, and to 0.35 ft. for regular (R-type) shapes. FEM analysis can be undertaken when V/S ratio exceeds these limits.

6.3 Recommendations for Further Studies

- During the preliminary laboratory studies with epoxy cubes (Appendix A), it was observed that the temperature measurements by thermocouples and by nondestructive thermograhic methods agreed quite well. Further studies are needed to evaluate the potential of thermography used as a nondestructive inspection technique or a data acquisition system facilitating the field temperature monitoring of epoxy grout pourback systems.
- While it can be concluded that the early age cracking is caused by thermal stresses associated with peak exothermic temperatures, the later age and subsequent cracking is most likely caused by shrinkage and/or other factors. Further studies are needed to identify these factors and investigate their effects.
- In general, higher peak exothermic temperature is associated with higher thermal stresses and cracking potential. The relationship between the laboratory peak exothermic test and the field cracking potential and/or tensile stresses needs to be further investigated.
- Studies should be undertaken to investigate performance/behavior of epoxy when batched with a fiber. Presence of fiber may help hold cracks together if they start to develop. To attain similar results use of stainless steel reinforcement can also be investigated.

REFERENCES

FDOT Structures Manual (2010), Florida Department of Transportation, Volume 1 – 9, Topic No. 625-020-018, Tallahassee, Florida.

Standard Specifications for Road and Bridge Construction (2010), Tallahassee, Florida, Available: http://www.dot.state.fl.us/construction/2010master.pdf.

Corven Engineering, Inc. (2002), *New Directions for Florida Post-Tensioned Bridges,* Report prepared for Florida Department of Transportation, Volume 1 – 10, Tallahassee, Florida.

Hamilton, H.R., and Alvarez, G. A. (2002), *Post-Tensioning Grout Bleed, Duct, and Anchorage Protection Test,* Final Report submitted to FDOT, Contract No. BC-354 RPWO #73, p. 54.

American Society for Testing Materials (ASTM), ASTM Headquarters, 100 Barr Harbor Drive, PO Box C700, West Conshohocken, PA 19428-2959, USA
http://www.astm.org/

Stolarski, T., Nakasone, Y., Yoshimoto, S. (2011), Engineering Analysis with ANSYS Software. Elsevier, Burlington, MA.

Kim, S. G. (2010), *Effect of heat generaAStion from cement hydration on mass concrete placement*, MS Thesis, Iowa State University, Ames, Iowa.

FDOT Bulletin 15-03 at http://www.dot.state.fl.us/structures/Bulletins/2015/SDB15-03.pdf.

Florida Department of Transportation (FDOT) (2015), *Approved Product List*, https://fdotwp1.dot.state.fl.us/ApprovedProductList/ProductTypes/Index/45.

Florida Department of Transportation (FDOT) (2016), *Design Standards*, (post-tensioning anchorage protection, FDOT 2016 Design Standards Index No. 21802 at http://www.dot.state.fl.us/rddesign/DS/16/IDx/21802.pdf).

Florida Department of Transportation (FDOT) (2014), *926-14 specifications.* http://www.dot.state.fl.us/specificationsoffice/Implemented/SpecBooks/2013/Files/926-2013.pdf

APPENDIX A: PRELIMINARY EVALUATION OF THERMAL BEHAVIOR

A.1 Laboratory Evaluation of Thermal Behavior

This task involved preliminary testing and evaluation of a 12 in. epoxy cube for developing full-scale field testing and measurement protocols and finite element model calibration. The main aim of this laboratory experiment is to use a cube of epoxy grout for continuously monitoring the temperature right after casting. Tests were conducted in the FIU structural lab. Ambient temperature was in the range of 71-73^0 F. The relative humidity was about 40%. The specimen temperature was monitored for a period of 22 hours.

A.1.1 Formwork

A cubic formwork with dimensions 1x1x1 ft was designed using 9/16 in. thick plywood built with five sides, four panels for walls and one panel for bottom surface. The form was placed on a metal stand (Figure A-1).

Figure A-1: Formwork for E3HP epoxy grout system

A.1.2 Embedded temperature sensors

A total of 9 sensors were embedded within the cube specimen, including 8 thermocouples and one vibrating wire strain gauge. Thermocouples were type K manufactured by Omega, and model 4200 vibrating wire stain gage was manufactured by Geokon. The Geokon Model 4200 Vibrating Wire Strain Gage is designed primarily for long-term strain measurement in mass concrete, in structures such as foundation, piles, bridges, dams, containment vessels, tunnel liners, etc. (Figure A-2). These Strain Gages are designed for direct embedment in concrete. The 4200 (standard model) has a 6 in. (152 mm) gage length and 1 µɛ sensitivity. These sensors are capable of measuring the temperature in the range of −20°C to +80°C as well.
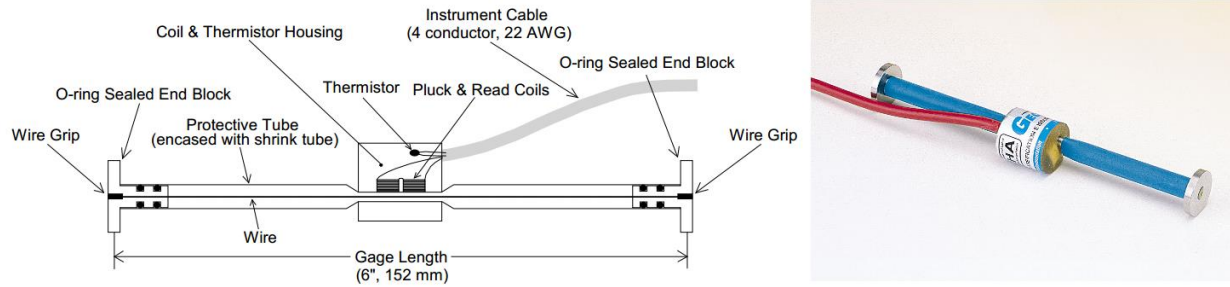
Figure A-2: Geokon Model 4200 vibrating wire strain gage

Thermocouples were labeled as TC1 to TC8. Six thermocouple sensors, TC1 to TC6, were embedded in the neighborhood of the surface shot by the thermography Camera 1, Figure A-3.

Figure A-3: Six thermocouple sensors were embedded in the neighborhood of the surface shot by the thermography Camera 1

One thermocouple, TC8, was inserted in the center of the cube and another one, TC7, 3 in. deep from top surface and 3 in. from two other lateral surfaces. Figure A-4 shows the overall view of sensor arrangements. The exact location of the sensors is depicted in Figure A-5. The thermocouples were supported by thermally insulated wire, which in turn were attached to the formwork. The vibrating wire strain gage was used in the core of the cube to measure the strain and temperature. The idea of having TC8 at the center was to compare the result from thermocouple with vibrating wire strain gage.
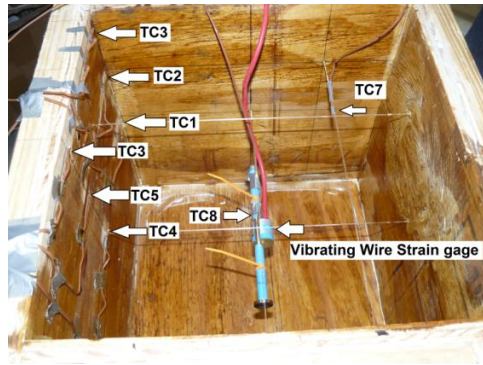
Figure A-4: The overall view of sensor arrangement
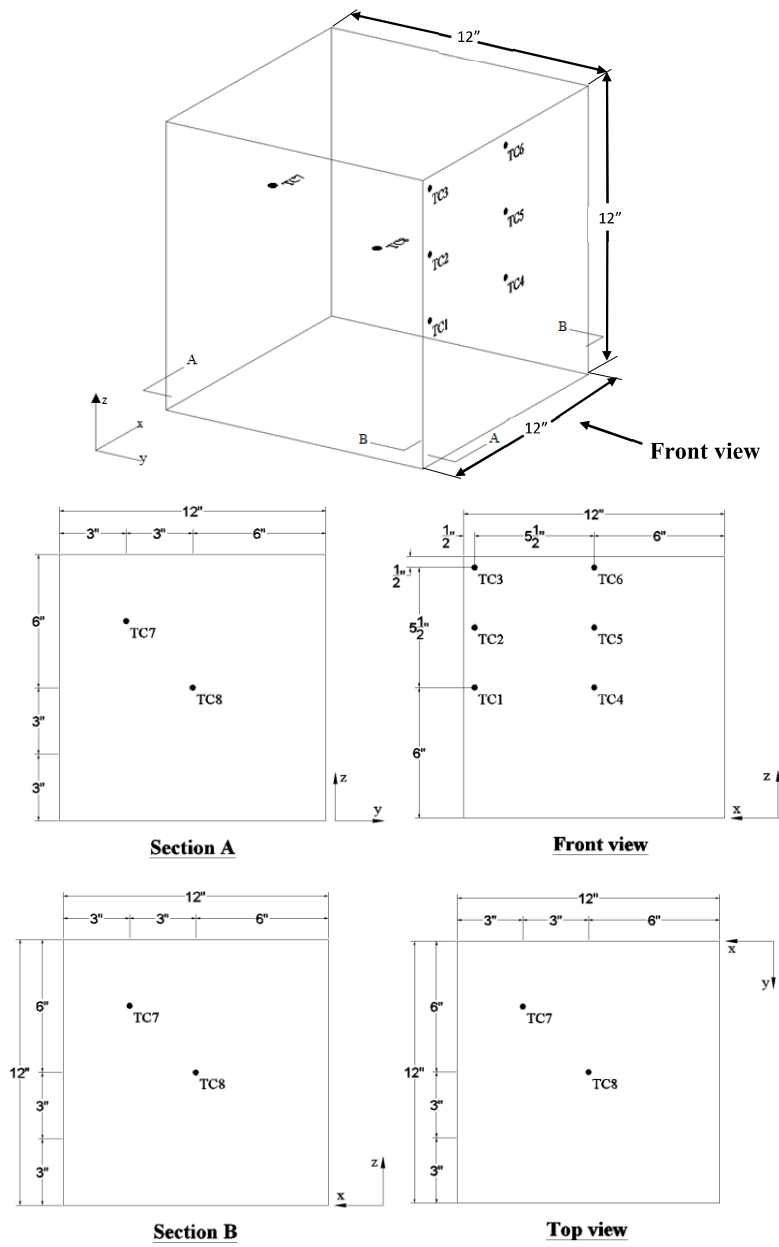
Figure A-5: Sensor arrangement

A.1.3 Data Acquisition System

All the sensors were connected to an automatic data acquisition system called CR1000 which has a capacity to measure 8 thermocouples at a time, and two vibrating wire strain gages by adding an interface called AVW200 (Figure A-6). AVW200 enables CR1000 to get measurements from an AVW200 Vibrating Wire Spectrum Analyzer.
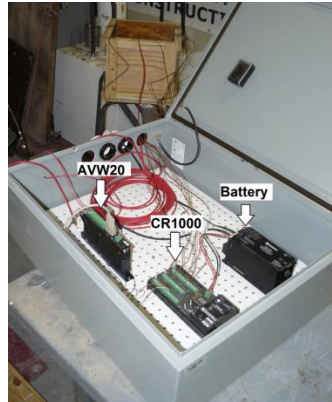
Figure A-6: CR1000automatic data acquisition system

CR1000 was set to record the sensors every 5 minutes. The test was initiated right after casting and continued until all sensors reached ambient temperature. This period took 22 hours.

A.1.4 Mixing material

The epoxy used for this experiment was E3HP from the Euclid Chemical Company. E3HP is a three part epoxy grout system which consists of a Part A (resin), Part B (hardener) and Part C (aggregate). After mixing and placing, the color is similar to that of concrete though the grout may always appear somewhat darker than the surrounding concrete. Table A-1 shows the mix proportion of E3-HP epoxy grout system.

Table A-1: Mix Proportion of E3HP Epoxy Grout

Resin Part A	2.54 gal
Hardener Part B	0.64 gal
Aggregate Filler Part C	180 lb

Before mixing, all E3HP materials, the three parts, were stored at the laboratory for 3 days, in order to bring the materials temperature close to ambient temperature. Parts A & B (resin & hardener) were mixed for 2 minutes using a drill and mixing prop (Figure A-7). For ease of mixing, the part B was added to the part A. The epoxy must be well mixed to ensure proper

chemical reaction. After the epoxy has been mixed, the part C (aggregate) was added and mixed for 5 minutes until the aggregate was completely wetted out (Figure A-8).

Figure A-7: Parts A & B (resin & hardener) mixed for 2 minutes using a drill and mixing prop

Figure A-8: The part C (aggregate) added and mixed for 5 minutes until the aggregate was completely wetted out

A.1.5 Placement

According to the manufacturer, epoxy grout should be placed at a minimum of 1" (25 mm) thickness and a maximum of 6" (152 mm) thickness per lift when placed in a large mass. In this experiment, the epoxy grout was placed in one lift (Figure A-9). Cold temperatures will significantly reduce flow characteristics and will increase the difficulty of placing, whereas higher temperatures will increase initial flow but cut down on working time. E3-HP requires no special curing procedures.

Figure A-9: The E3-HP epoxy grout was placed in one lift

A.1.6 Formwork removal

Formwork removal was started at the time of 130 min with surface 2 and finished at 165 min with surface 4. Although inside the wooden form was fully coated with oil, at the time of formwork removal, it was bonded to the specimen (Figure A-10). Thus it took about 35 minutes to remove the 4 lateral formwork panels, resulting in five surfaces in contact with the ambient environment. (Figure A-11).

Figure A-10: Formwork removal

Figure A-11: Five surfaces of specimen in contact with the ambient environment

A.1.7 Thermography

Two FLIR B400 infrared cameras with a 320 x 240 pixel infrared image resolution were used in this experiment, having an accuracy of ±3.6 F or ±2% of reading and an object temperature range of -4 F to +248 F. The overall view of the position of the cameras and specimen are shown in Figure A-12.
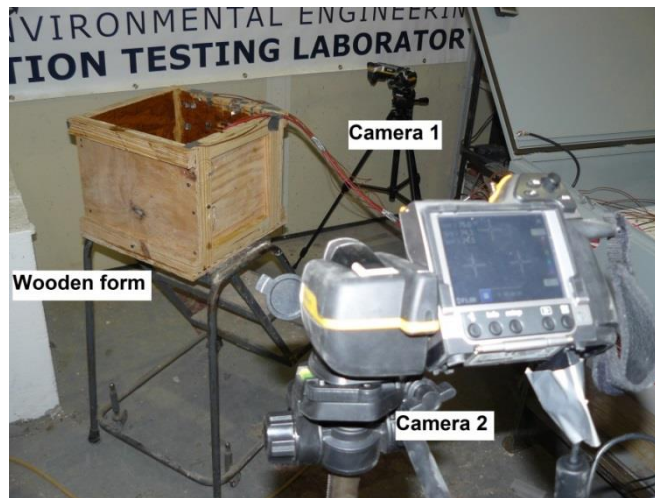
Figure A-12: The overall view of the position of the cameras and form

The first camera (Camera 1) was placed in front of side 4, where the thermocouples was inserted, at the level of mid-height of the specimen, in a direction which was perpendicular to the specimen surface (see Figure A-13). This camera was able to monitor all the thermocouples on 6 surfaces.

The second camera (Camera 2) was placed at a distance of 43 in. from the specimen, and 12 in. above its top surface (Figure A-14), in order to allow the simultaneous visibility of three surface of the cube (Figure A-15).The observation angles were α =22.7 deg. for the top surface and α =50 deg. for the vertical surfaces. The reason for using the second camera was to monitor the top surface temperature, and also the center of two other surfaces, in order to compare the results obtained with camera 1 for detecting any error associated with the observation angle. The differences are described later.

Figure A-13: Position of Camera 1 and specimen

Figure A-14: The second camera (Camera 2)

Figure A-15: Camera 2 simultaneously monitored three surface of the specimen

A.1.8 Setup of Thermal cameras

The epoxy grout emissivity value was obtained through the calibration of the thermography image to match the corresponding temperature resulting from temperature sensors. This value was assumed constant throughout the entire experiment, with the value of 0.90, which lies within the usual range considered for concrete. The cameras were set to monitor the temperature from 67 F, almost ambient temperature, to 220 F, somewhat higher than expected surface temperature. The camera has the capability to set up to 5 spotmeters (Figure A-16).

Figure A-16: Three spot-meters set for Camera 2 (left), and five spot-meters for Camera 1 (right)

A.2 Thermal Behavior of Laboratory Specimen (E3-HP)

This section describes the laboratory evaluation of the thermal behavior of the laboratory cube specimen. As described before in section A.1, Camera 2 was used to compare the results with Camera 1 in order to see the effect of angle view. Spot 1 on surface 1, Spot 2 on surface 2 and Spot 4 on surface 4 showed almost identical temperature, which was different for Spot 3 on top surface of the cube. Figure A-17 represents some thermography images for E3-HP epoxy grout system monitored by both cameras side by side. Spot 1 and Spot 2 in Camera 2 and Spot 4 in Camera 1 were set to measure the center temperature of lateral surfaces. Because of symmetry and boundary conditions, these three spots were expected to present an identical temperature. In other words, Spot 1 and Spot 2 measured by camera 2 are relevant with Spot 4 from camera 1. Figure A-18 shows a similar comparison of the T–t (Temperature-time) evolutions obtained through thermocouple measurement and thermography for the center location of three lateral surfaces. In this case, both cameras and thermocouple TC4 yield similar results. Consequently, errors associated with the observation angle are not relevant.
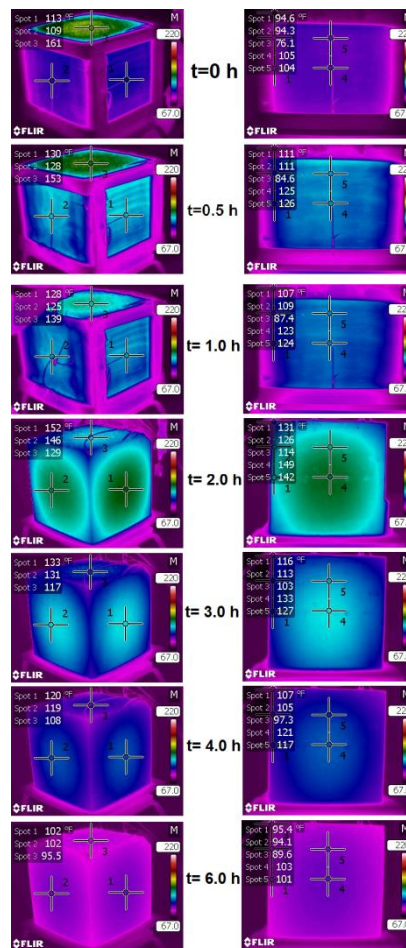
Figure A- 17: Some of thermography images for E3-HP epoxy grout system, camera 2 (left), camera 1 (right)
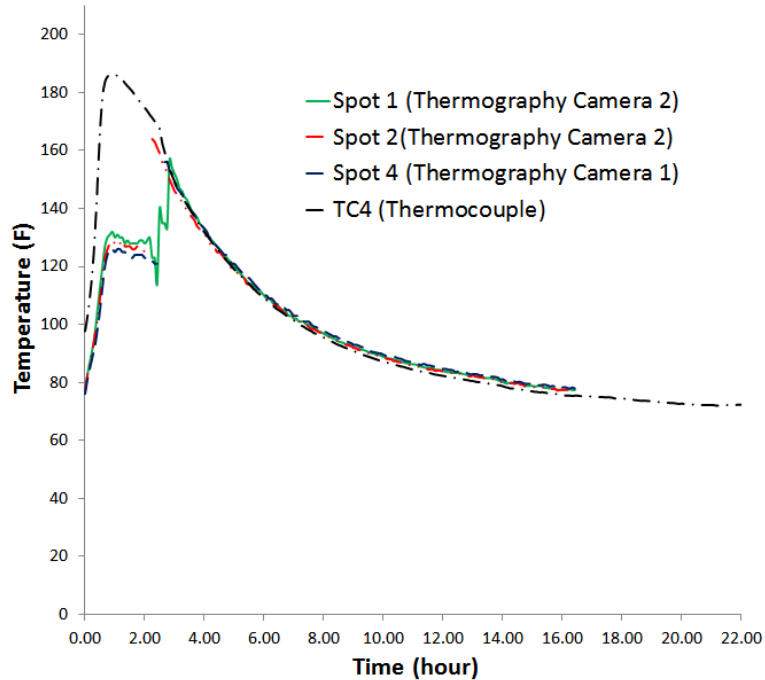
Figure A- 18: Temperature measurement from Camera 1, Camera 2 and thermocouples for the center of lateral surfaces

The results obtained from thermography and sensors are depicted in Figure A-19 to Figure A-20. Some general comments can be made at this point. The reported initial temperature of epoxy grout at 95 F can be confirmed at all sensors. The maximum recorded temperature occurred at the age of 65 minute reaching 205.2 F at the center of the specimen (sensor TC8), which corresponds to a temperature rise of 110.2 F with respect to the starting temperature of 95 F. The maximum recorded temperature gradient occurred between sensors TC8 (in the core) and TC3 (near the upper corner of the specimen), with a value of 65.9 F at the age of 1.75 h (Figure A-19). Furthermore, the expected tendency of higher temperatures in areas near the core versus lower temperatures near the surfaces was confirmed, and it took about 22 hours for all the sensors to return to the environmental room temperature of 72 F. From the results plotted in Figure A-20 to Figure A-25, a discontinuity in the slope of temperature diagrams for sensors near the lateral surfaces was observed at the age of 130-165 hours, coinciding with the instant at which the lateral wooden formwork panels were removed, causing a sudden increase in the boundary transfers, as expected.
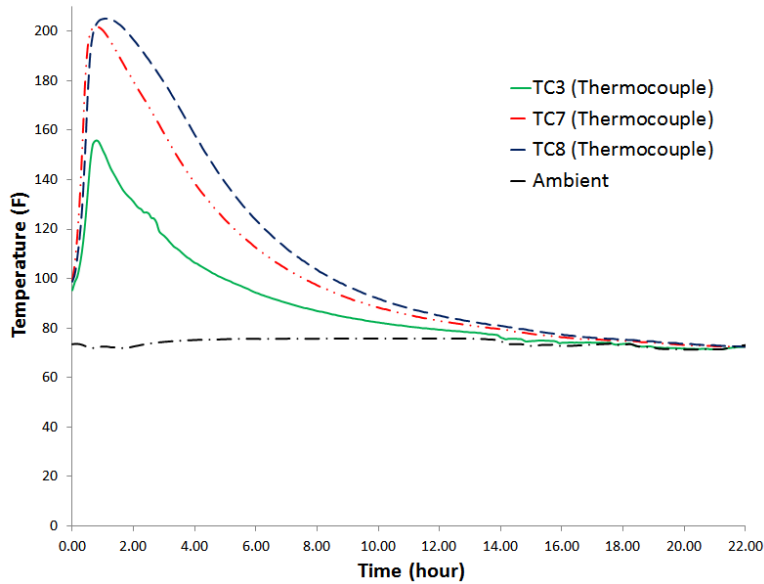
Figure A-19: The most three critical thermocouples

In view of the capacity of post-processing the images from thermography to obtain the time evolution of temperature at any specific pixel, comparisons can be made between the embedded thermocouple results and the corresponding monitored temperatures with thermography (based on the nearest pixel of the image).

Such a comparison is made in Figure A-23 for sensor TC4, located 6 in. deep with respect to the center of a vertical surface of the cube. Comments about this figure are divided in two phases, with the first pertaining to the period before removal of the vertical formwork panels (i.e., until the age of t = 165 minutes), and the second phase regarding the period that follows. During the first phase, while sensor TC4 is really monitoring the temperature in epoxy grout, the camera is measuring the temperature on the formwork surface, which explains the quite different evolution of the T-t curve provided by thermography with respect to the one defined by sensor TC4. Conversely, during the second phase (after formwork removal), the thermography camera measures a pixel temperature at almost the same location as sensor TC4 (Spot 4), with both T-t curves becoming practically coincident.
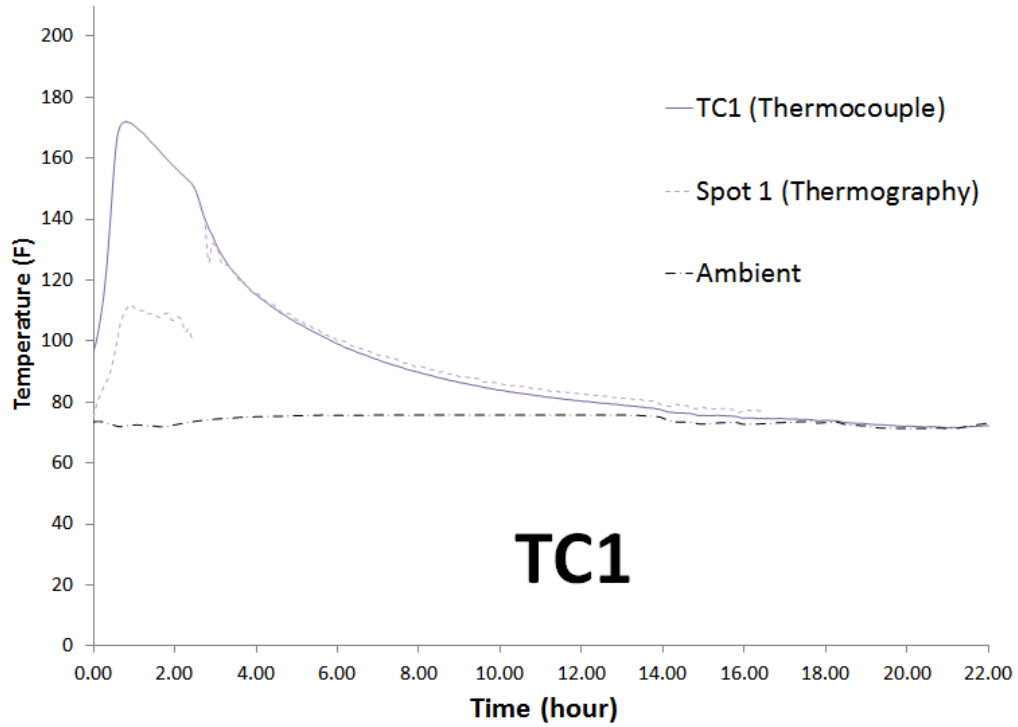
Figure A- 20: Monitored temperature by sensors and thermography
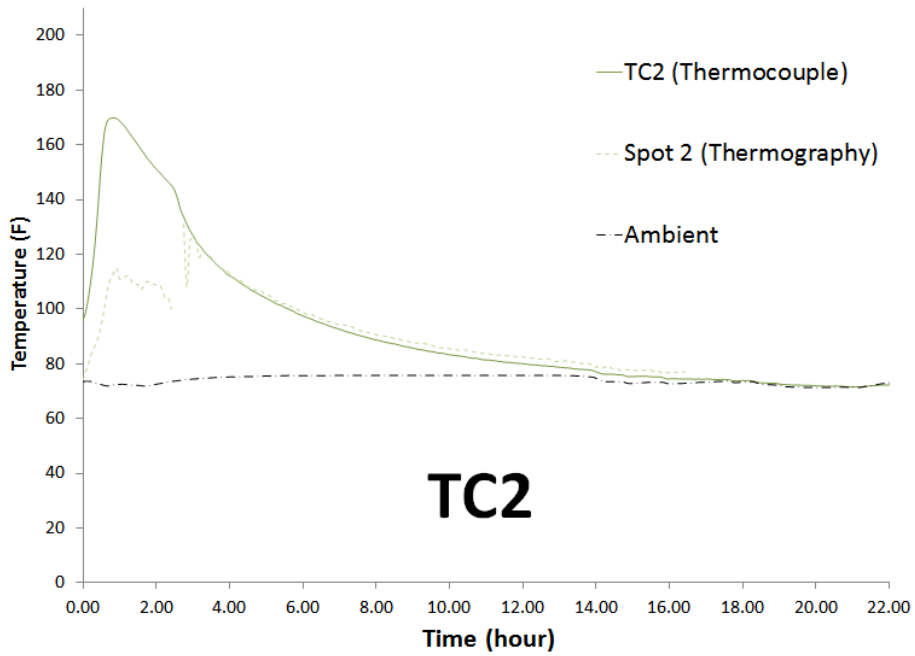
Figure A- 21: Monitored temperature by sensors and thermography
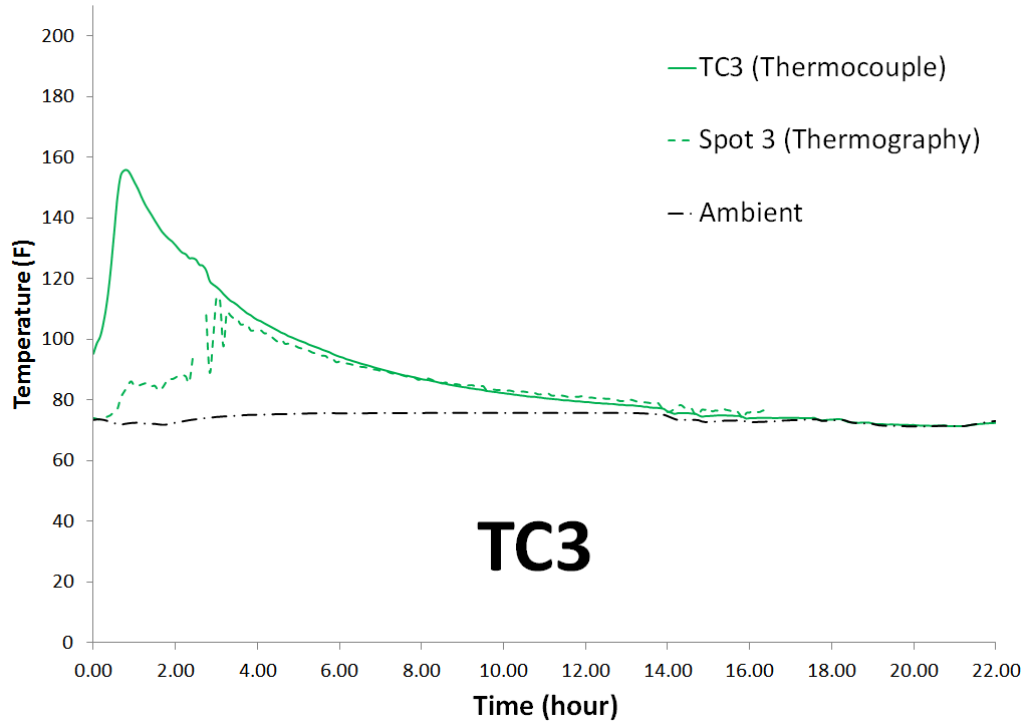
Figure A-22: Monitored temperature by sensors and thermography
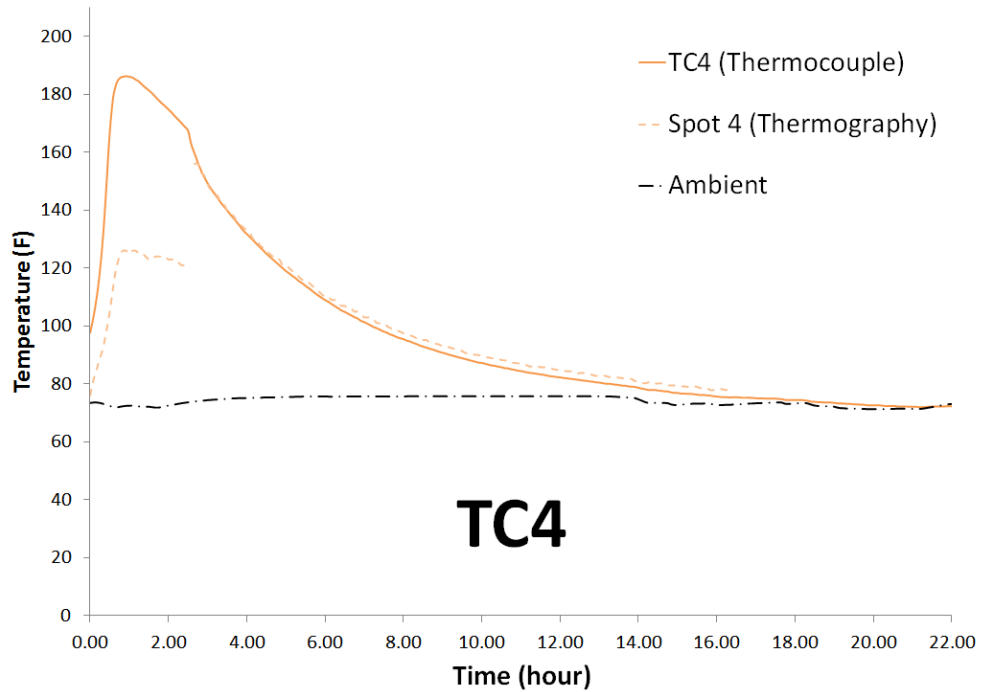
Figure A-23: Monitored temperature by sensors and thermography
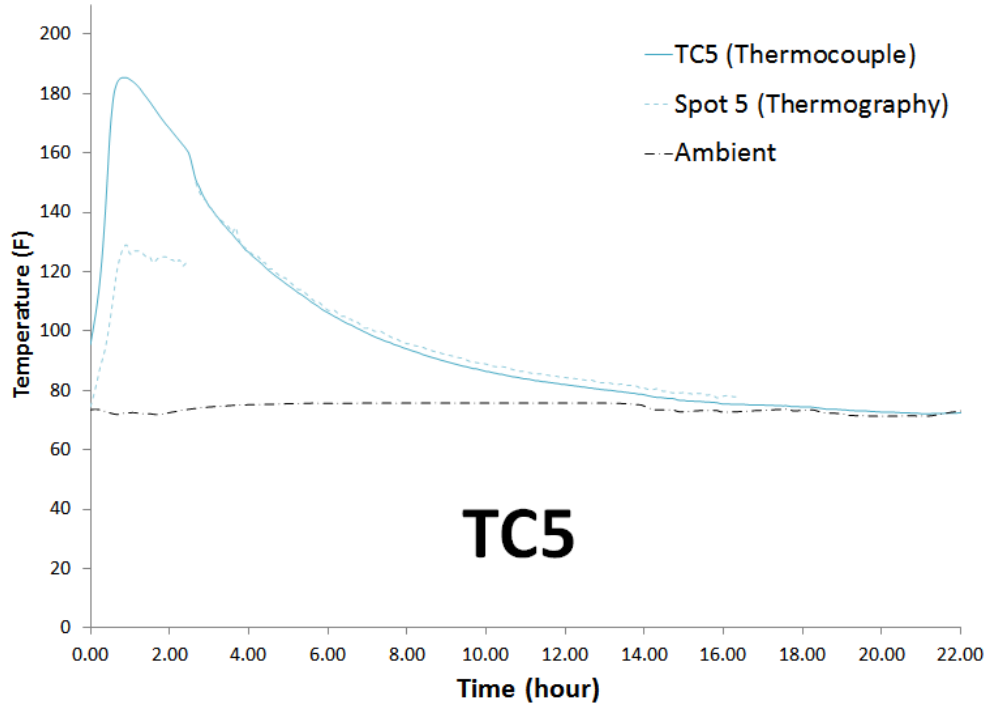
Figure A-24: Monitored temperature by sensors and thermography
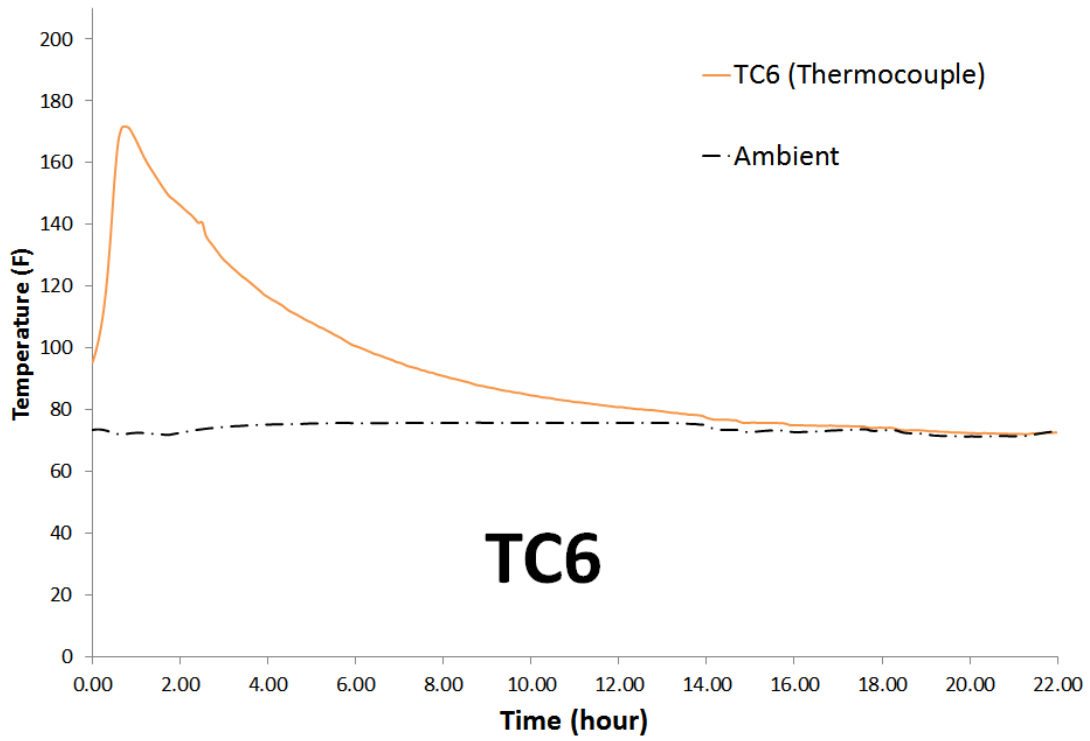
Figure A-25: Monitored temperature by sensors

Figure A-26 demonstrates that both thermocouple and vibrating wire strain gage measured temperatures. Vibrating wire strain gage perfectly matched with thermocouple at center of the specimen.
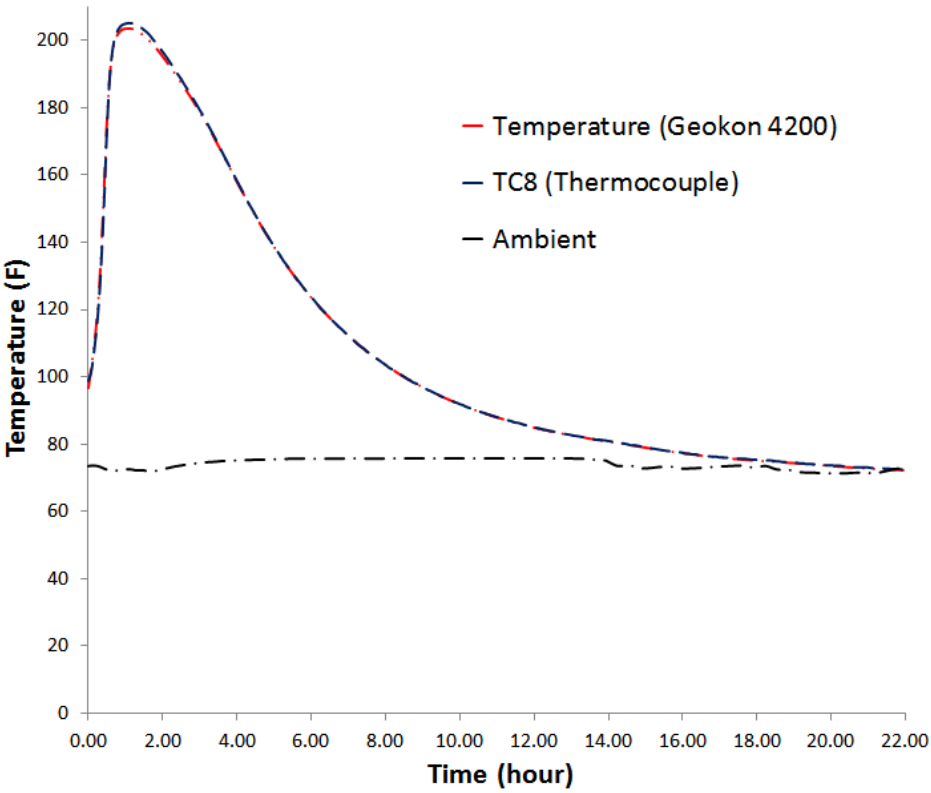
Figure A-26: The temperature measurement with thermocouple TC8 and Geokon vibrating wire strain gage at the center of the specimen

Thermocouples TC6 and TC1 showed almost identical temperature during the test because of symmetry, as expected. From the start to peak exotherm of 171.7 F and 171.9 F at times of 45 min and 50 min, respectively, both are showing identical trends (Figure A-27). Thereafter, TC1 showed higher temperature than TC6 until some time after the formwork removal, followed by identical temperature history.
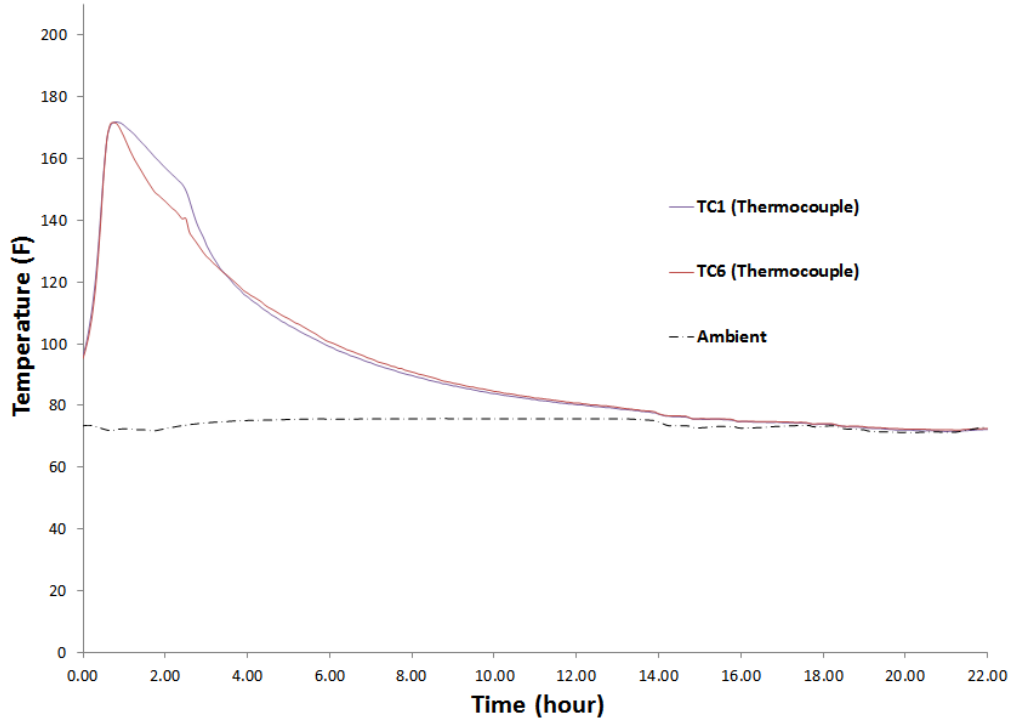
Figure A-27: Recorder temperature by TC1 and TC6

The strain in the center of the specimen measured by vibrating wire stain gage is presented in Figure A-28.
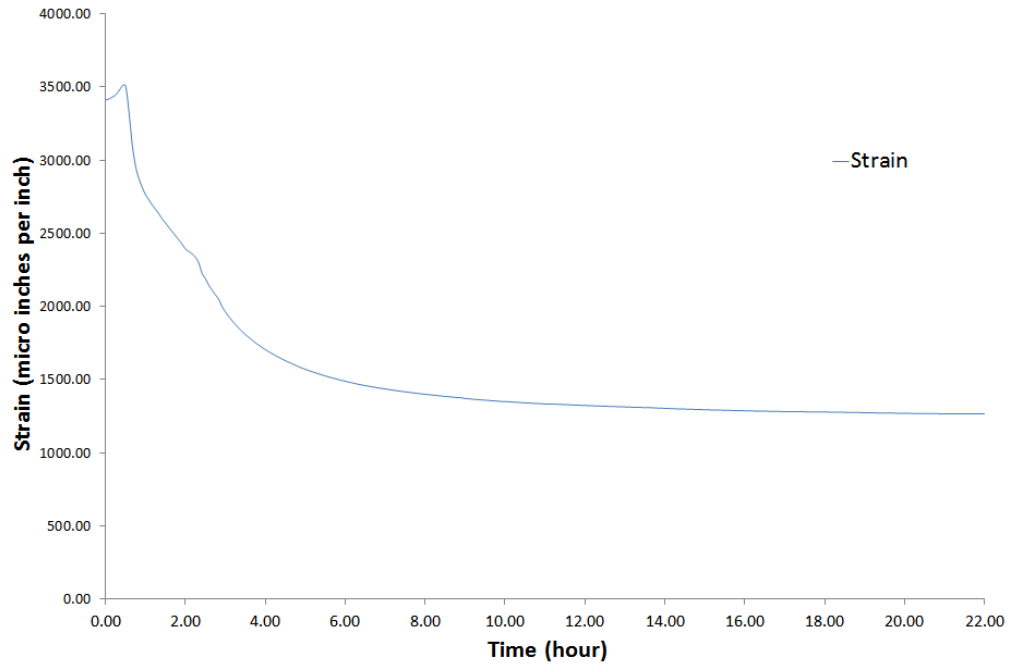
Figure A-28: The strain measured with Geokon vibrating wire strain gage in center of cube specimen

A.3 Laboratory Evaluation of Thermal Behavior (E-Bond 420)

E-Bond 420 PT Epoxy system was tested in the FIU structural lab. Ambient temperature was in the range of 70-78 F. It was almost constant at 76 F during the time of 2-13 hours.. The relative humidity was 45%. The specimen was then left and monitored for a period of 20 hours.

Mixing

For best results, components were stored prior to mixing in the laboratory at 70°- 78°F for 3 days. The three components were mechanical mixed. Component B (hardener) was poured into 7 gallon pail followed by component A (Resin). A mixing paddle driven by a low speed electric drill was used for mixing. Both A & B components were mixed to a uniform mix (approx. 2-3 minutes). The paddle was kept below the surface material to avoid entrapment of air. Component C (Sand) was then slowly poured into the epoxy. The mixing took another 3-5 minutes. The mixed epoxy grout was then poured into a plastic form.

In this test, a thin plastic form was used, with dimensions 8.5 in x 8.5 in x 6.75 in. Two thermocouples type K were embedded, one at the center of the specimen, and one at the center of the lateral surface. Camera locations and specimen are shown in Figure A-30.

Figure A-29: Location of camera and specimen

Figure A-31 represents some thermography images for E-Bond 420 PT Grout System. Ambient temperature was 69.58 to 77.77 F, and remained almost constant at 76 F during the age of 2 to13 h. The data acquisition system was set to record the temperature every one minute. The test started right after casting and continued for 20 hours, until all thermocouples reached room temperature. The maximum temperature was recorded at the age of 1.85 h with 194.5 F in the

center of the specimen. The lateral surface experienced temperature of 179.6 F at the age of 1.82 h (see Figure A-32). From Figure A-3333, it is clear that both techniques verified each other.
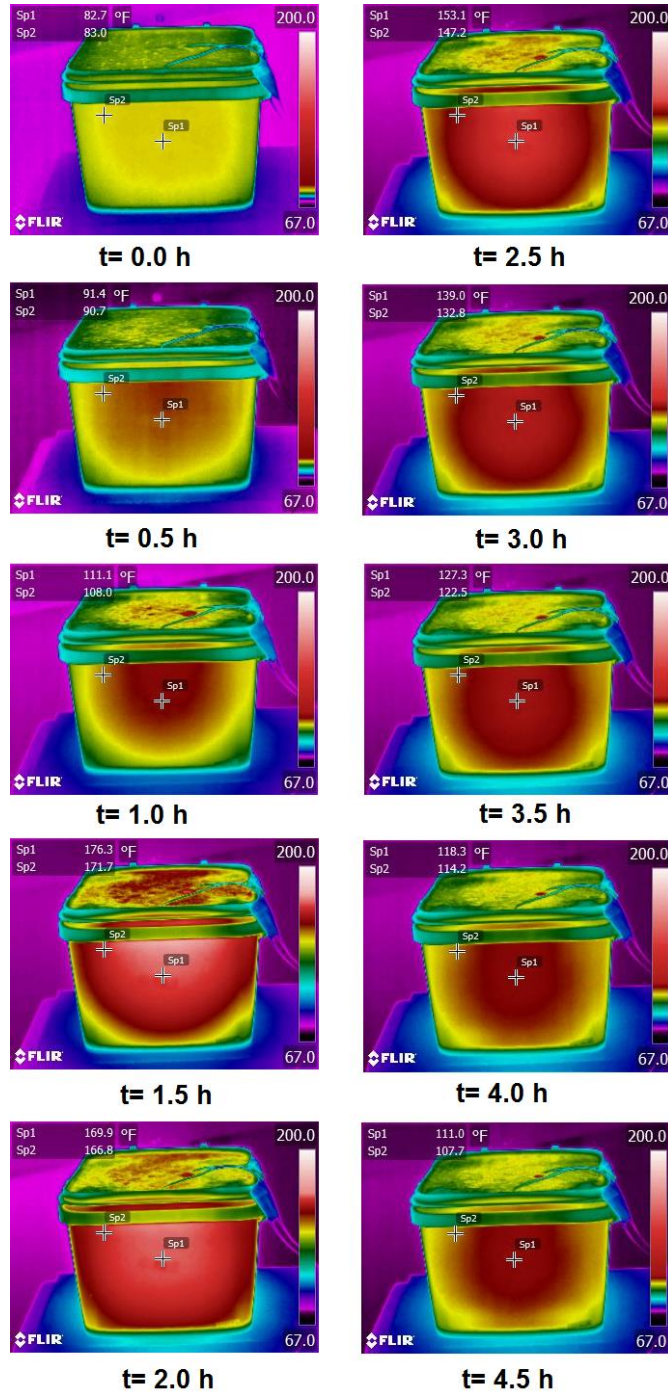
Figure A-30: Some thermography images for E-Bond 420 PT Grout System
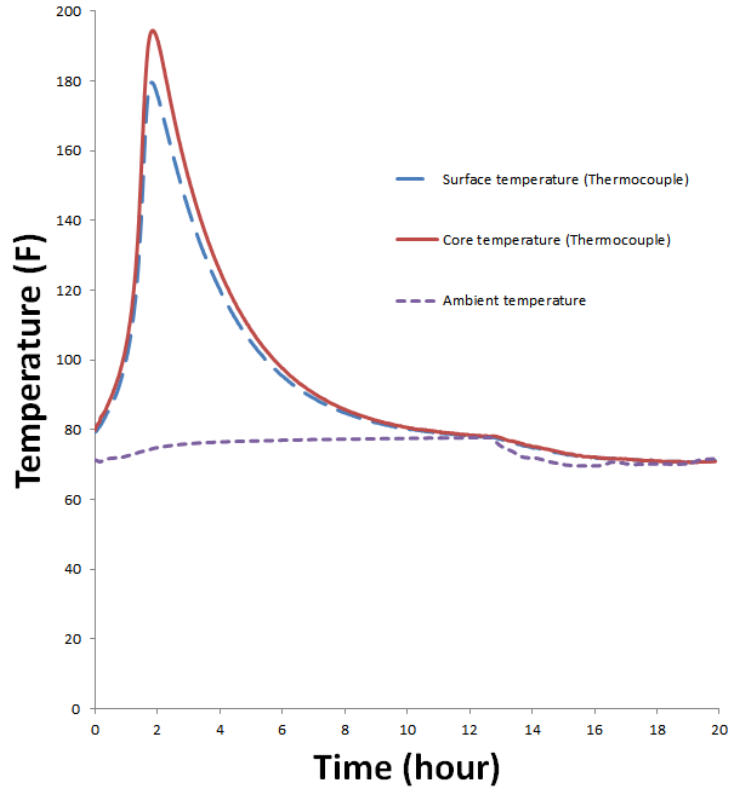
Figure A-31: The temperature profile for E-Bond 420 PT Grout System
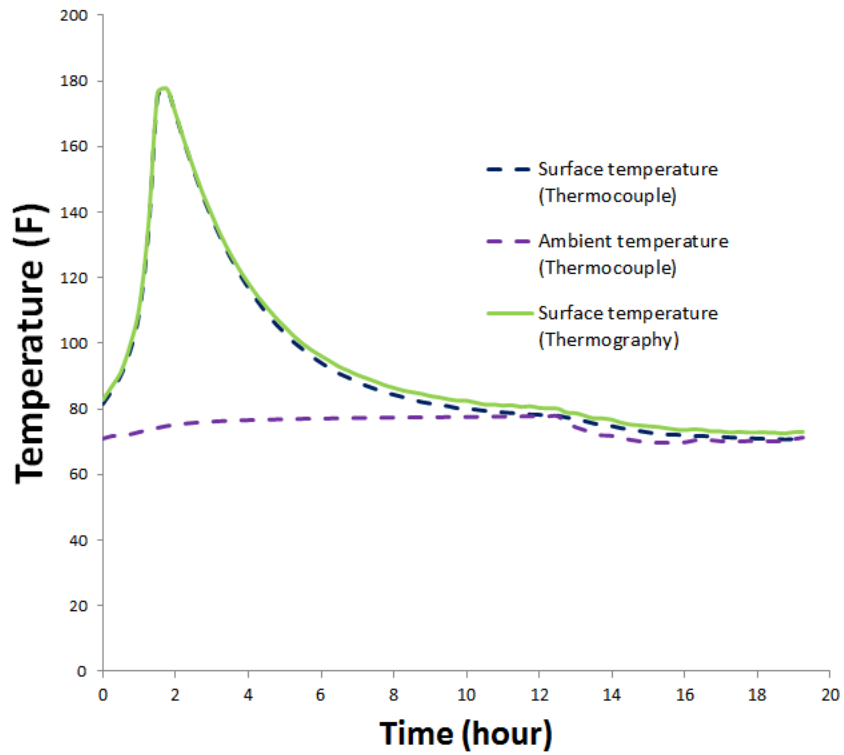
Figure A-32: Temperature changes in center of surface for E-Bond 420 PT Grout System, thermocouple and thermography

A-21

Table A-2: Summary of Tests on Epoxy Grouts

	E-Bond 420 PT Grout System	E3-HP Epoxy Grout System
Initial temperature	79 F	95 F
Test duration	20 h	
Max core temprature and time	194.5 F / 1.85 h	205.2 F / 1.1 h (65 min)
Max surface temprature and time	179.6 F / 1.82 h	
Max temperature gradient	16 F / 2.0 h	65.9 F / 1.75 h
Ambient temperature (min, max)	69.58 F, 77.77 F	71.31 F , 75.79

A.4 Finite Element Modeling of Thermal Behavior (Masterflow 648CP Plus)

Masterflow 648CP Plus epoxy grout, included in the FDOT's qualified product list, was simulated using the Finite Element Analysis software ANSYS. Figure **A-**34 shows the geometry of the pourback. The task was to replicate a temperature profile developed by Degussa Technical Center in Cleveland, Ohio, for a Florida Key's project (Figure A-35). Given the absence of some material properties in the manufacturer data sheet, some values were assumed to be similar to concrete.
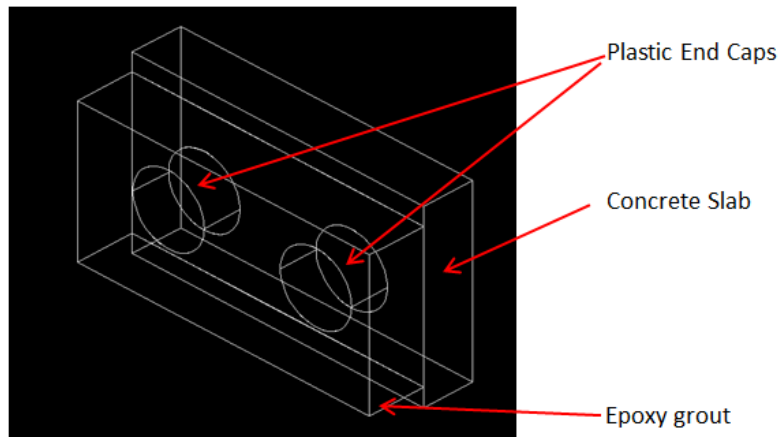
Figure A-33: Masterflow 648CP epoxy pourback geometry
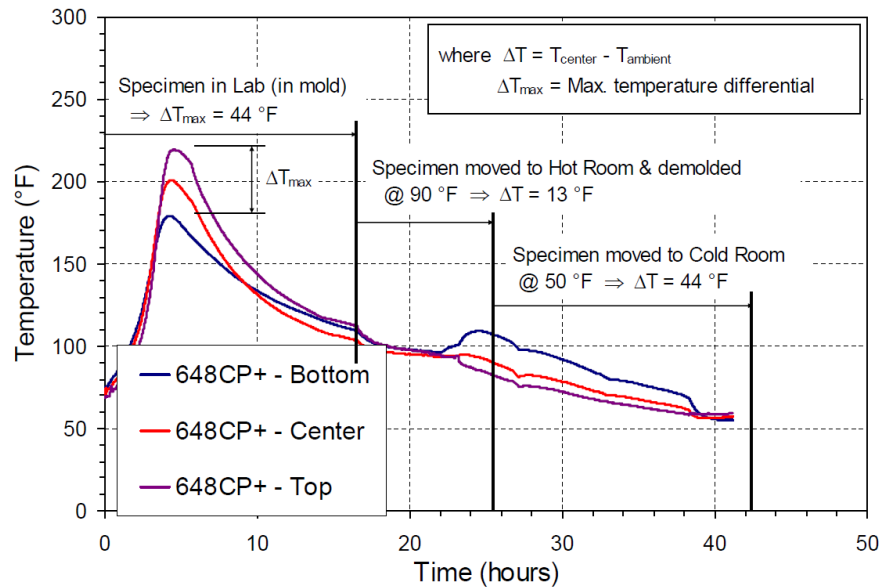
Figure A-34: Experimental temperature profile for masterflow 648CP

The epoxy pourback dimensions were 24"x48" and 9" deep. The analysis was performed for the first 45 hours after the epoxy grout casting. The boundary conditions used for thermal analysis were as follows: bottom surface in contact with previously cured concrete block and plastic end caps; and all other surfaces in contact with wood forms (treated as convection load). The three-dimensional solid element PLANE 70–3D was used for the analysis. The reference temperature was the temperature of the epoxy at the moment of placing in the formwork (70 F).

Figure A-36 shows the results of the thermal analysis for the top, middle, and bottom sections of the epoxy pourback. For the stress analysis, the three-dimensional solid element PLANE 185-3D was used.

Figure A-37 shows the stress results for the top, middle, and bottom sections of the epoxy pourback. Table A-3 shows the properties used for the thermal and stress analysis.
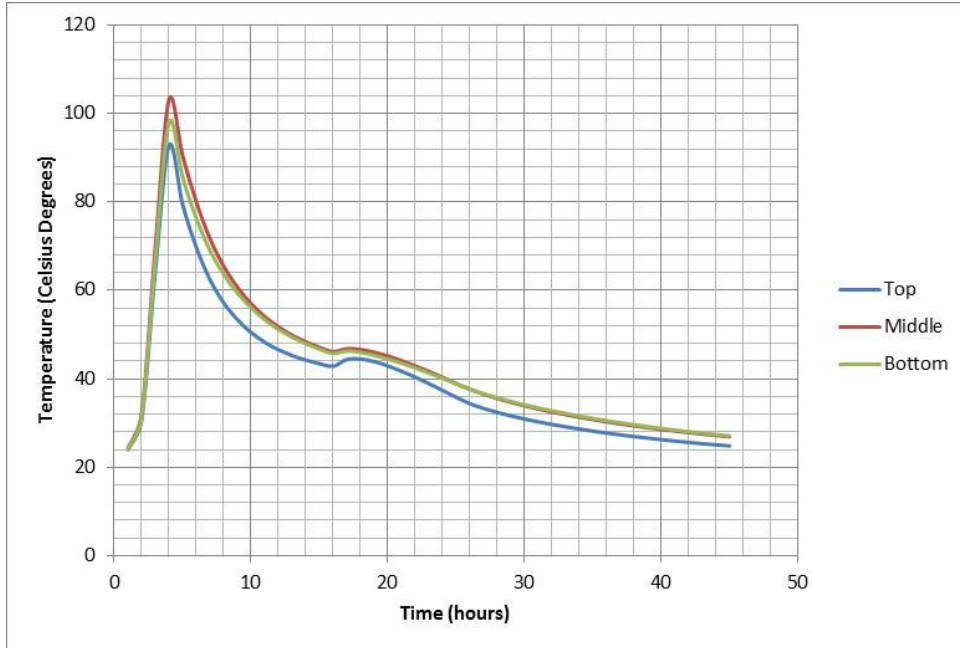
Figure A-35: Masterflow 648CP thermal analysis
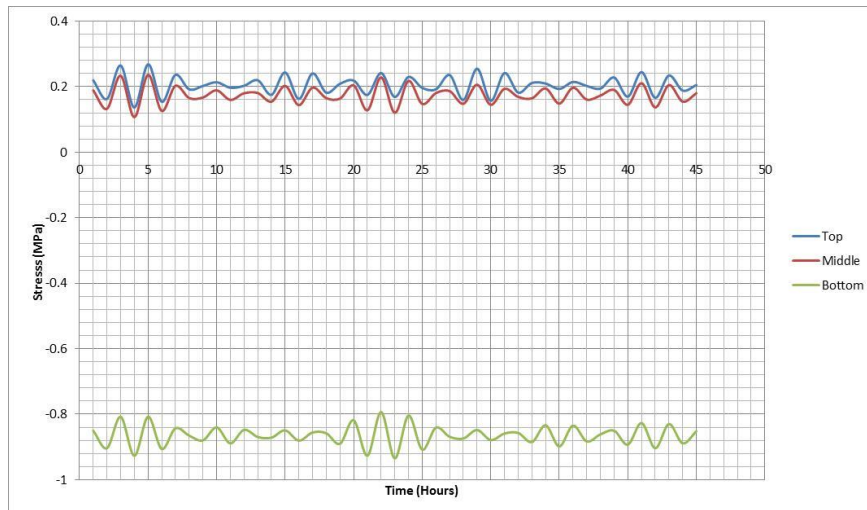
Figure A-36: Masterflow 648CP stress anlysis

The tensile strength of the Masterflow 548CP epoxy grout is 15MPa as indicated by the manufacturer. According to the FE analysis performed, no cracks were developed in the pourback given that the stresses developed in the epoxy block did not exceed the 15Mpa tensile strength. This coincided with the results from the Degussa Technical Center, which did not find any cracks during the experimental procedure.

Table A-3: Concrete, Plastic Caps, and Masterflow 548CP Epoxy Grout Properties

Concrete Slab	Standard Test	Units	Value
Thermal conductivity		kJ/m.h.C	2.3
Specific heat	ASTM E1269 - 11	kJ/kg.C	0.23
Heat-transfer film coefficient (air exposure)		kCal/m^2.h.C	4.3
Density		Kg/m^3	2400
Young Modulus	ASTM C580	MPa	5000
Poisson's ratio		--	0.18
Thermal Expansion Coefficient	ASTM C531	mm/mm/C	1.0x10^{-6}
Epoxy Grout Masterflow 648	**Standard Test**	**Units**	**Value**
Thermal conductivity		kJ/m.h.C	2.3
Specific heat	ASTM E1269 - 11	kJ/kg.C	0.23
Heat-transfer film coefficient (wood forms)		kCal/m^2.h.C	8.5
Heat-transfer film coefficient (air exposure)		kCal/m^2.h.C	4.3
Density		Kg/m3	1986
Young Modulus	ASTM C580	MPa	8500
Poisson's ratio		--	0.4
Thermal Expansion Coefficient	ASTM C531	mm/mm/C	3.6x10^{-5}
Plastic End Caps	**Standard Test**	**Units**	**Value**
Thermal conductivity		kJ/m.h.C	0.68351
Specific heat	ASTM E1269 - 11	kJ/kg.C	1.05
Density		Kg/m^3	1400
Young Modulus	ASTM C580	MPa	8000
Poisson's ratio		--	0.4
Thermal Expansion Coefficient	ASTM C531	mm/mm/C	3.6x10^{-5}

APPENDIX B

Time-temperature plots at all sensor locations for both S-type and R-type models

Comparison of experimental observation and FEM analysis
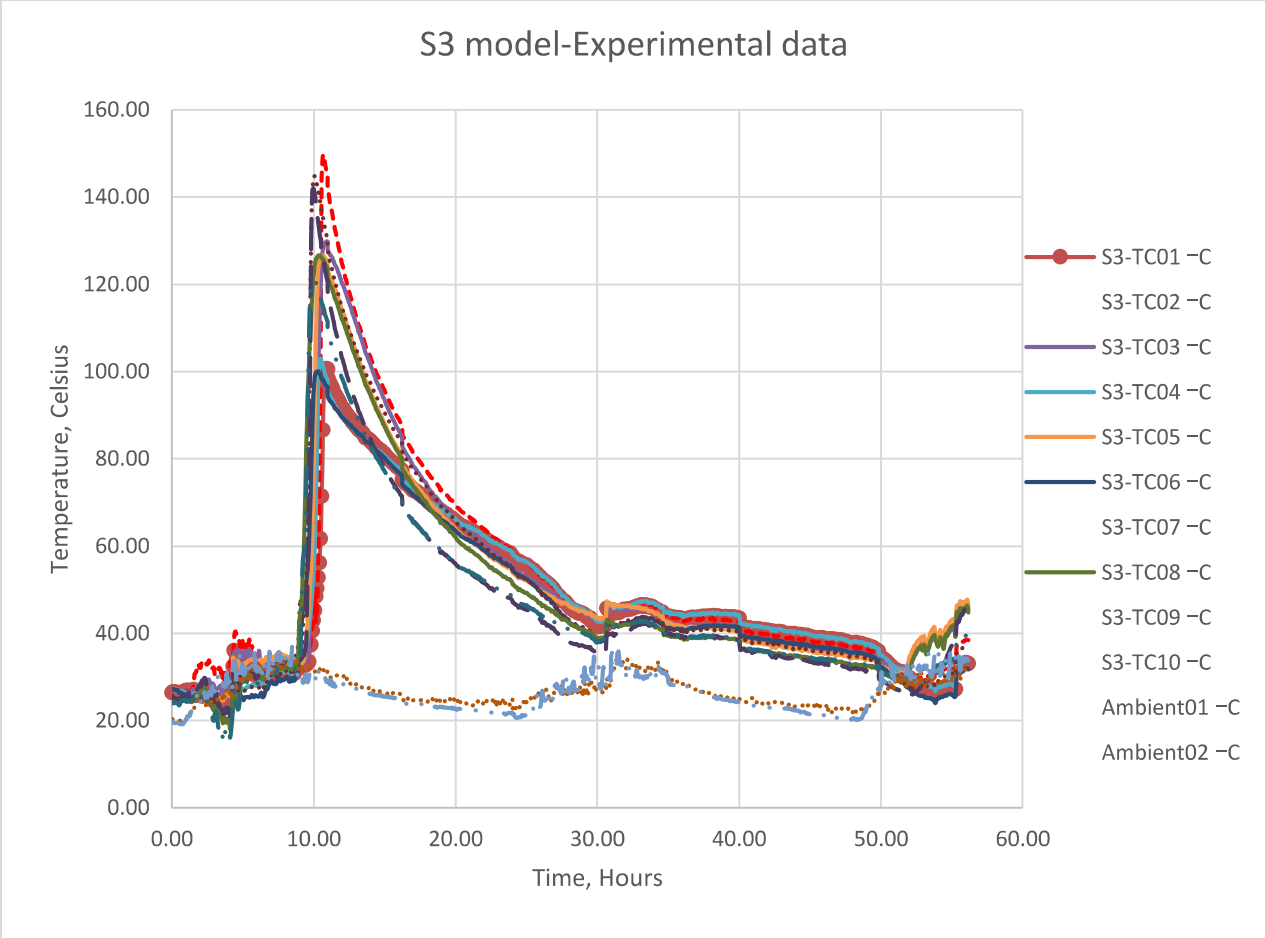
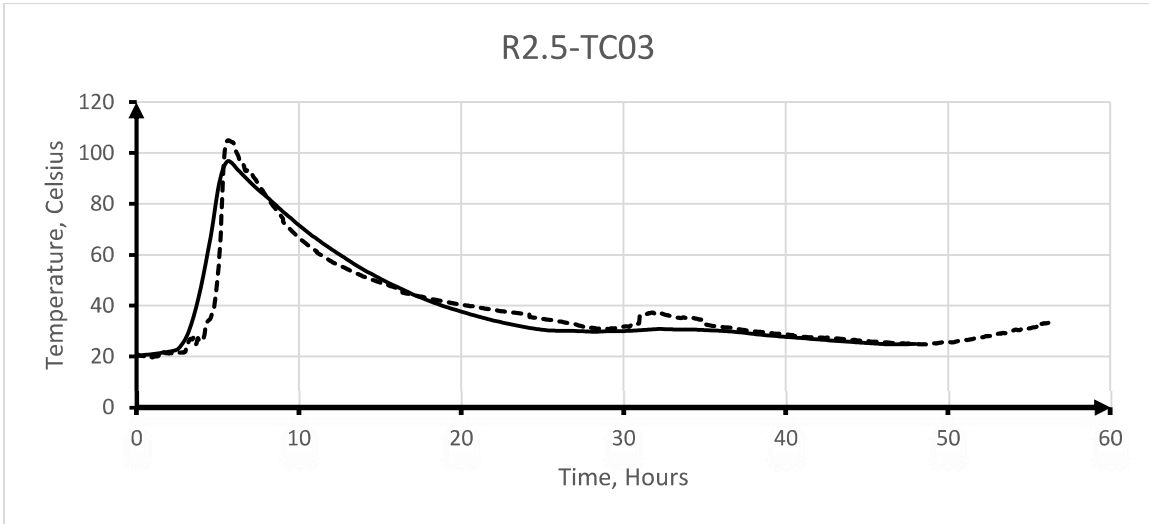Figure B- 1: Time temperature curve for all sensor locations
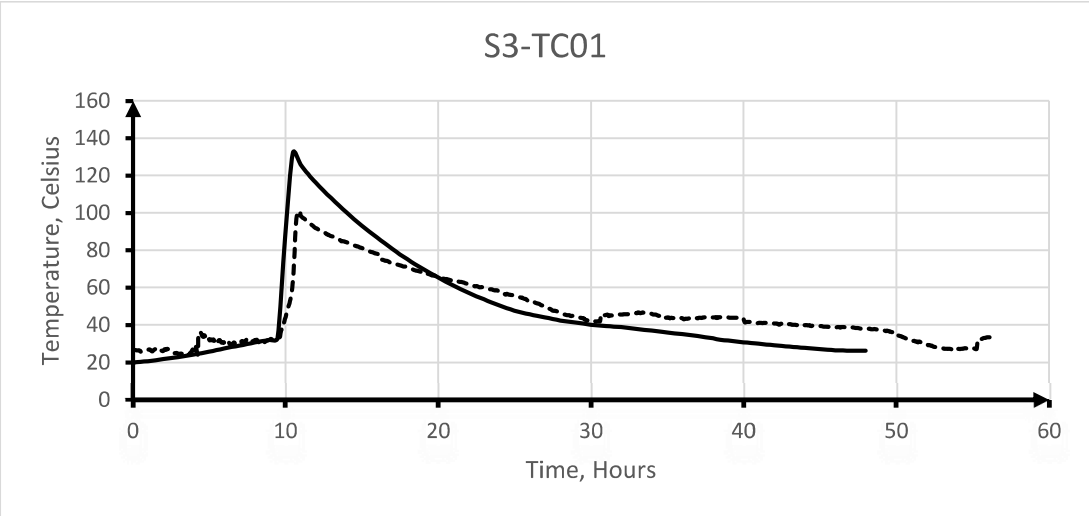
Figure B- 2: Time temperature curve for sensor S3-TC01

B-2
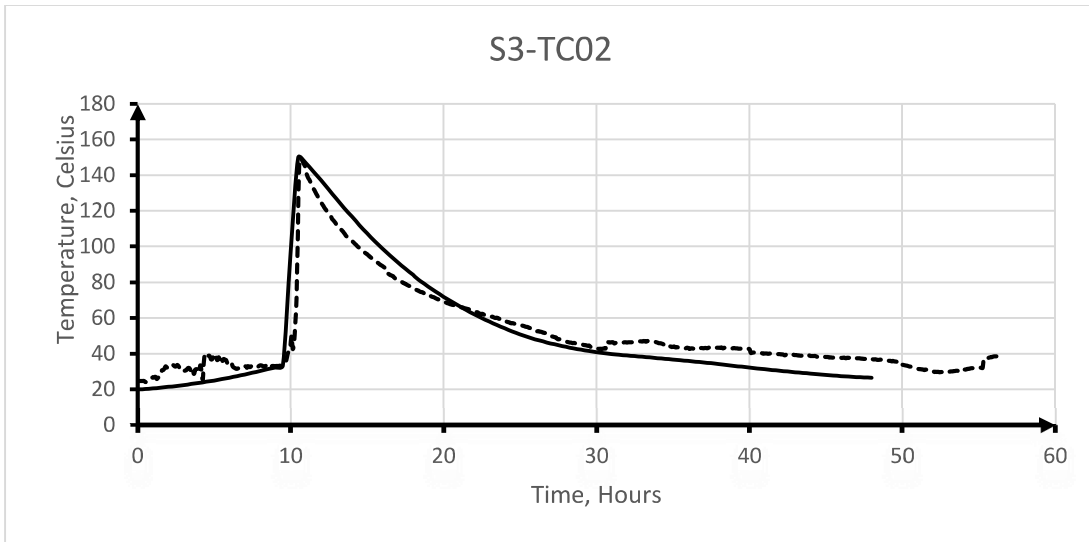
Figure B- 3: Time temperature curve for sensor S3-TC02
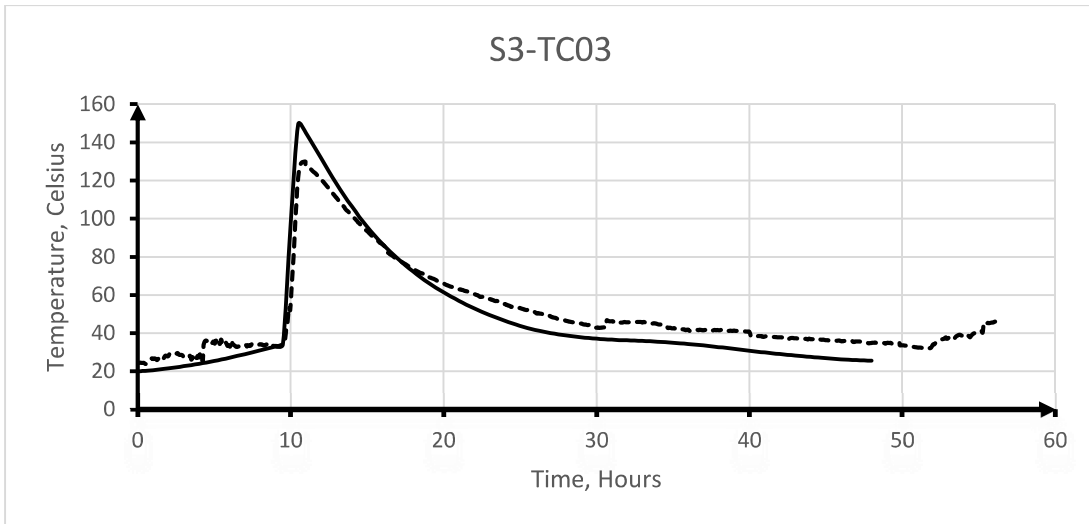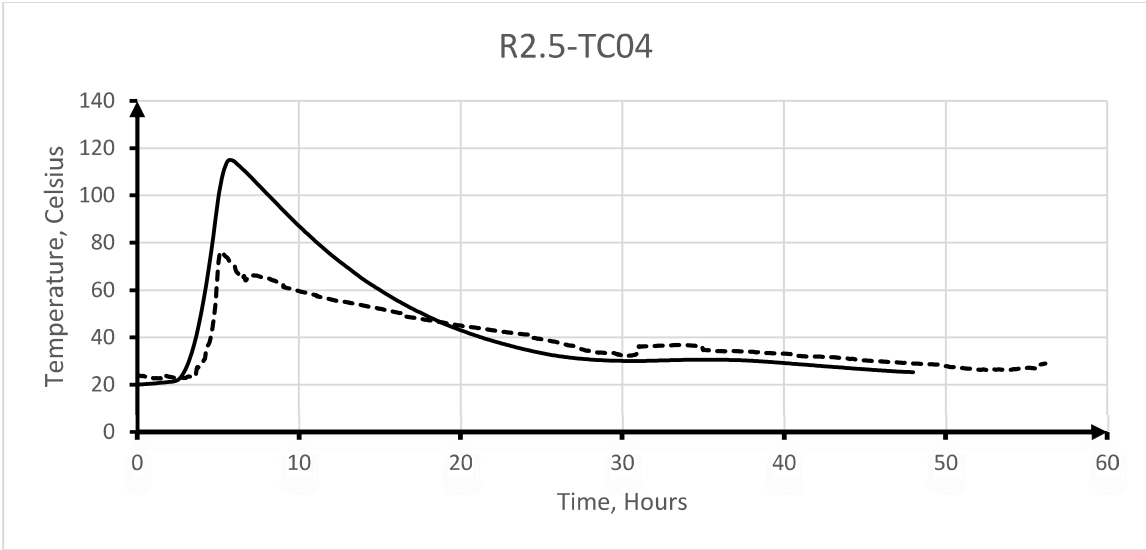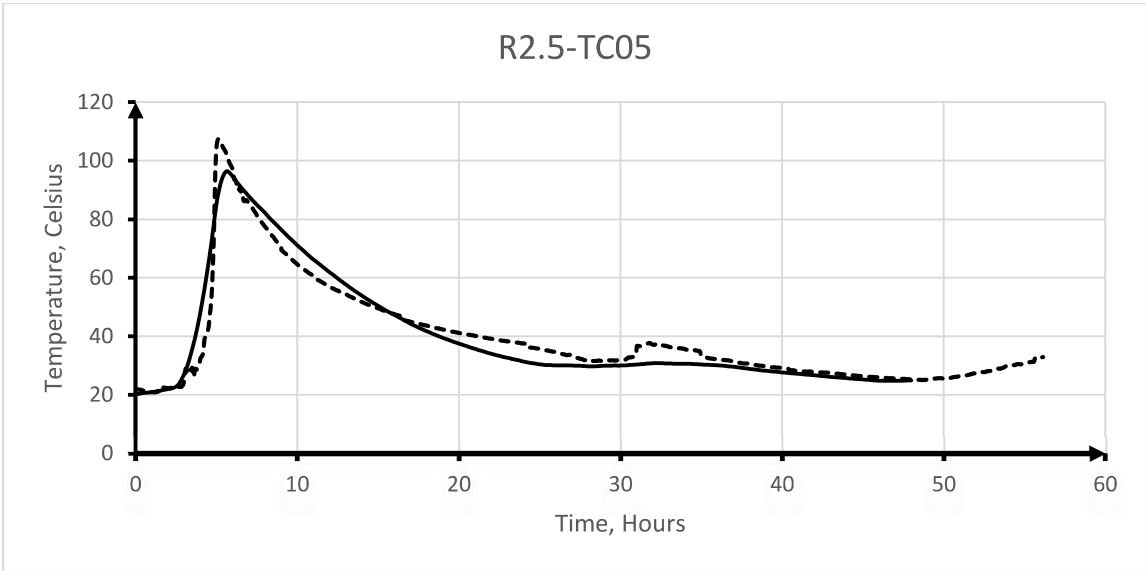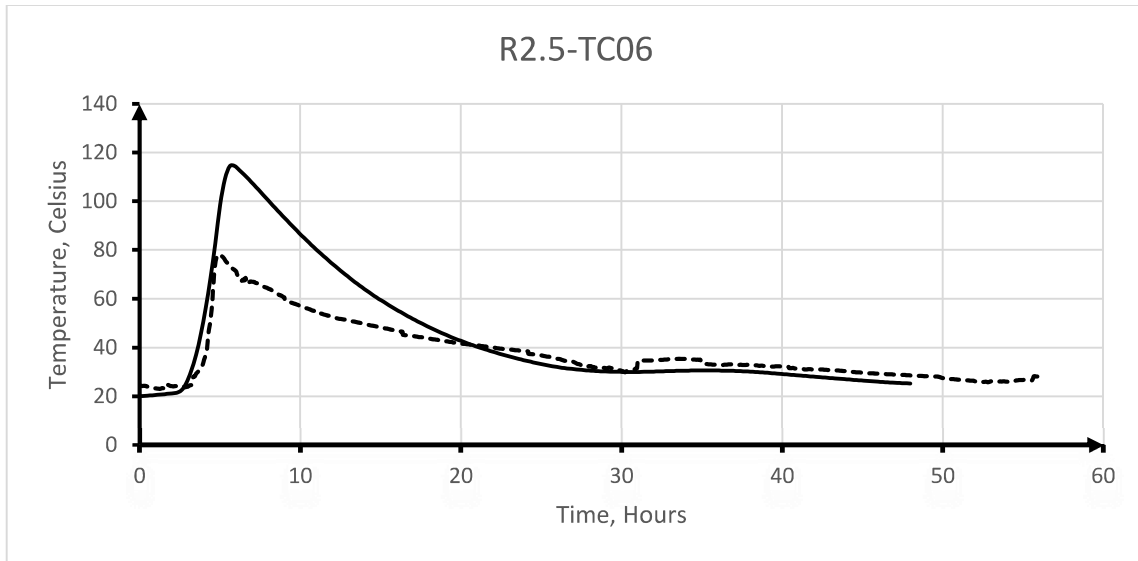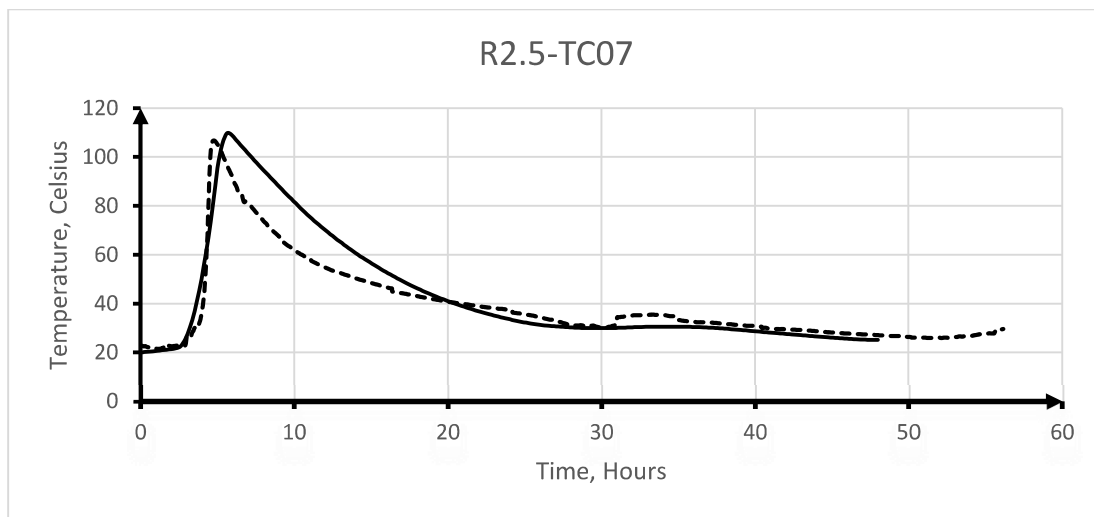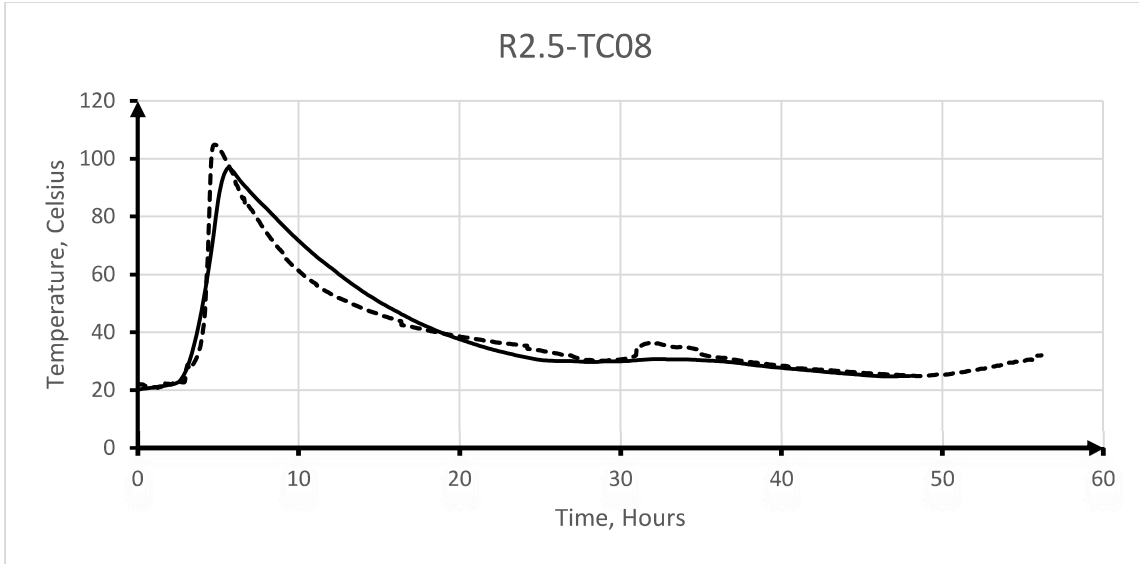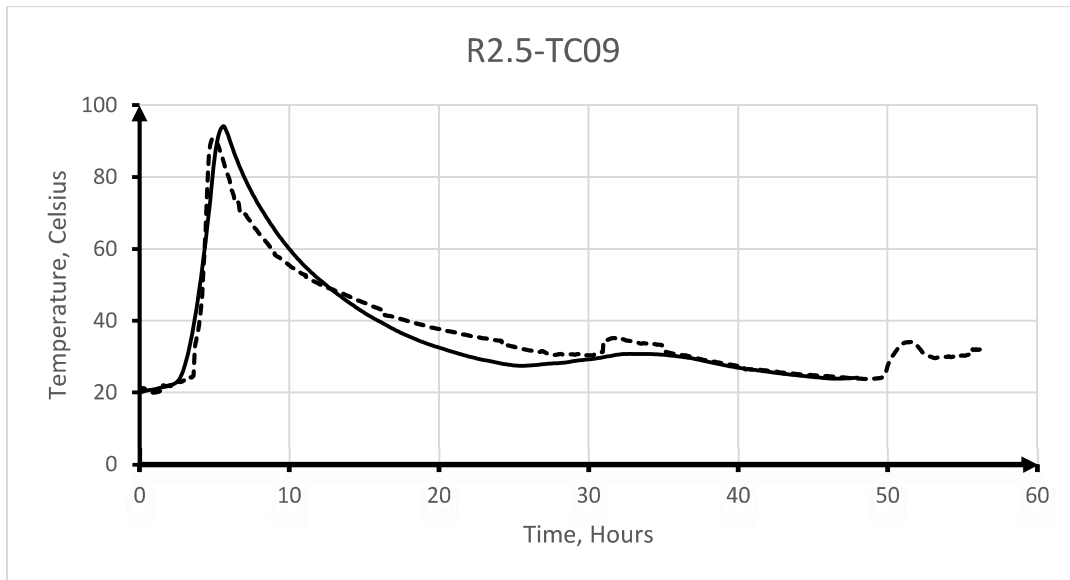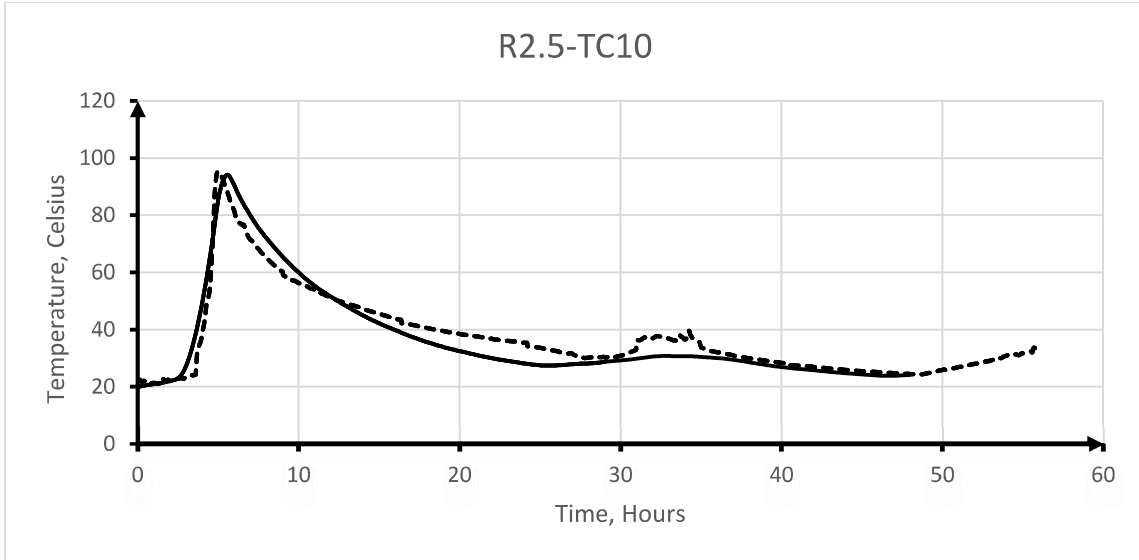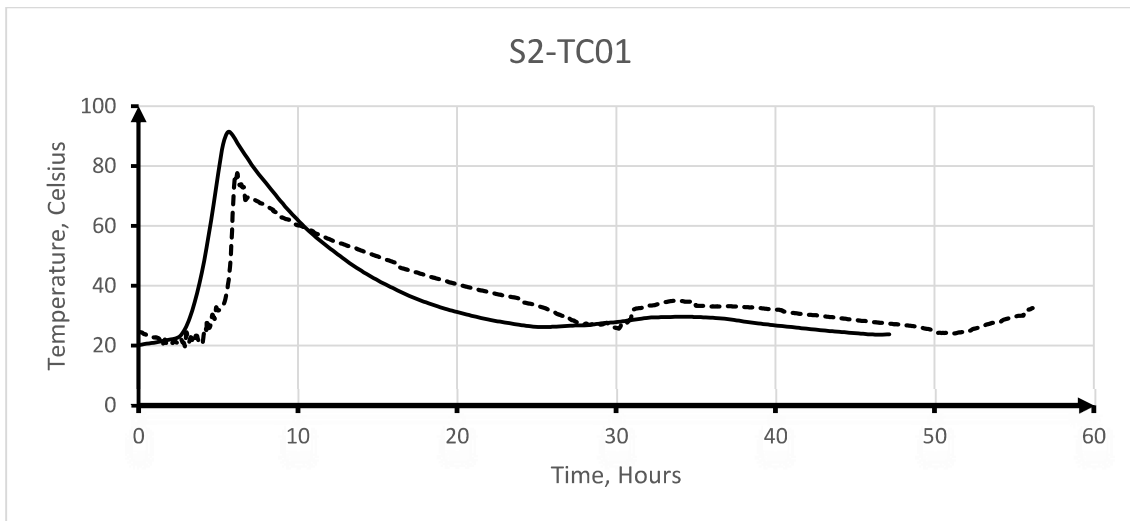

Figure B- 4: Time temperature curve for sensor S3-TC03
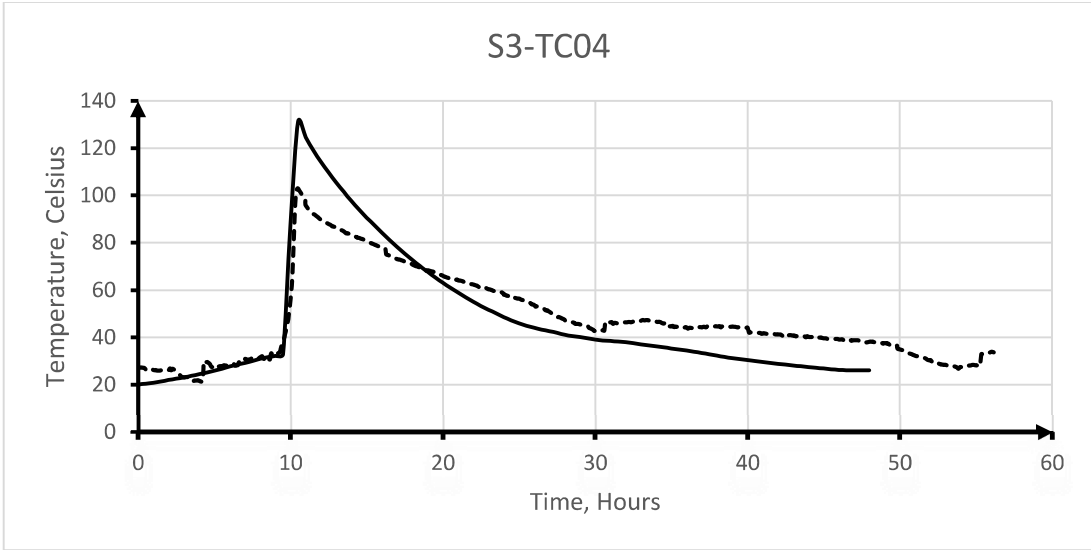
Figure B- 5: Time temperature curve for sensor S3-TC04
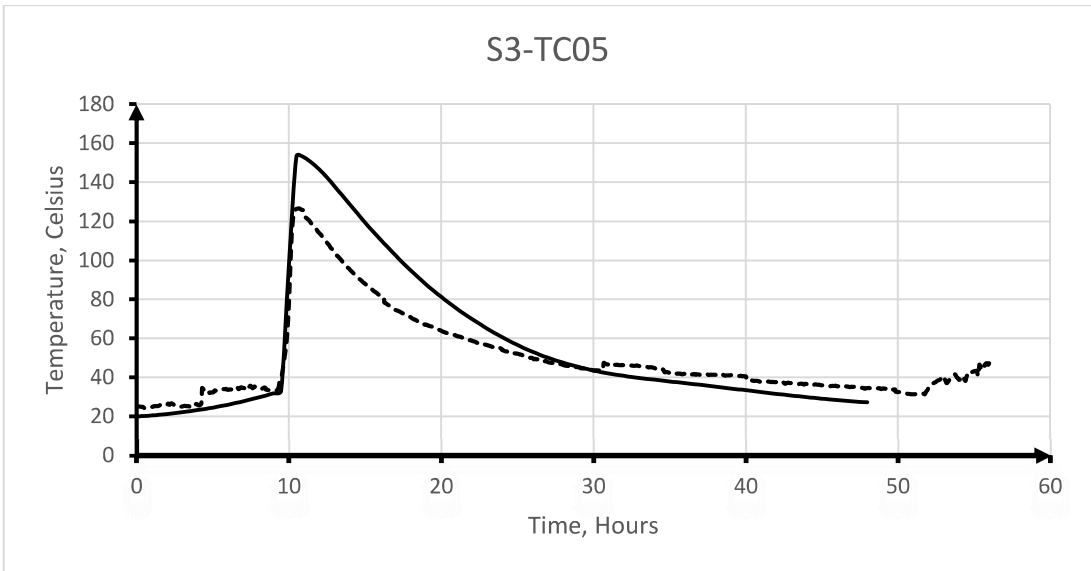
Figure B- 6: Time temperature curve for sensor S3-TC05
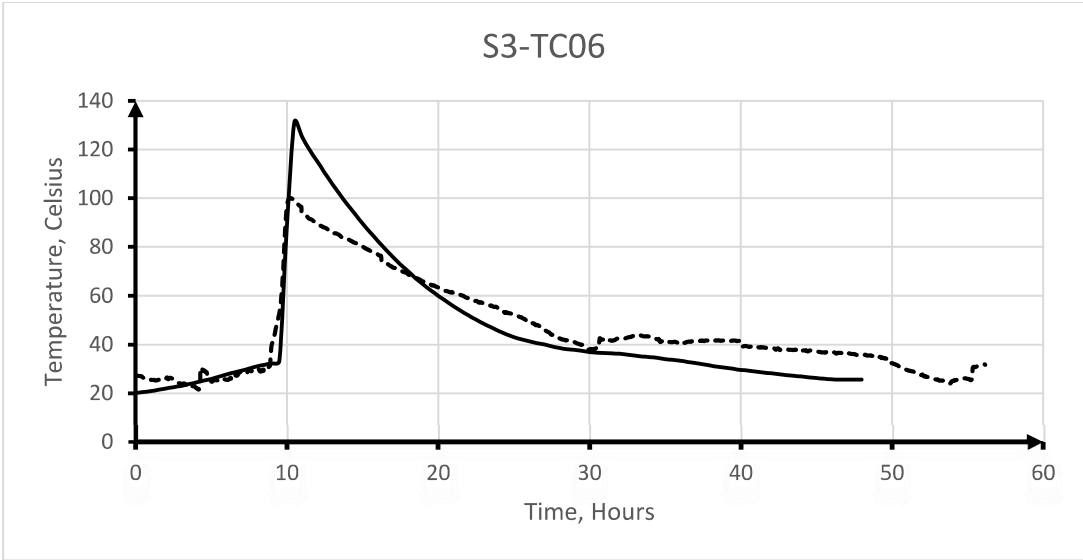
Figure B- 7: Time temperature curve for sensor S3-TC06
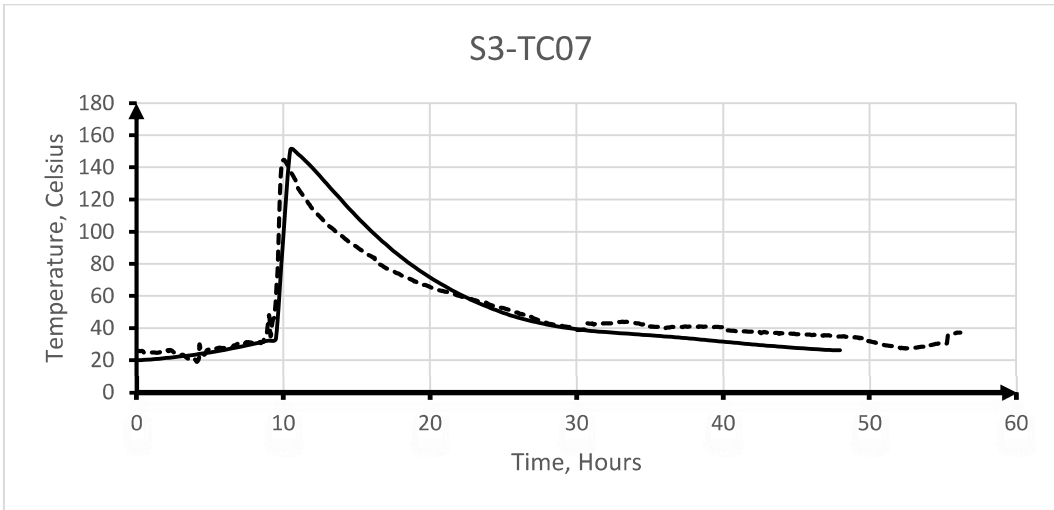
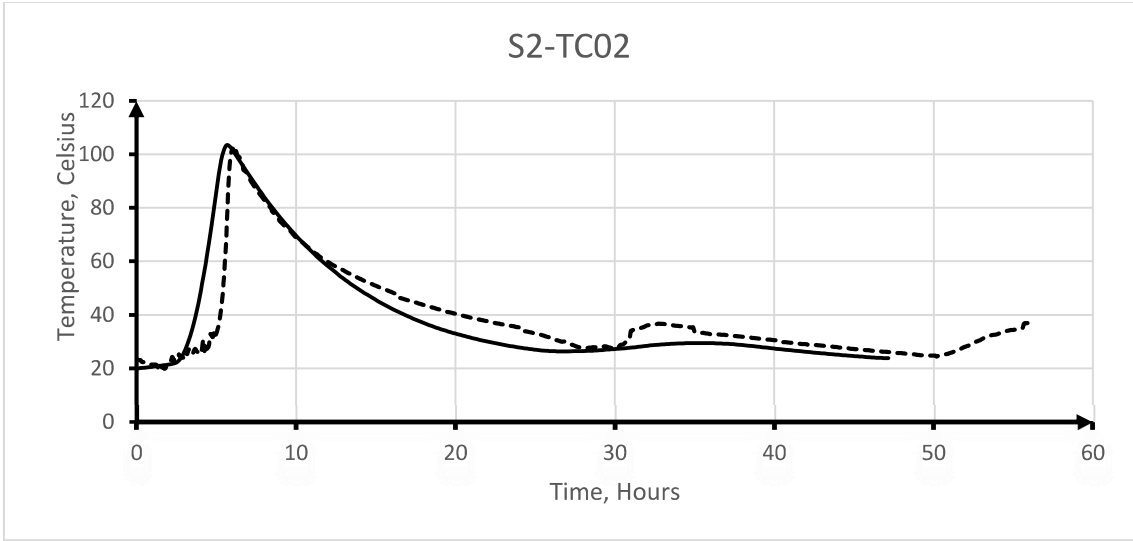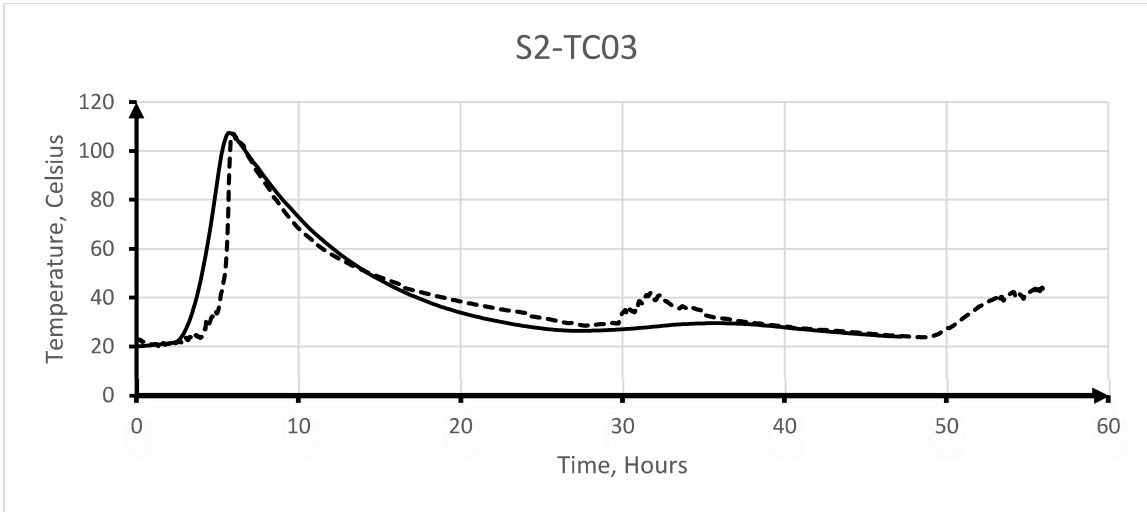
Figure B- 8: Time temperature curve for sensor S3-TC07
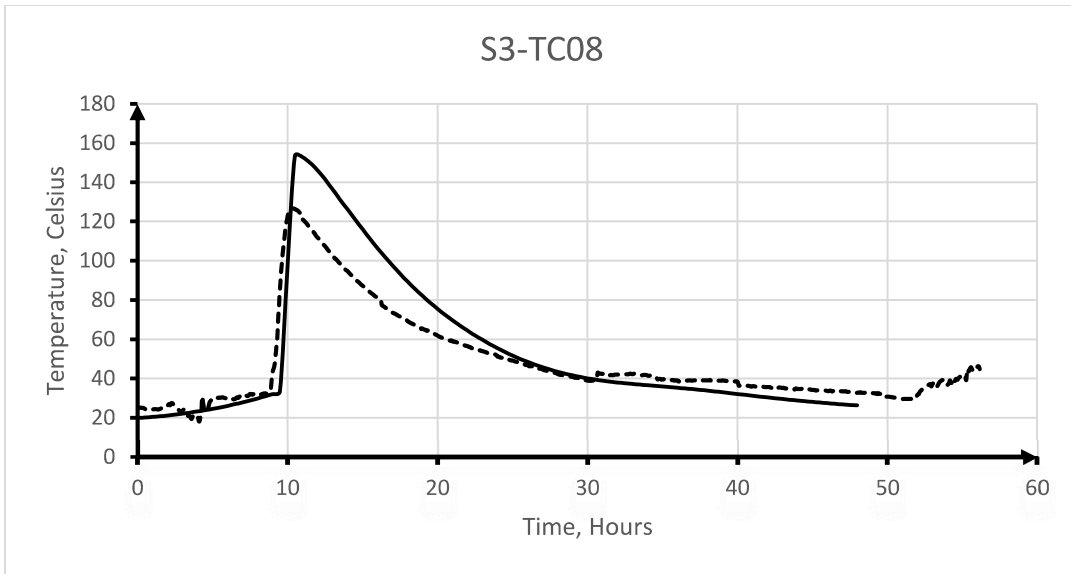
Figure B- 9: Time temperature curve for sensor S3-TC08
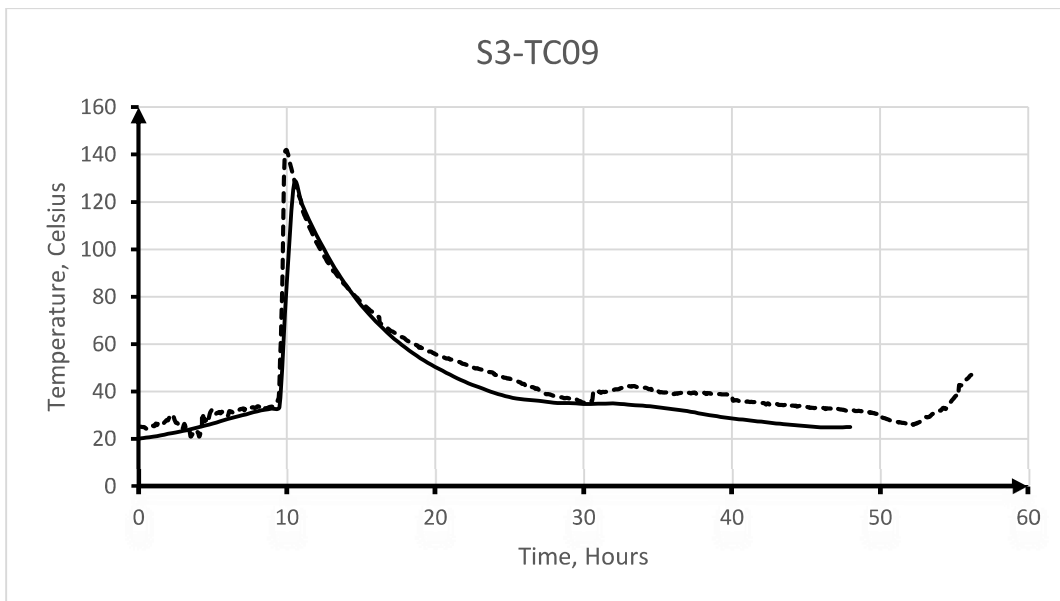
Figure B- 10: Time temperature curve for sensor S3-TC09
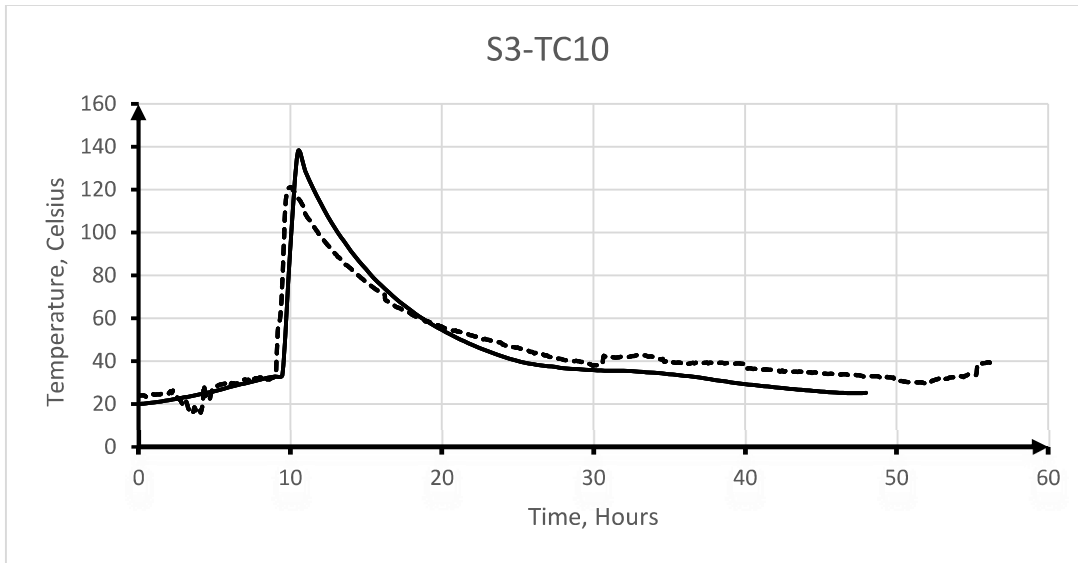
Figure B- 11: Time temperature curve for sensor S3-TC10
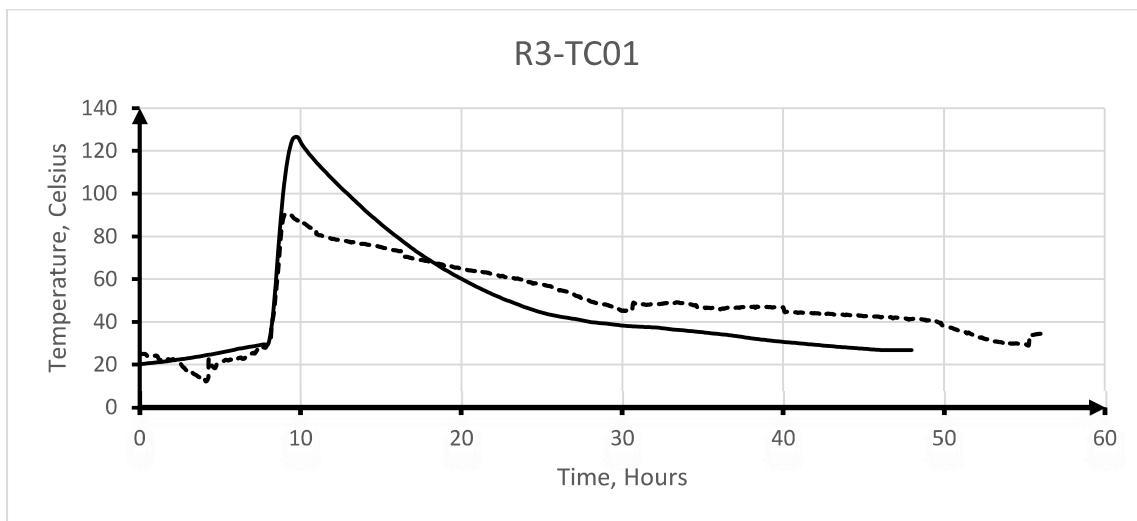
Figure B- 12: Time temperature curve for sensor R3-TC01
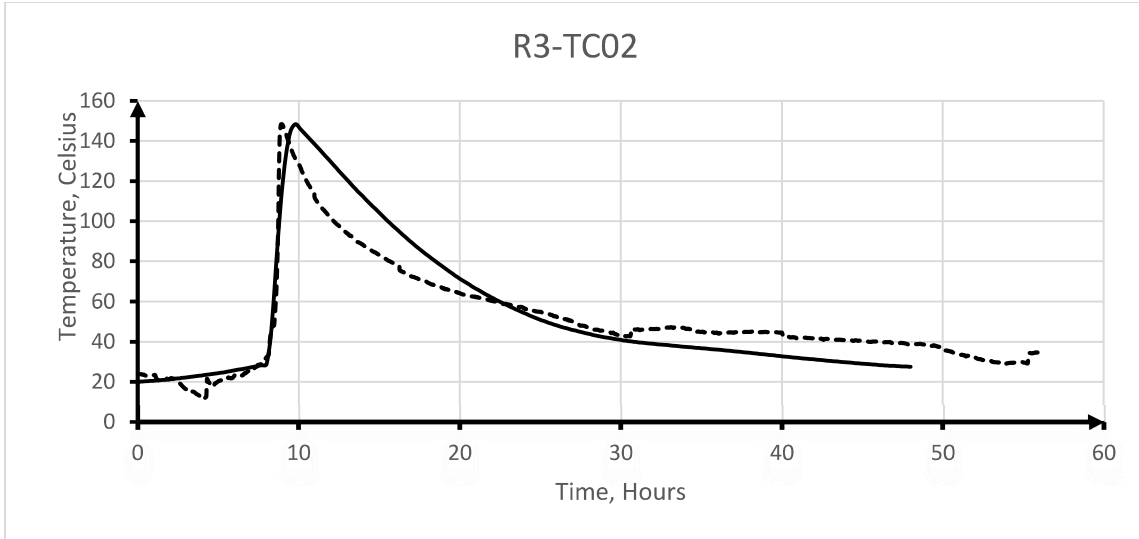
Figure B- 13: Time temperature curve for sensor R3-TC02
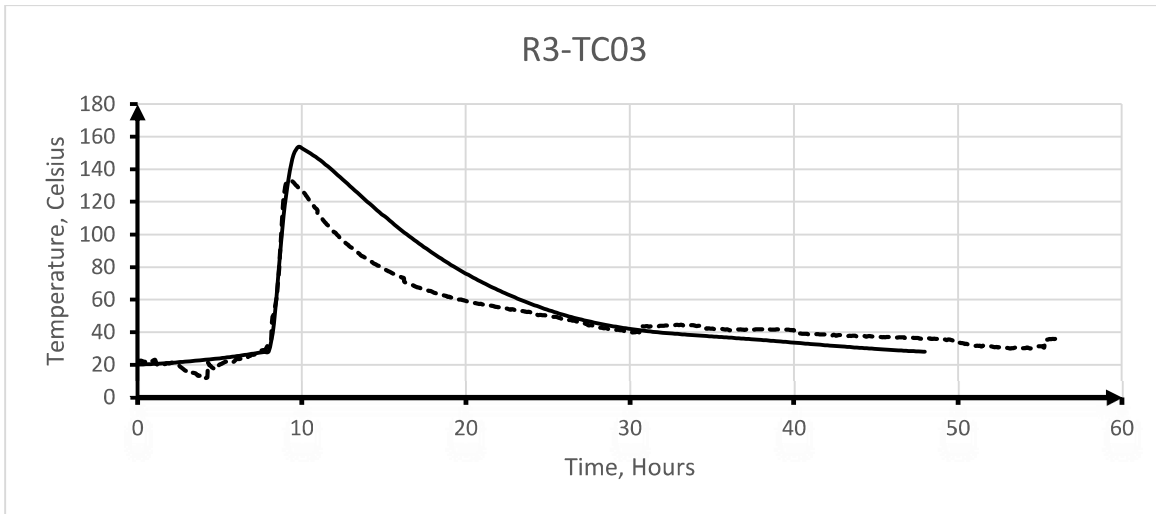
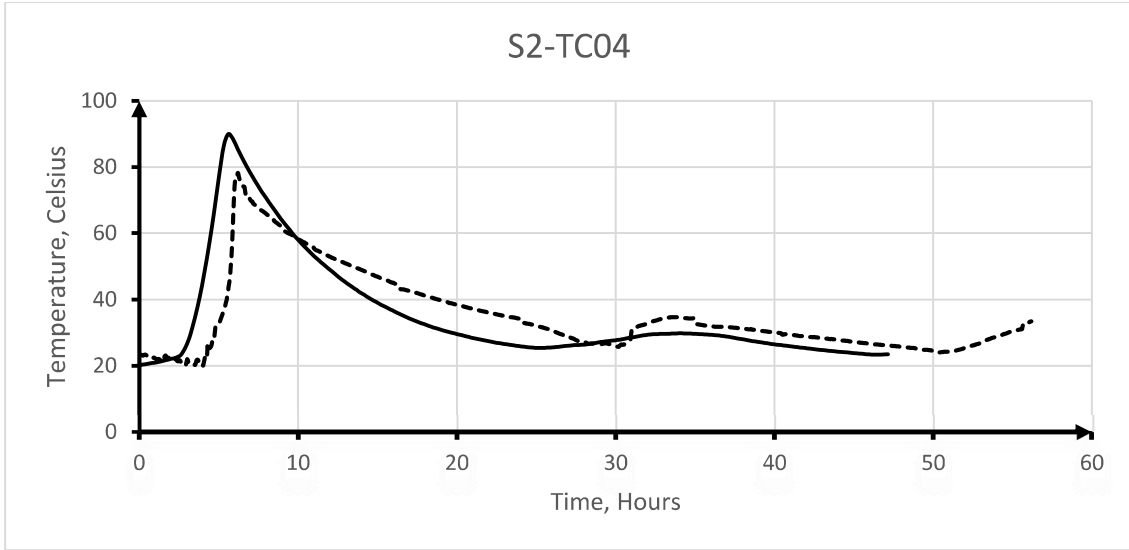Figure B- 14: Time temperature curve for sensor R3-TC03
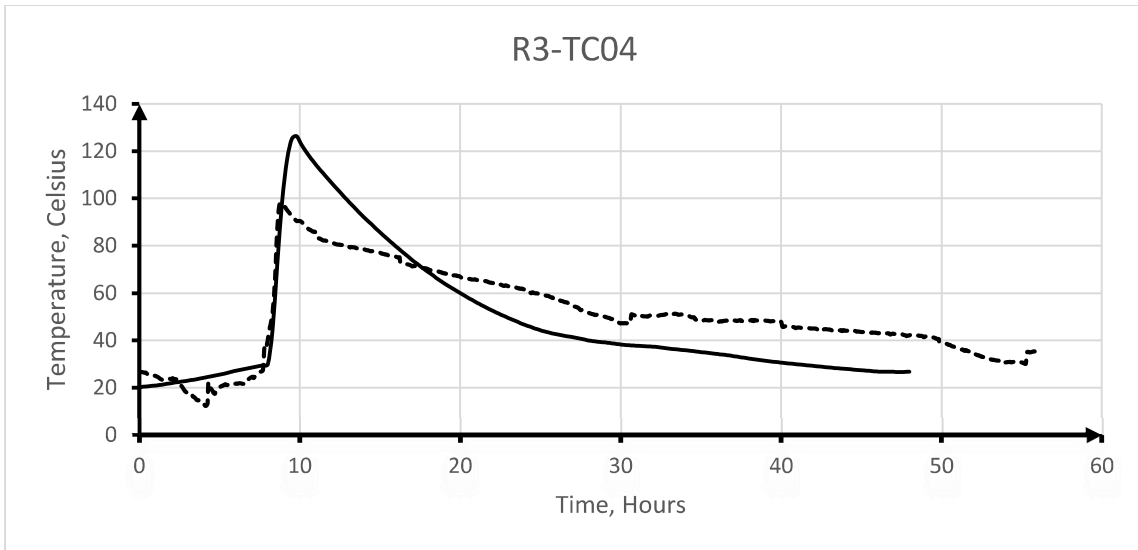
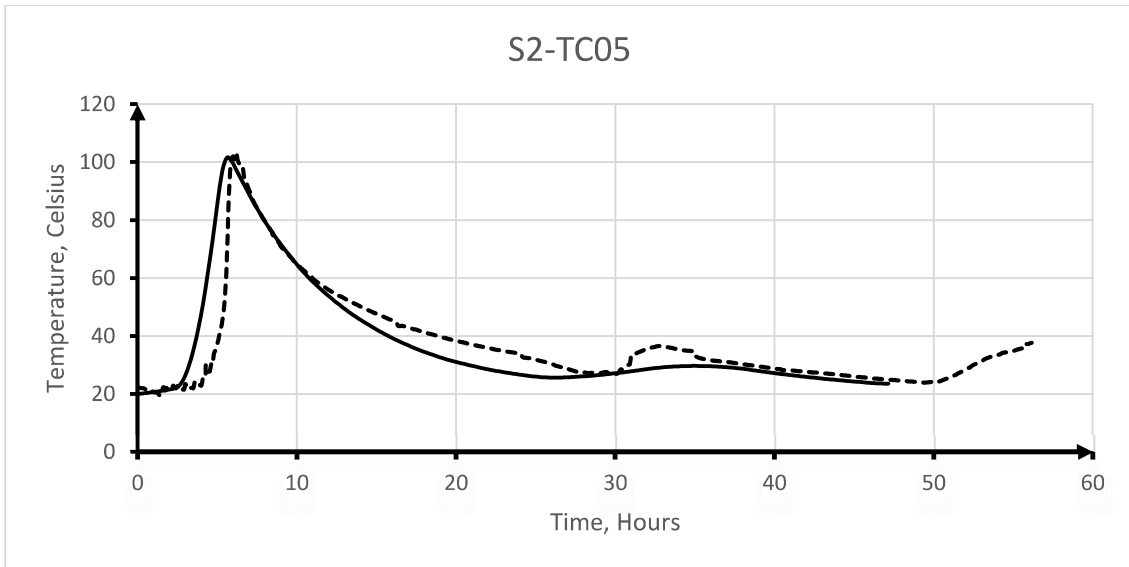Figure B- 15: Time temperature curve for sensor R3-TC04
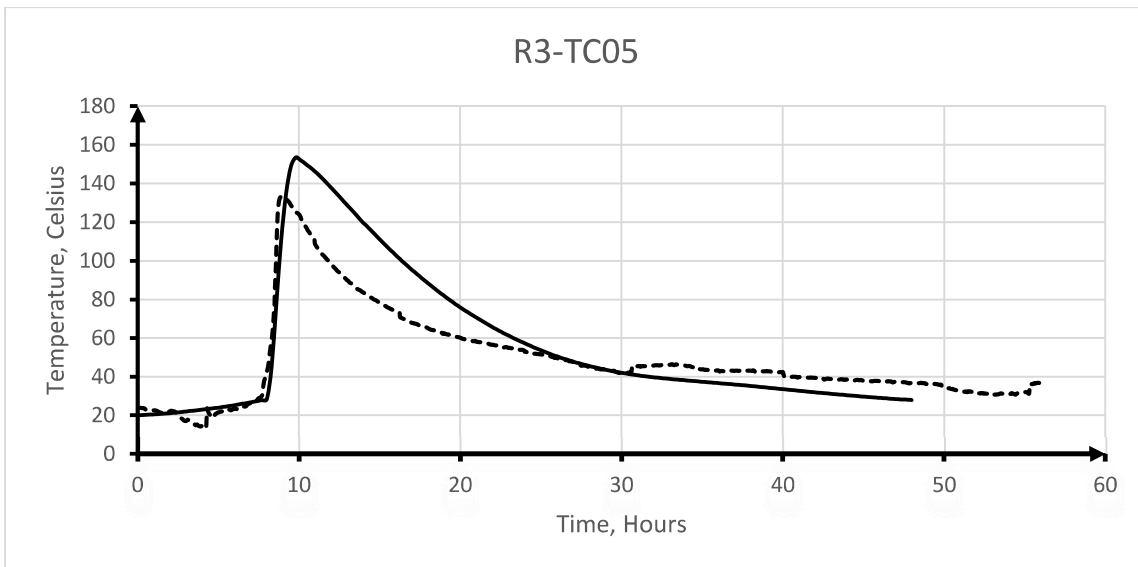
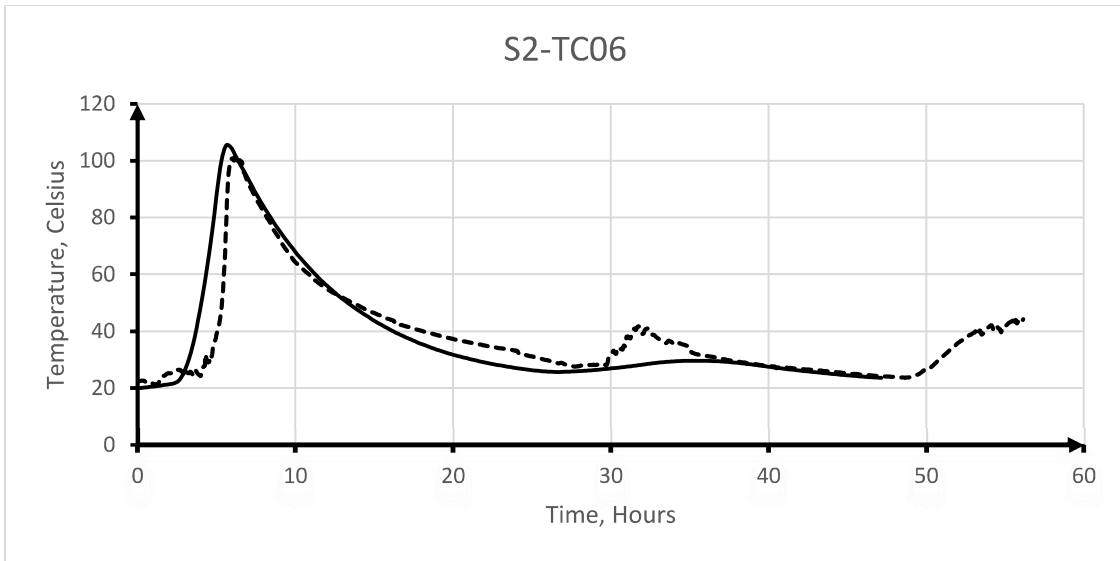Figure B- 16: Time temperature curve for sensor R3-TC05
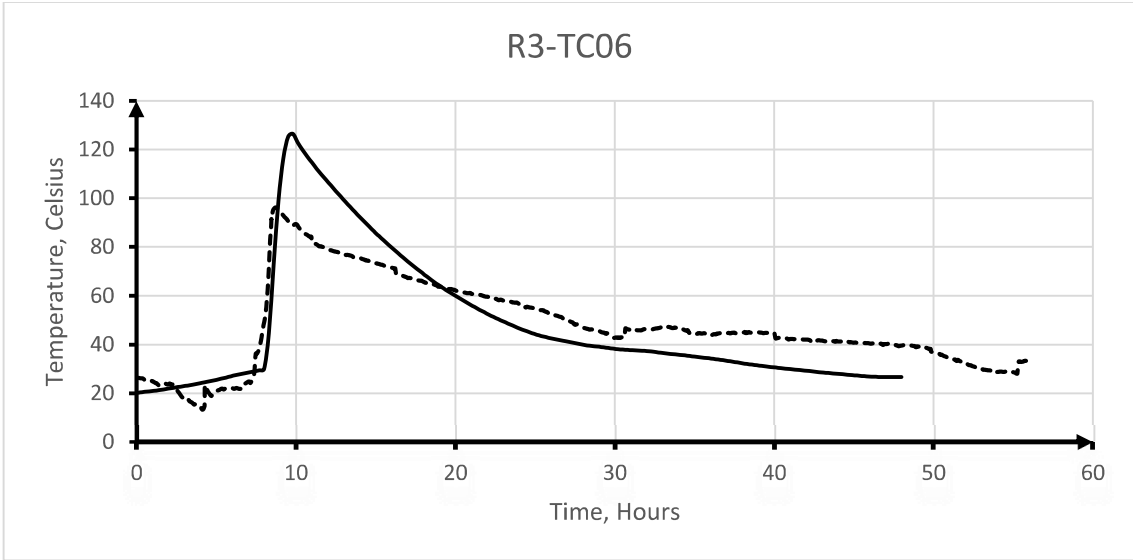
Figure B- 17: Time temperature curve for sensor R3-TC06
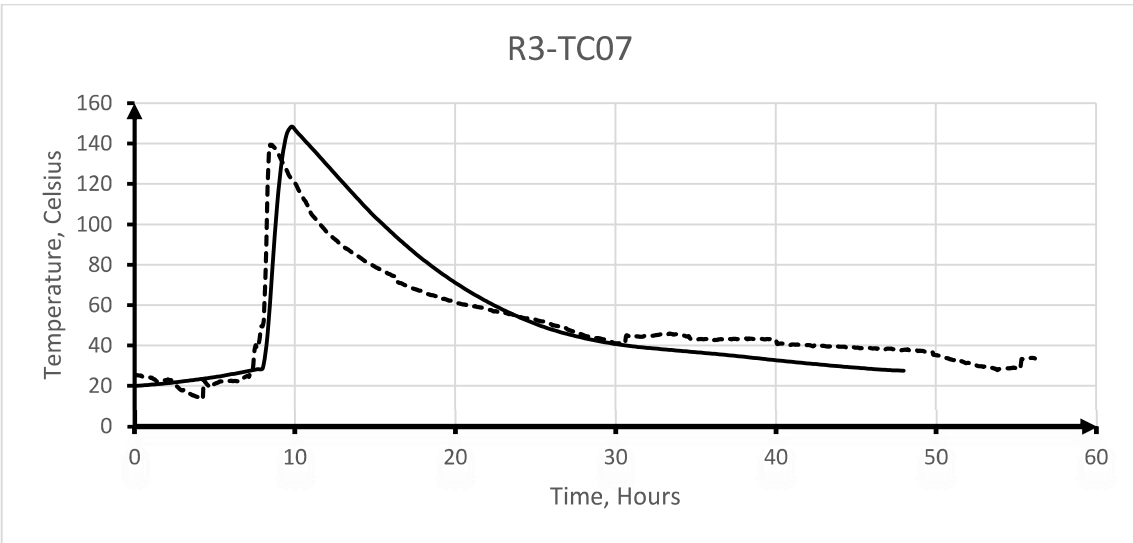
Figure B- 18: Time temperature curve for sensor R3-TC07
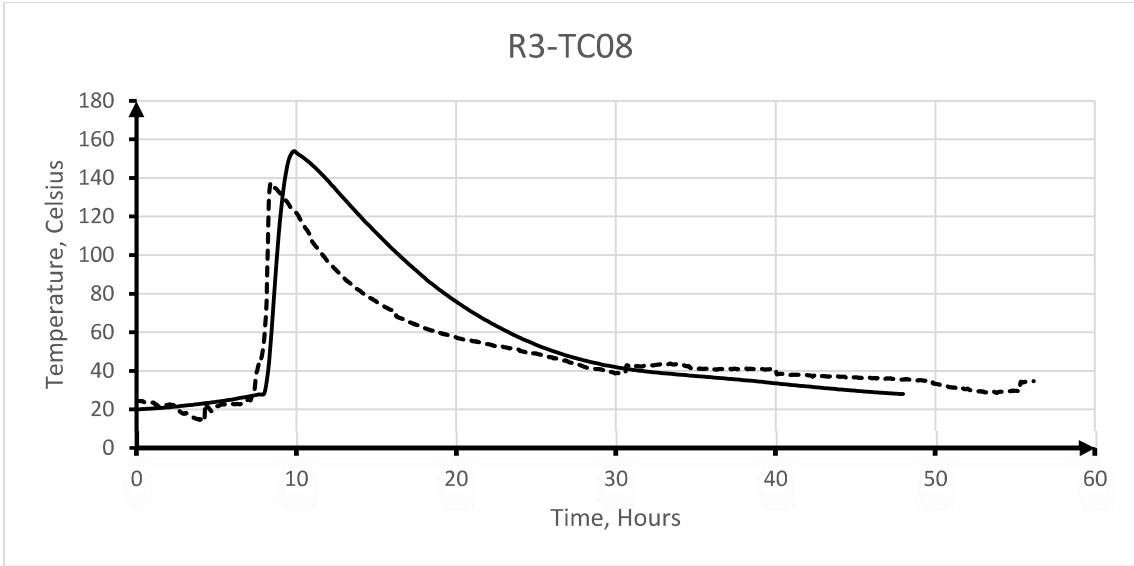
Figure B- 19: Time temperature curve for sensor R3-TC08
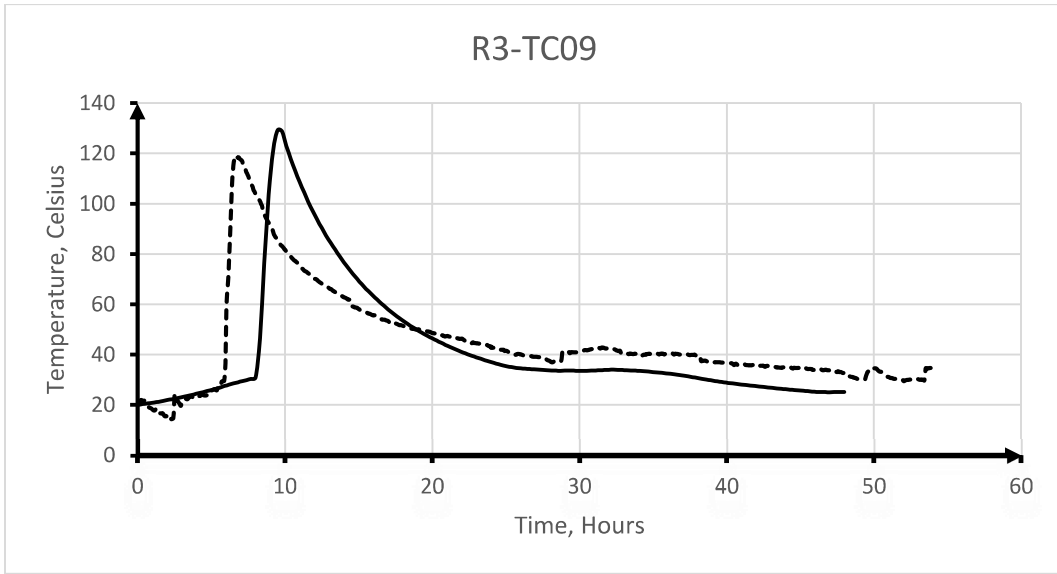
Figure B- 20: Time temperature curve for sensor R3-TC09
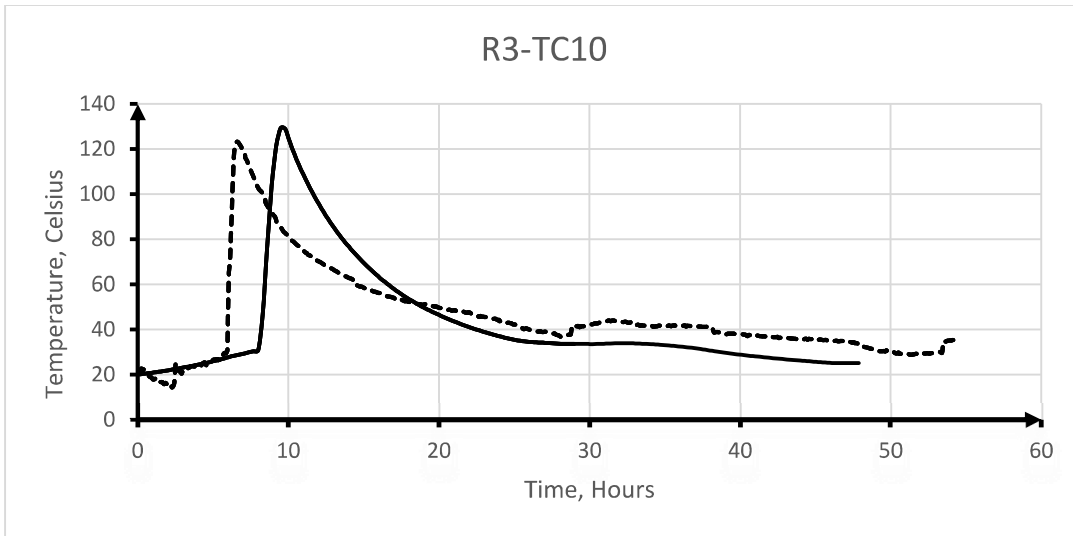
Figure B- 21: Time temperature curve for sensor R3-TC10
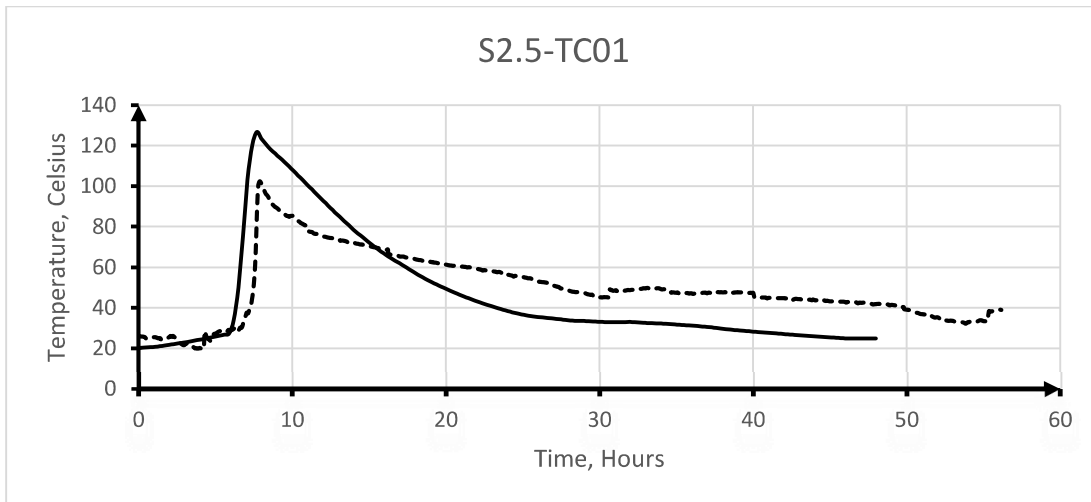
Figure B- 22: Time temperature curve for sensor S2.5-TC01
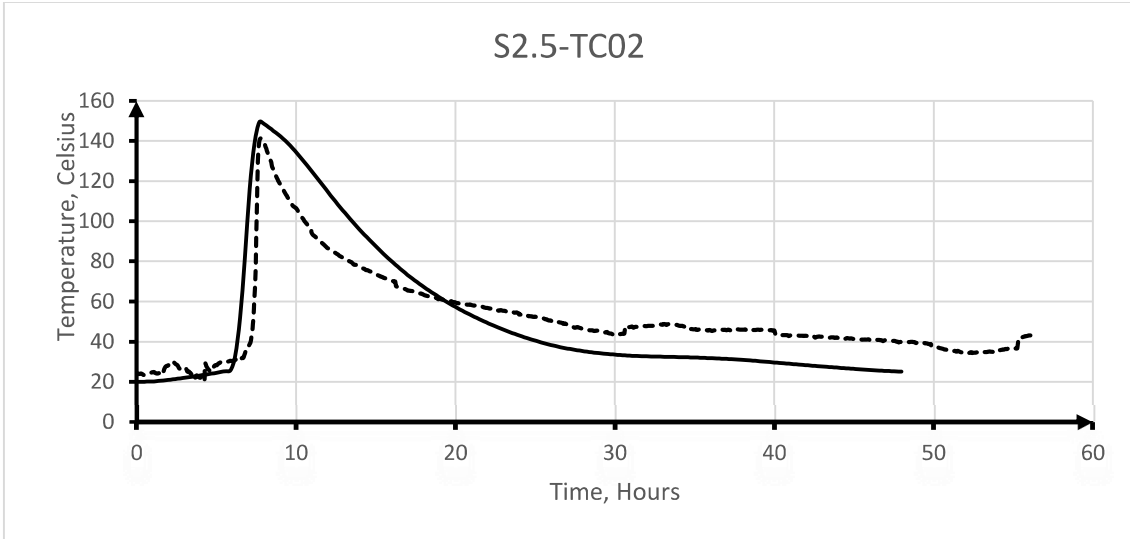
Figure B- 23: Time temperature curve for sensor S2.5-TC02
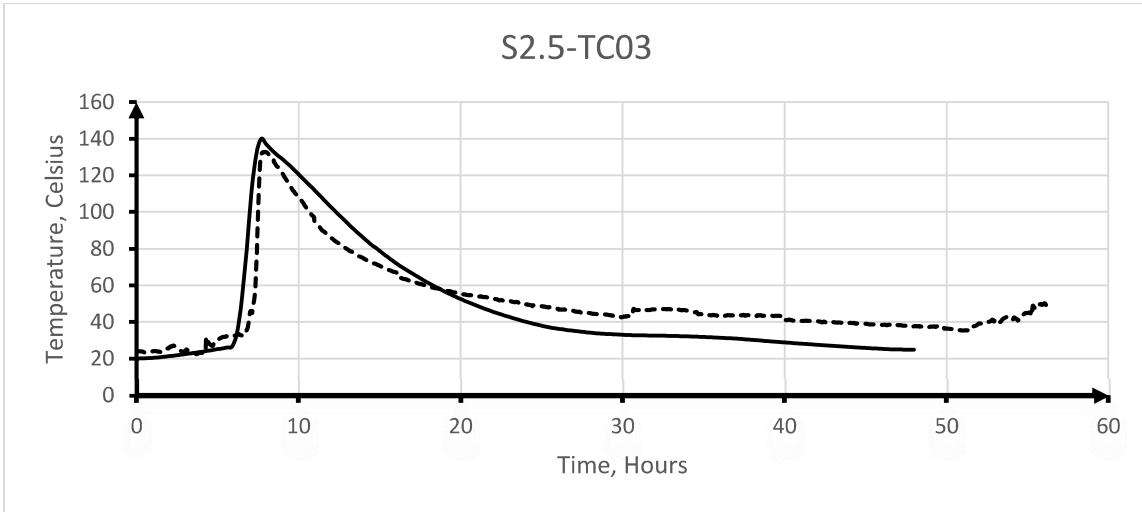
Figure B- 24: Time temperature curve for sensor S2.5-TC03
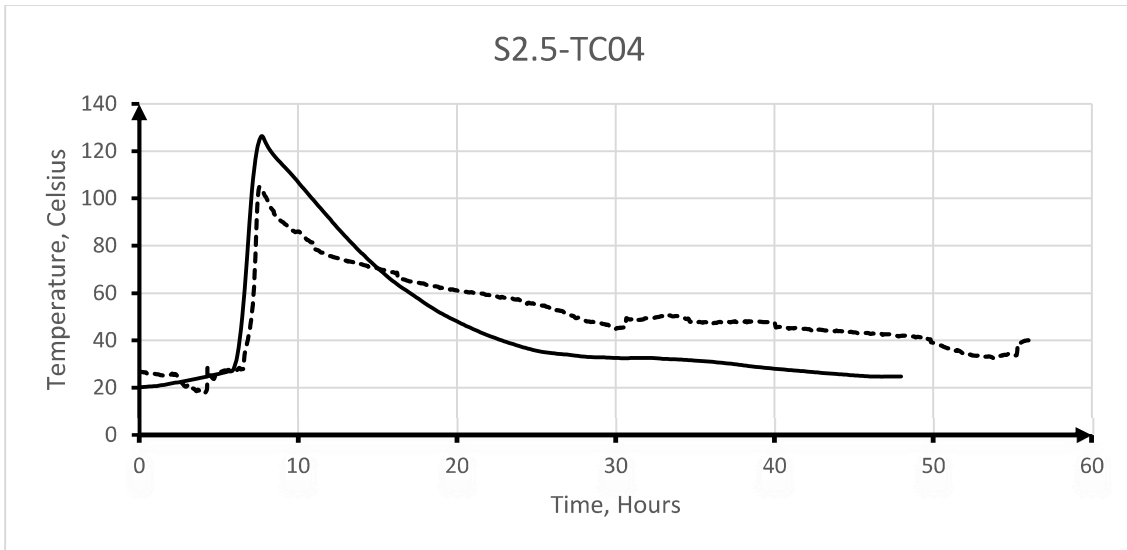
Figure B- 25: Time temperature curve for sensor S2.5-TC04
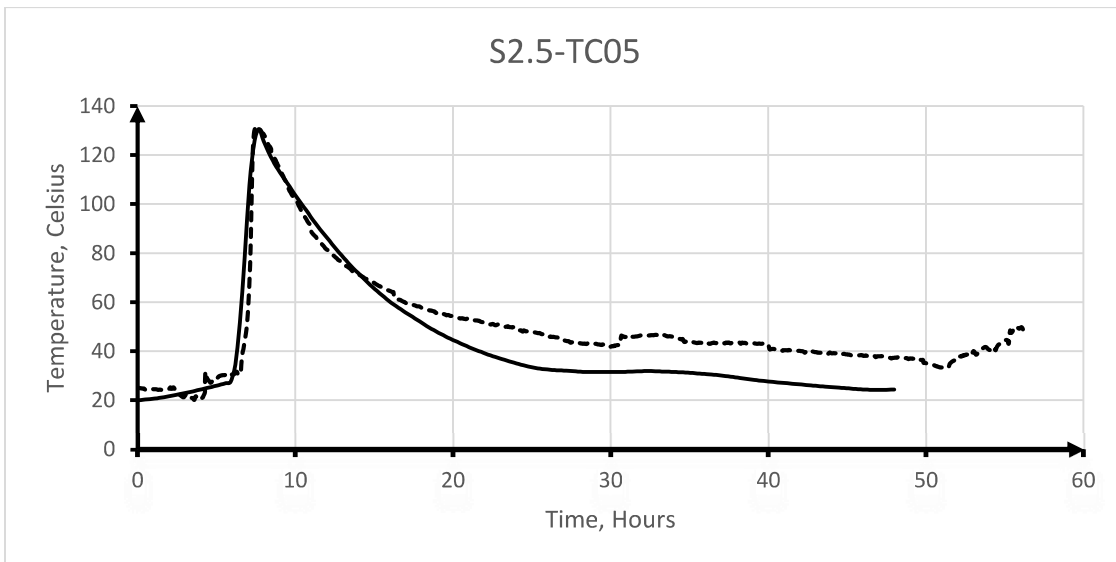
Figure B- 26: Time temperature curve for sensor S2.5-TC05
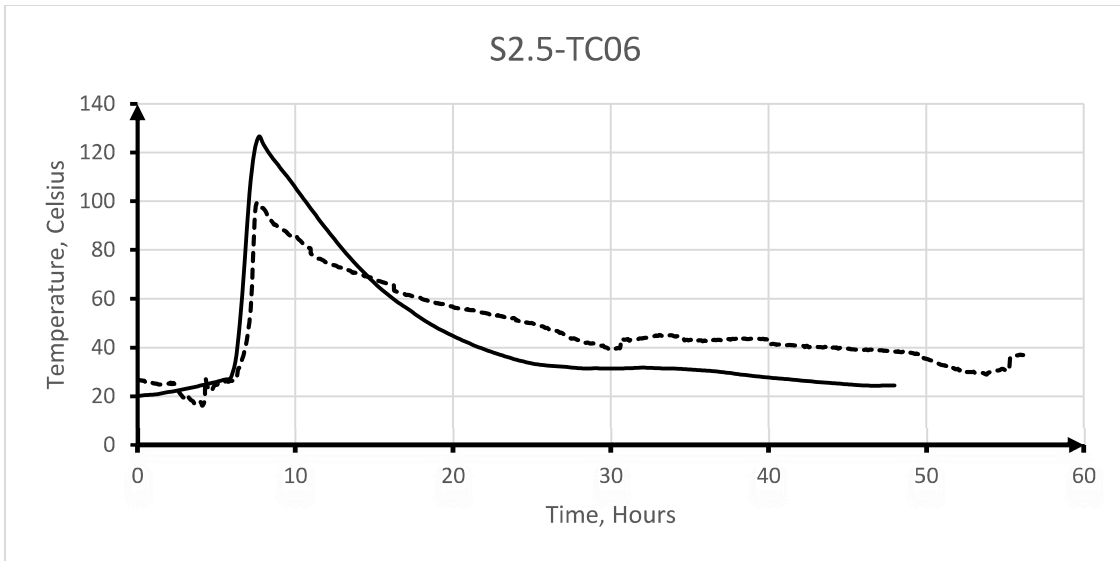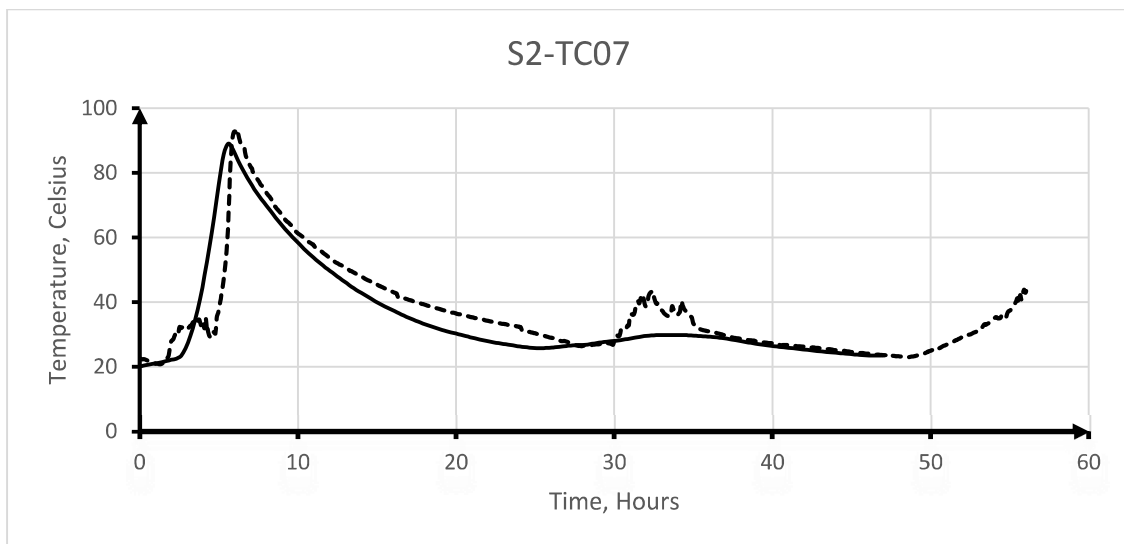
Figure B- 27: Time temperature curve for sensor S2.5-TC06
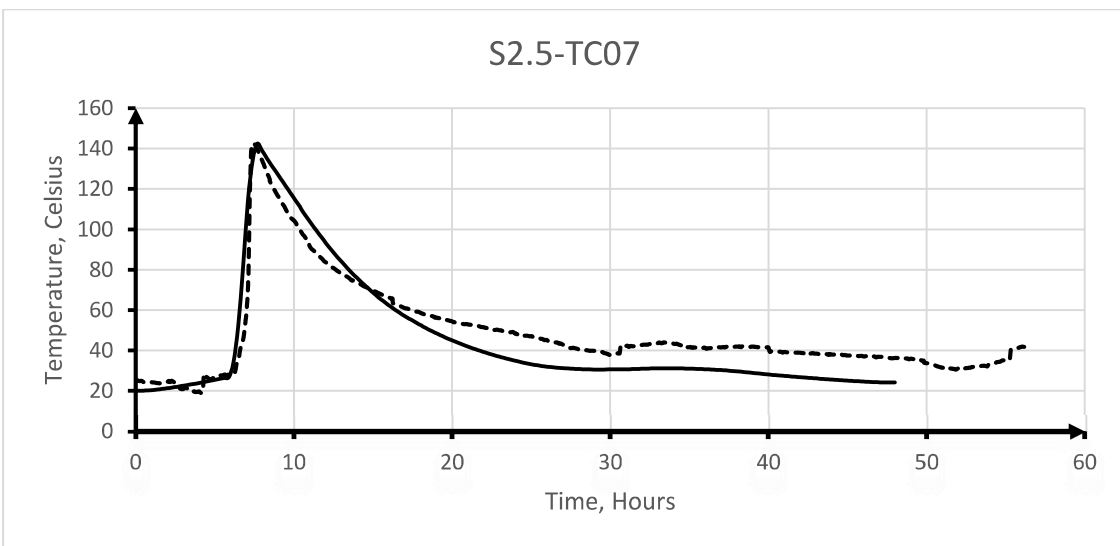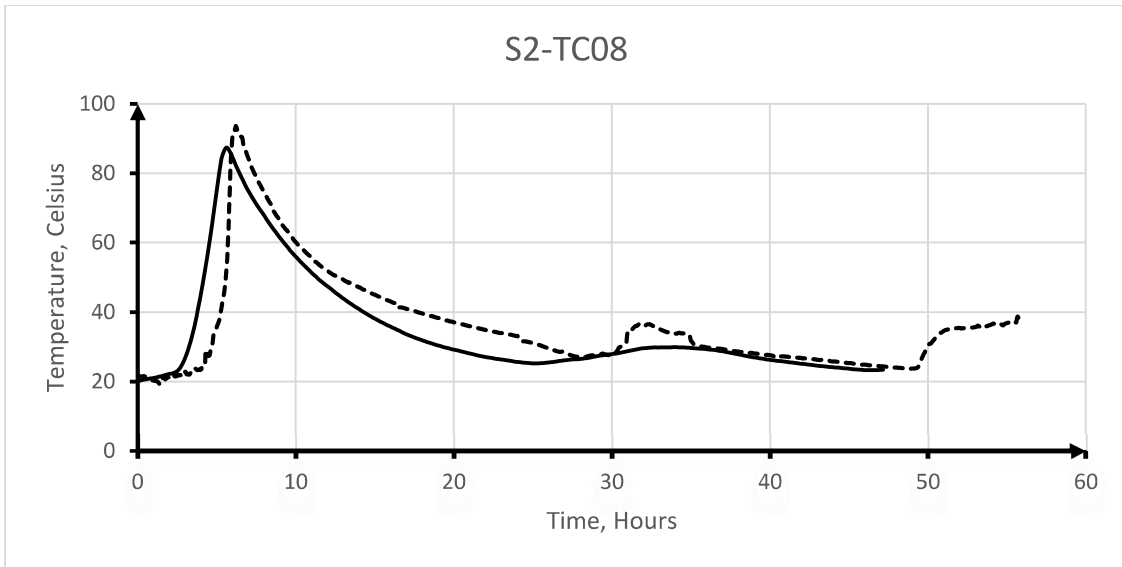

Figure B- 28: Time temperature curve for sensor S2.5-TC07
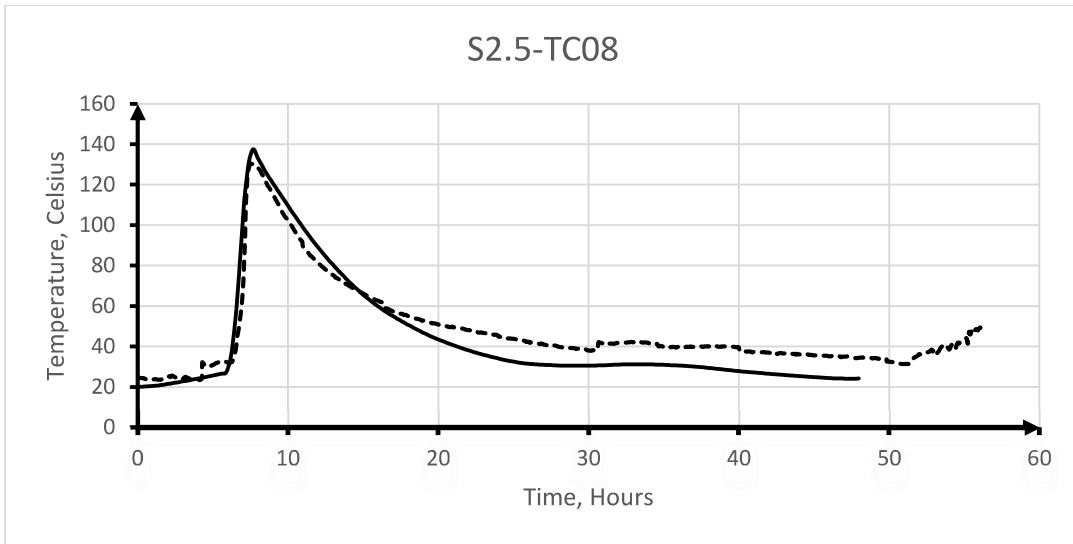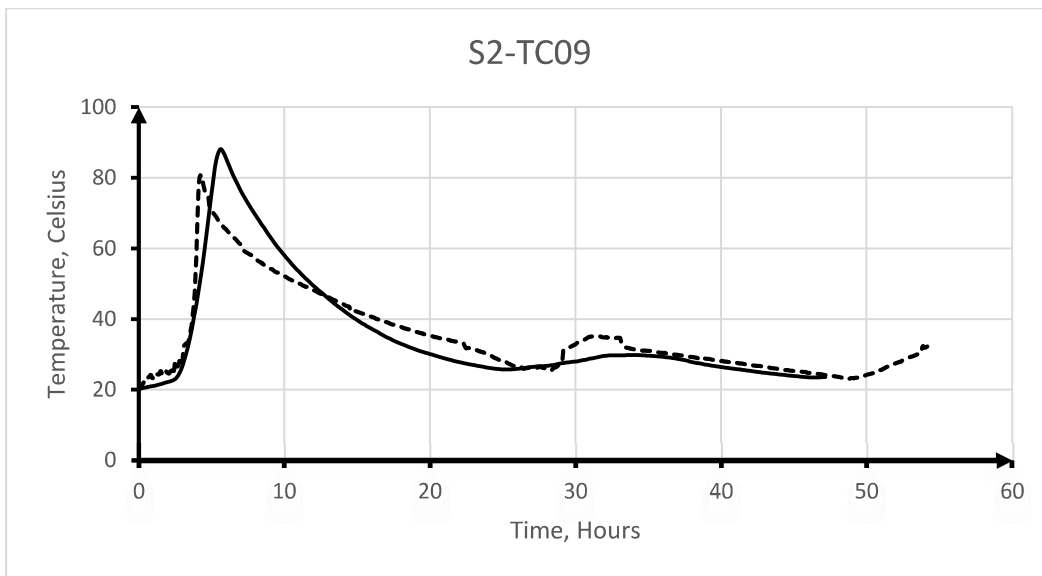
Figure B- 29: Time temperature curve for sensor S2.5-TC08
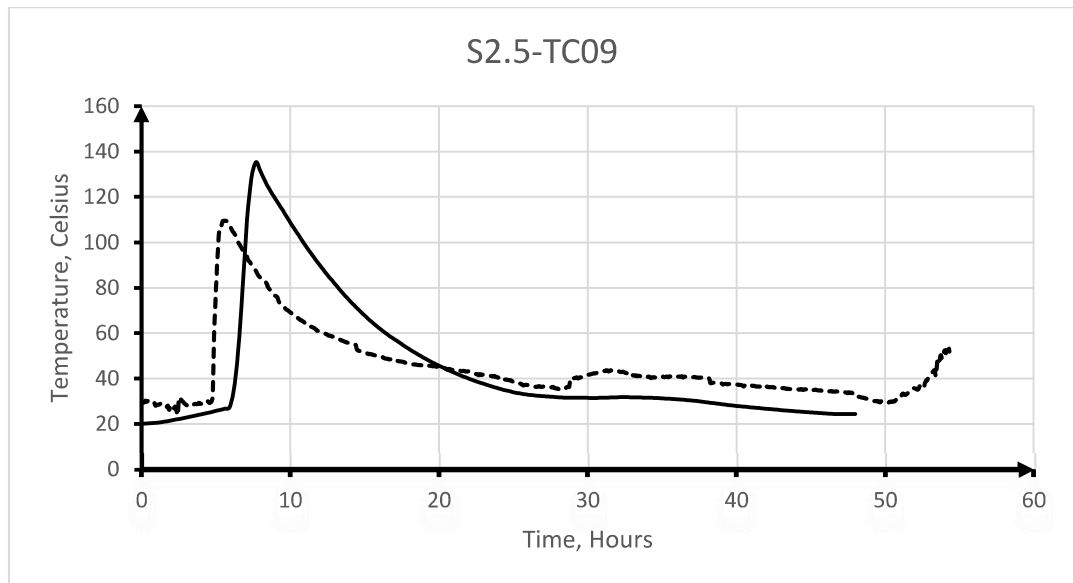
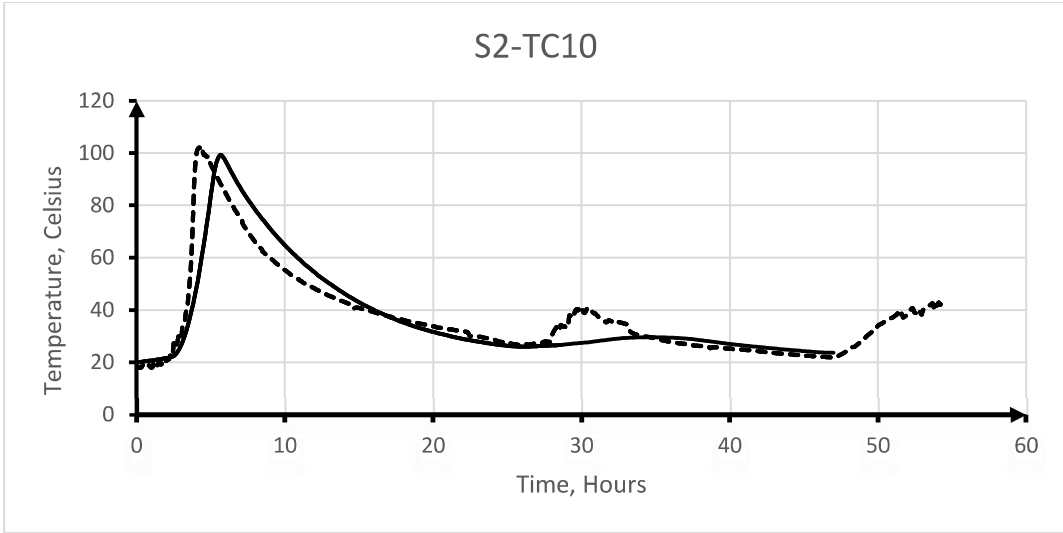Figure B- 30: Time temperature curve for sensor S2.5-TC09
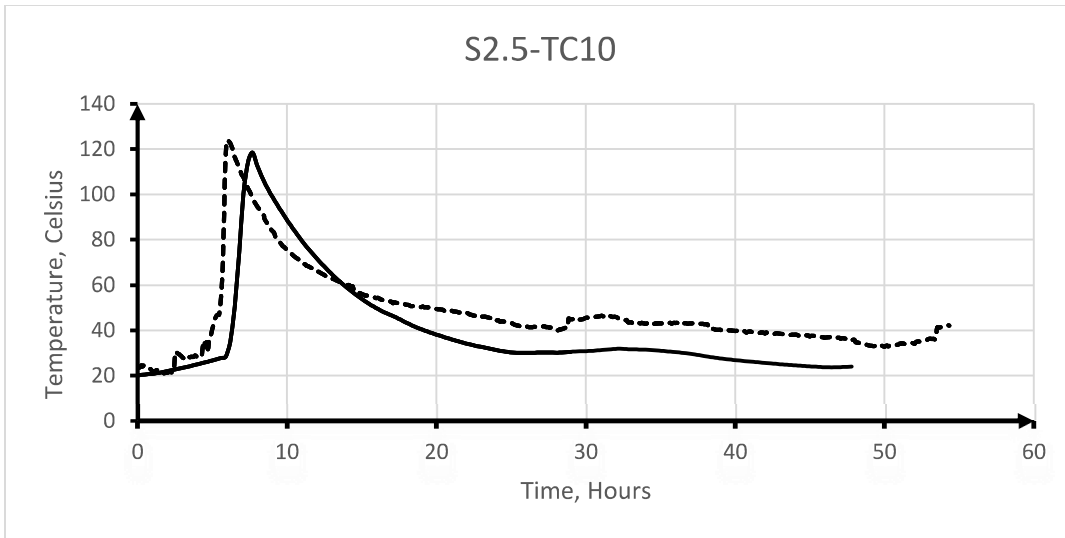
Figure B- 31: Time temperature curve for sensor S2.5-TC10
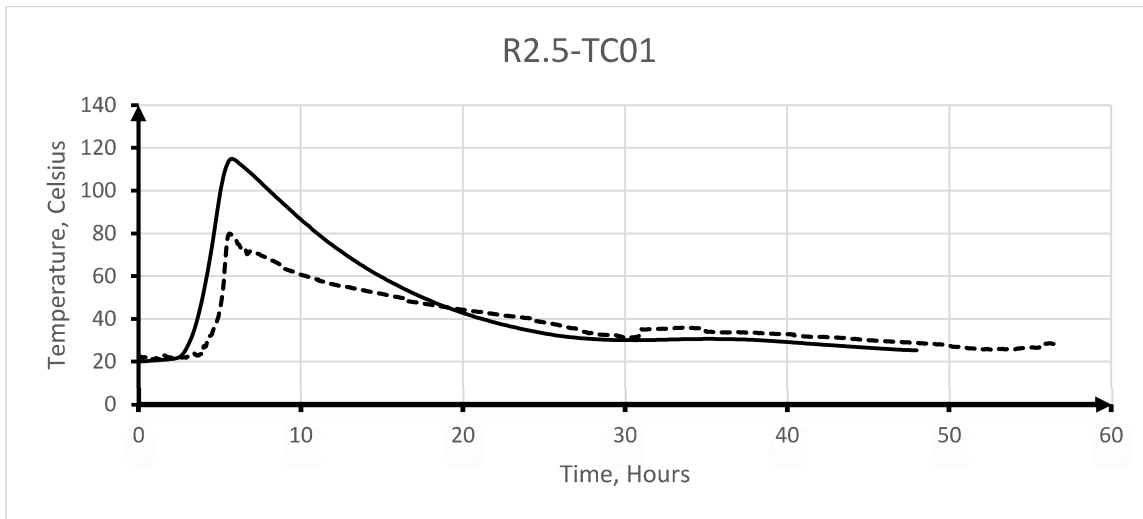
Figure B- 32: Time temperature curve for sensor R2.5-TC01
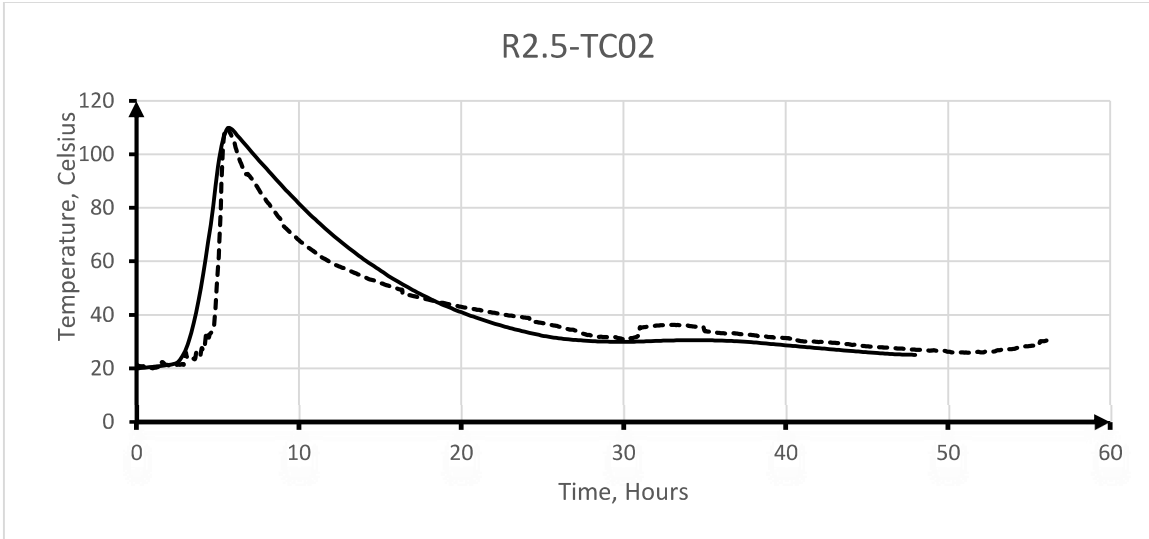
Figure B- 33: Time temperature curve for sensor R2.5-TC02

Figure B- 34: Time temperature curve for sensor R2.5-TC03

Figure B- 35: Time temperature curve for sensor R2.5-TC04

Figure B- 36: Time temperature curve for sensor R2.5-TC05

Figure B- 37: Time temperature curve for sensor R2.5-TC06

Figure B- 38: Time temperature curve for sensor R2.5-TC07

Figure B- 39: Time temperature curve for sensor R2.5-TC08

Figure B- 40: Time temperature curve for sensor R2.5-TC09
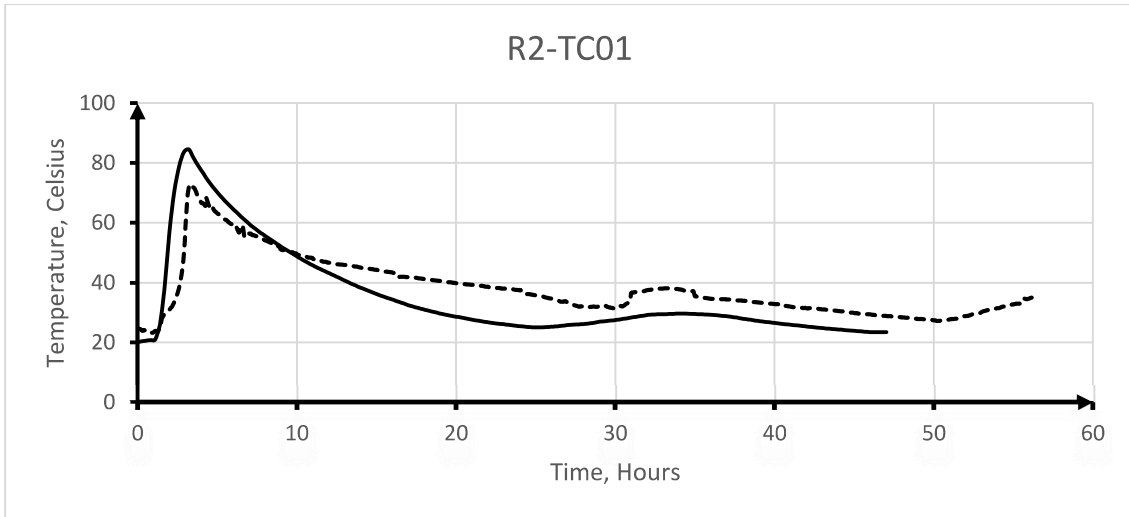
Figure B- 41: Time temperature curve for sensor R2.5-TC10

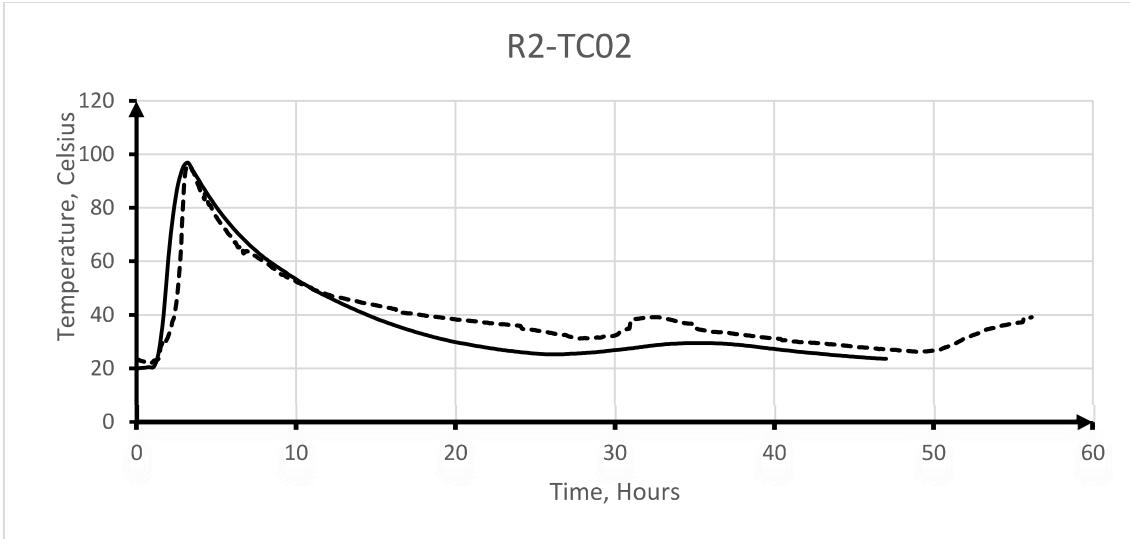Figure B- 42: Time temperature curve for sensor S2-TC01

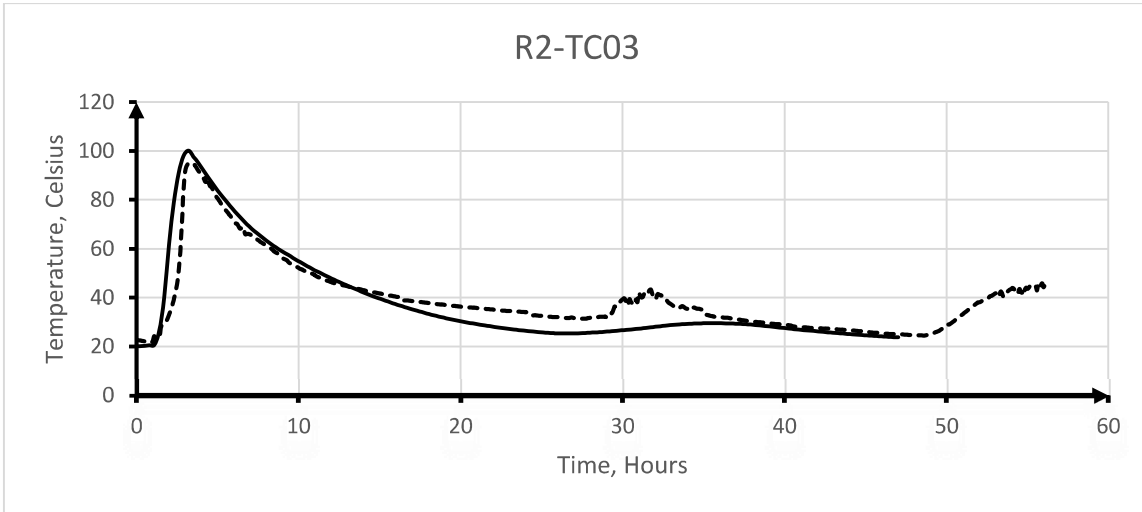Figure B- 43: Time temperature curve for sensor S2-TC02

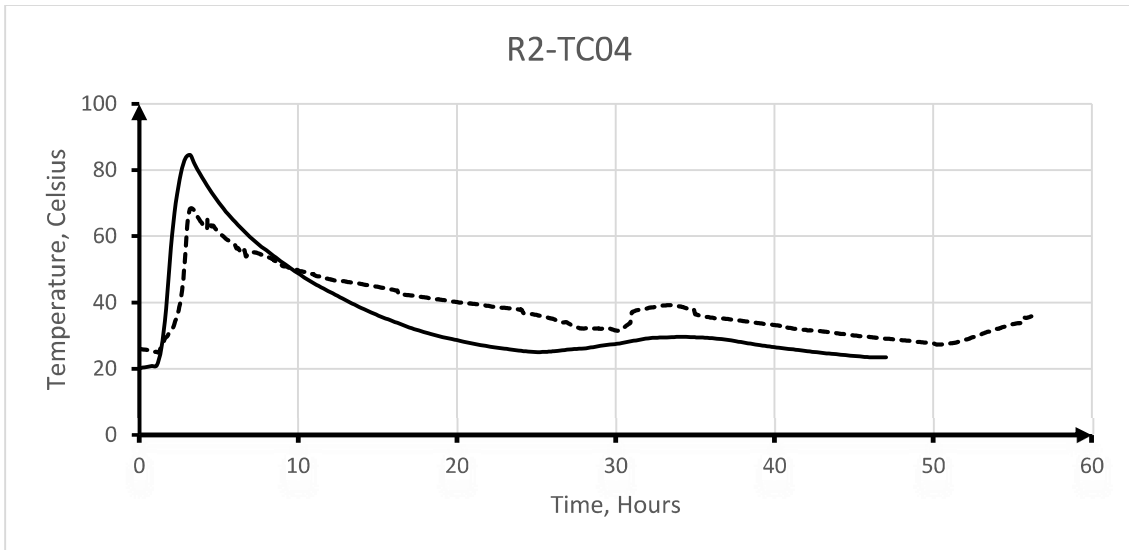Figure B- 44: Time temperature curve for sensor S2-TC03

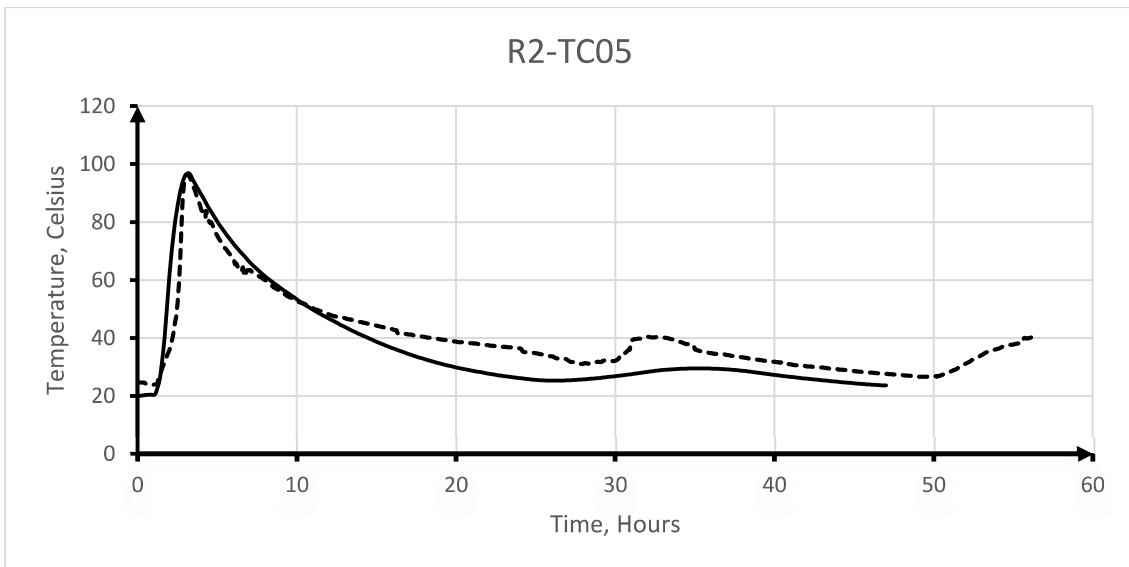Figure B- 45: Time temperature curve for sensor S2-TC04

Figure B- 46: Time temperature curve for sensor S2-TC05

Figure B- 47: Time temperature curve for sensor S2-TC06

Figure B- 48: Time temperature curve for sensor S2-TC07

Figure B- 49: Time temperature curve for sensor S2-TC08

Figure B- 50: Time temperature curve for sensor S2-TC09

Figure B- 51: Time temperature curve for sensor S2-TC10

Figure B- 52: Time temperature curve for sensor R2-TC01

Figure B- 53: Time temperature curve for sensor R2-TC02

Figure B- 54: Time temperature curve for sensor R2-TC03

Figure B- 55: Time temperature curve for sensor R2-TC04

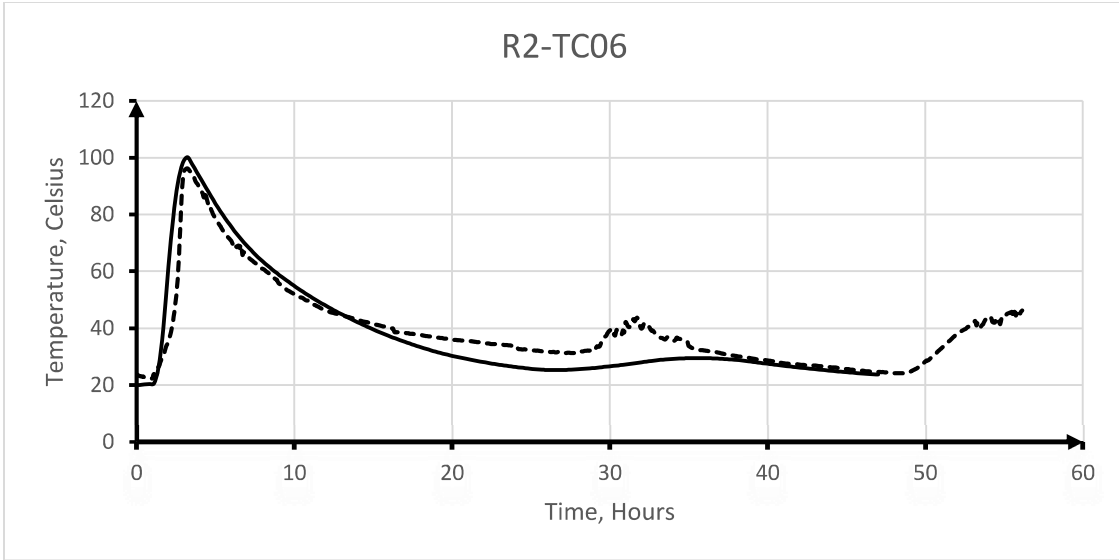Figure B- 56: Time temperature curve for sensor R2-TC05
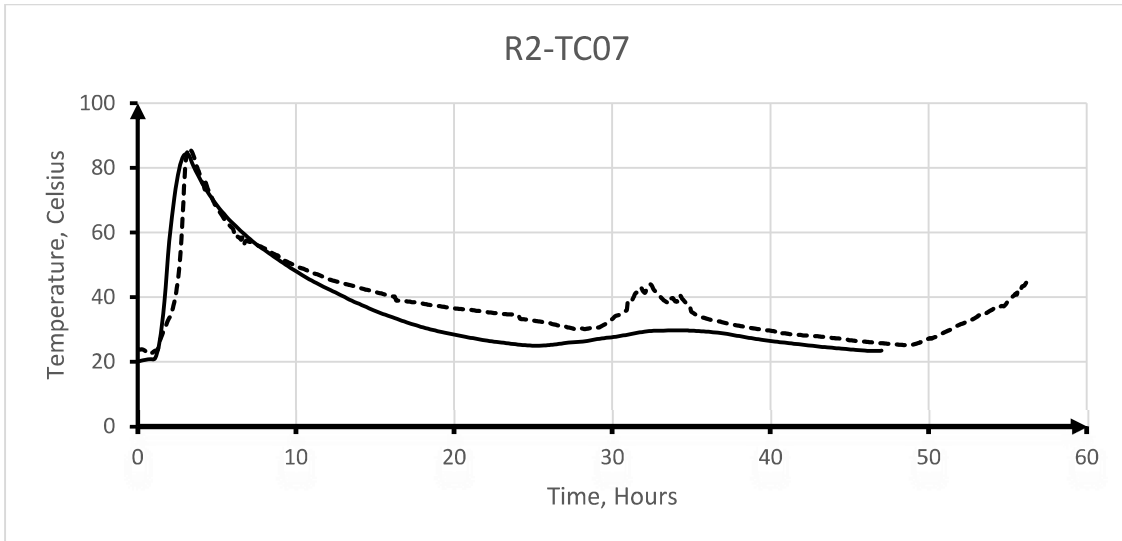
Figure B- 57: Time temperature curve for sensor R2-TC06
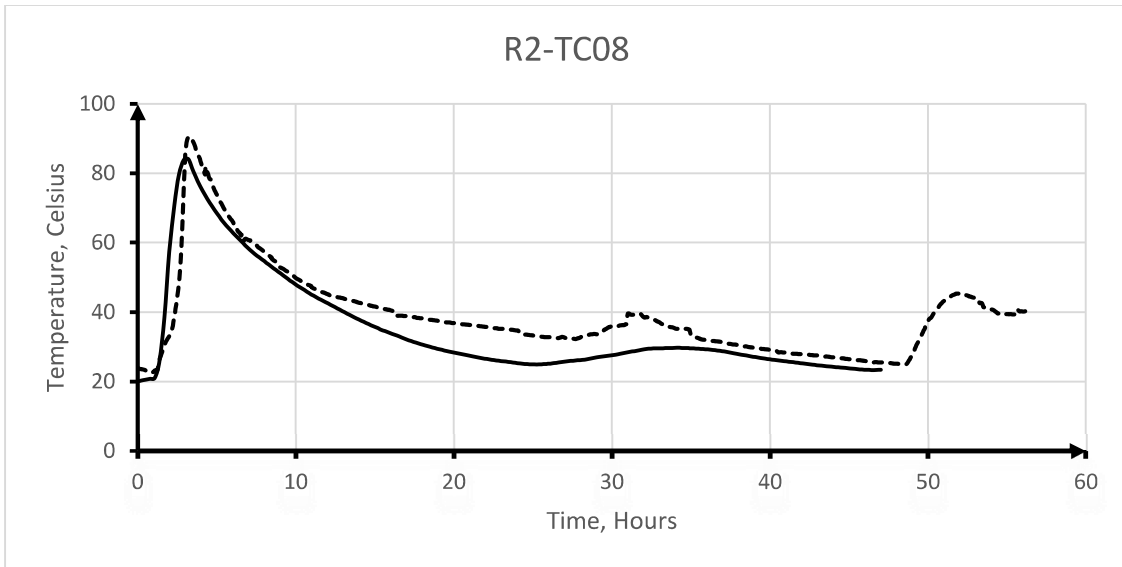

Figure B- 58: Time temperature curve for sensor R2-TC07

Figure B- 59: Time temperature curve for sensor R2-TC08